Addis Ababa University

College of Technology and Built Environment

School of Mechanical and Industrial Engineering

Experimental Investigation of Electrically Powered Stove for Areke Distillation

A Thesis Submitted to the School of Graduate Studies of Addis Ababa University in Partial Fulfillment of the Requirements for the Award of the Degree of Master of Science in Energy Technology

By: Dawit Debash

Advisor: Kamil Dino Adem (PhD)

June 16, 2025

Addis Ababa University

College of Technology and Built Environment

School of Mechanical and Industrial Engineering
School of Graduate Students

Experimental Investigation of Electrically Powered Stove for areke Distillation

By: Dawit Debash Birhanu

Submitted in accordance with the requirements for the degree of Masters of Science (M.Sc)

Approved by board of examiners

Kamil D. Adem (Ph.D.)		
Advisor	*Date*	*Signature*
Wondwossen Bogale (Ph.D.)		
Internal Examiner	*Date*	*Signature*
Habtamu Tkubel (Ph.D.)		
External Examiner	*Date*	*Signature*
Abdulkadir Aman (Ph.D.)		
Interim Head of Mechanical & Industrial Engineering	*Date*	*Signature*
Shegaw Ahmed (Ph.D.)		
Interim Vice Executive Dean for Academic Affairs	*Date*	*Signature*

Declaration

I hereby declare that the work which is being presented in this MSc thesis entitled as "Experimental Investigation of Electrically Powered Stove for areke Distillation" is the original work of my own, has not been presented for a degree of any university and all the resource of materials used for this thesis have been duly acknowledged.

Dawit Debash		
Name	*Date*	*Signature*

This is to certify that the above declaration made by the candidate is correct to the best of my knowledge.

Kamil D. Adem (Ph.D.)		
Advisor	*Date*	*Signature*

Acknowledgement

First and foremost, I thank Almighty God and the Blessed Virgin Mary for their endless grace, guidance, and strength throughout this journey.

I am deeply grateful to my advisor, Dr. Kamil Dino Adem, for his invaluable support, mentorship, and encouragement.

My heartfelt thanks go to my beloved wife, Bezawit Assefa, for her unwavering love, patience, and constant support.

I also wish to express my deepest gratitude to my parents, Tigist Abebaw and Debash Birhanu, for their sacrifices, prayers, and boundless love that have carried me to this point. Last but not least, special thanks to my friend, Habtamu Afework, for his encouragement, and support along the way.

Abstract

Areke, a traditional Ethiopian distilled spirit, is primarily produced using biomass-fueled stoves, which are characterized by inefficiency, deforestation, and significant contributions to indoor air pollution which poses serious health risks. This research aims to design, manufacture, and experimentally investigate an electrically powered distillation stove for areke production to address inefficiencies, improve product quality, and reduce environmental and health impacts. A prototype electric stove was developed, incorporating a clay pot, coil-based heating element, bamboo shell-and-tube condenser, and a PID temperature control system. Performance was evaluated through controlled tests, including Water Boiling Tests (WBT) and Controlled Cooking Tests (CCT), comparing the prototype to traditional methods in terms of thermal efficiency, energy consumption, distillation time, and product quality.

Through controlled testing and design modifications, the stove successfully produced high-quality areke. The custom-designed electric areke distillation stove achieved thermal efficiencies of 52.2% during cold start and 75.8% during hot start conditions, significantly outperforming traditional biomass stoves, which typically operate at 10-23% efficiency, and surpassing the Ethiopian standard requirement of 40%. With an average energy consumption of 7.9 kWh to produce 1.5 liters of areke, the prototype achieved a 49% reduction in estimated energy costs and a 69% decrease in energy consumption compared to traditional methods. Precise temperature control with PID controller provided consistent regulation over the distillation rate and duration. Testing revealed that rate of distillation had a direct impact on the final product's alcohol content. A longer distillation time resulting in higher alcohol concentration in the final areke.

The prototype’s design, which integrates locally available materials and aligns with traditional practices, proved compatible with existing distillation setups, enhancing its potential for widespread adoption. Additionally, the stove completely eliminated harmful emissions associated with biomass combustion, addressing key environmental and health concerns. The electrically powered distillation stove offers a sustainable and efficient alternative to traditional biomass stoves, addressing critical environmental and health issues.

Key words: A*reke distillation, electric stove, thermal efficiency, biomass alternatives, indoor air pollution, sustainable technology, Ethiopia.*

Contents

List of Figures

List of Tables

Abbreviations

ABV	Alcohol by Volume
CCT	Controlled Cooking Test
CO_2	Carbon Dioxide
GTZ-SUN	Deutsche Gesellschaft für Internationale Zusammenarbeit – Special Unit for Sustainable Energy (Stove type identifier)
IAP	Indoor Air Pollution
IR	Infrared
NI cDAQ	National Instruments Compact Data Acquisition
NI-DAQmx	National Instruments Data Acquisition Driver Software
PC	Personal Computer
PID	Proportional-Integral-Derivative (controller)
PM	Post Meridiem (after noon)
PVC	Polyvinyl Chloride
RTD	Resistance Temperature Detector
SSR	Solid-State Relay
TC	Thermocouple
WBT	Water Boiling Test
WHO	World Health Organization

Chapter 1

Introduction

1.1 Introduction

Ethiopia, known for its cultural richness and diversity, is home to a variety of traditional beverages, including *tela*, *tej*, and *areke*. *Areke* is a traditional distilled spirit widely consumed in Ethiopia, known for its strong alcoholic content and cultural significance in social gatherings and ceremonies fostering communal bonds and serving as a shared experience. Areke is made primarily from fermented grains, such as maize, barley, or wheat, using age-old techniques passed down through generations. It is widely enjoyed, especially in rural areas where its manufacture and consumption are still an important part of local traditions and communal life. Areke's popularity extends across various Ethiopian regions each with its unique variations and consumption customs, with notable mentions in Debre Berhan, Arsi Negele, Debre Markos, and beyond. Especially in these areas, areke production serves as a primary source of livelihood, generating income for producers, vendors, and related businesses. For instance, in 2008, the municipality of Arsi Negele town reported collecting approximately 1 million Birr annually from formal areke business operations, underscoring its significant economic contribution at the local level (Gezahegne, 2008). This figure excludes the numerous informal businesses, which are believed to surpass formal ones in number and operate without contributing to tax revenue.

According to Ethiopia National Clean Cook Stoves Program, more than 99% of the rural households depend on firewood for cooking and heating purpose. In Ethiopia, 90 percent of energy consumption comes from biomass (Alemayehu Zeleke Urge & Motuma Tolera Feyisa, 2019). Despite its deep cultural and economic importance, the energy needed for areke production and processing depends entirely on fuelwood (Gezahegne, 2008), which come with significant drawbacks. These thermally inefficient methods, which heavily use biomass fuel, raise concerns on environmental sustainability due to deforestation and health risks due to pollution. And from a modern perspective, these traditional methods face a

significant limitation in their inability to consistently produce high-quality areke.

Indoor air pollution, stemming from the combustion of biomass, is a significant concern associated with traditional areke production method. Traditional biomass stoves exhibit low efficiencies primarily due to the incomplete combustion of biomass. This incomplete combustion leads to the generation of health-damaging pollutants, with suspended particulates and carbon monoxide being particularly prominent among them. These pollutants exceed acceptable levels inside poorly ventilated houses, especially those without chimneys (Goldemberg et al., 2000).

Due to its complete reliance on biomass, traditional areke production contributes to the alarming deforestation rate in Ethiopia. In 2022, Ethiopia lost 19.9 kha of tree cover, equivalent to 11.7 Mt of CO_2 emissions (Vizzuality, 2022). As we strive to improve areke production, addressing these environmental, health and quality issues becomes imperative.

Despite concerns about pollution and inefficiency, the traditional process of areke distillation has seen surprisingly few attempts at improvement by the existing body of research (Getachew et al., 2022). While several attempts have been undertaken to address key challenges, such as pollution reduction and enhanced efficiency for traditional stoves, but much progress is still needed. For example, attempts to design improved biomass stoves, such as the Mirt areke stove (Assefa & Adem, 2022), the GTZ-SUN stove (Gezahegne, 2008), and the Darfur areke stove (Bekele, 2019), have shown promise but they still emit pollution on part or even above WHO-recommended levels. Exploring alternative energy sources like biomass and solar energy also offered some promise (Demissie et al., 2016; Getachew et al., 2022), but biomass options proved expensive, and solar-powered solutions, while pollution-free, restricted production to daylight hours, significantly hampering producer flexibility. Consequently, most of these inventions struggled to gain traction in the community, highlighting the need for innovative solutions that address both environmental and practical concerns while respecting the needs of areke producers. Overall, while marginal improvements have been made, the fundamental constraints of the traditional distillation process remain largely unaddressed. To achieve significant improvements more groundbreaking innovations, likely driven by new technologies are essential.

The solution may lie in adopting a cleaner and more modern approach: electrically powered distillation stoves. This technology, already utilized by spirit producers on both small and large scales worldwide, presents unique benefits that could effectively address the

challenges currently facing the areke production industry. Among these advantages, electric heating stands out for its ability to eliminate harmful emissions associated with biomass combustion. Furthermore, it facilitates precise temperature control, ensuring higher and more consistent product quality. Ethiopia's majority electricity production from large hydro-power plants further ensures a clean and environmentally friendly energy source for areke production.

While electrical stoves have been proven effective for distilling other types of spirits, no efforts have been made to design and develop electric distillation stoves specifically for producing areke. Although commercial electric distillation stoves exist, they are neither customized for areke production nor economically feasible for producers in Ethiopia.

This study seeks to fill this significant gap by developing an accessible, efficient, and culturally sensitive electrically powered distillation stove designed specifically for Ethiopian areke producers. The lack of comprehensive data on areke distillation from a thermal engineering perspective further highlights the challenges and potential impact of this project. Filling this knowledge gap will not only benefit this project but also future studies by laying the groundwork.

1.2 Problem statement

Traditional methods of areke production in Ethiopia are heavily dependent on biomass as the primary fuel source (Gezahegne, 2008). This widespread use of wood fires raises major concerns around indoor air pollution, deforestation, thermal inefficiency, and product quality and consistency.

The use of biomass as a fuel for areke distillation contributes significantly to harmful emissions, posing serious health risks. According to the World Health Organization (WHO), indoor air pollution (IAP) resulting from biomass combustion is among the top ten global health risks (Elbayoumi & Albelbeisi, 2023). In 2020 alone, household air pollution was linked to approximately 3.2 million deaths annually, including over 237,000 deaths of children under the age of five (*Household Air Pollution*, 2024). The adverse health impacts of air pollution disproportionately affect the poorest and most vulnerable populations, with women and children being the most affected (Fullerton et al., 2008; *Household Air Pollution*, 2024).

Deforestation remains a pressing concern in Ethiopia. In 2022 alone, the country lost 19.9 thousand hectares of tree cover, resulting in an estimated 11.7 million tons of CO_2 emissions (Vizzuality, 2022). Traditional methods of producing areke exacerbate this issue, with a single household consuming an average of 450 kilograms of firewood to distill 150 liters of areke over six working days (Getachew et al., 2022). In Arsi Negele, one of Ethiopia's largest areke-producing cities, the demand for fuelwood is particularly high. In addition to wood transported by donkeys, carts, and individuals, approximately eight trucks, each with a loading capacity of 10 cubic meters, deliver various types of fuelwood to the market daily, underscoring the significant reliance on wood for areke production (Gezahegne, 2008).

Traditional stoves, such as the three-stone fire and mud stoves, are predominantly used for areke production in Ethiopia. However, these stoves are highly inefficient, with an energy efficiency of no more than 15% (Ikpambese et al., 2014; Koffi et al., 2014; Someswararao et al., 2012; Tesfay et al., 2024), which is significantly lower than other stove types that utilize modern energy sources. This inefficiency results in excessive fuel consumption, increasing the demand for firewood and, consequently, accelerating deforestation and environmental degradation. A significant amount of energy is lost as heat during the combustion process, leading to higher fuel consumption, which in turn increases production costs and reduces profits. Additionally, traditional stoves provide limited temperature control, resulting in inconsistent distillation and causing variations in product quality between batches.

Some attempts have been made to address aspects of these challenges through improved biomass stoves or alternative energy sources. However, these interventions have achieved limited real-world traction, with traditional methods still dominating. Fundamentally, the core issues of deforestation, indoor air pollution, thermal inefficiency and batch inconsistency persist unresolved. Therefore, this study aims to investigate the potential of electrically powered distillation methods to transform areke production. By eliminating biomass combustion and enabling precise temperature control, electric stoves could provide a cleaner, more efficient, and consistent distillation process aligned with modern quality and sustainability standards.

The purpose of this research is to design, build and experimentally test a prototype electric stove tailored to areke distillation. Through controlled testing, it will evaluate the technology's ability to reduce emissions, enhance efficiency, improve product consistency and offer a viable modern solution to Ethiopian areke producers.

1.3 Research Gap

A review of existing literature reveals that while some progress has been made in improving areke distillation, previous solutions, while valuable, have not provided a practical answer. Previous studies have primarily focused on:

- Improving Biomass Stoves: Innovations like the Mirt and GTZ-SUN stoves (Assefa & Adem, 2022; Gezahegne, 2008) have enhanced fuel efficiency and reduced some emissions. However, they do not eliminate indoor air pollution entirely and still rely on a depleting biomass resource.
- Exploring Alternative Renewable Sources: Solar-powered and biogas systems have been proposed (Getachew et al., 2022; Demissie et al., 2016). Solar solutions are limited by daylight hours and weather dependency, while biogas requires significant infrastructure (digesters) and a consistent supply of feedstock, which may not be practical for all producers.

Existing improvements are either incremental (still polluting) or have significant practical limitations (cost, complexity, daylight dependency). No efforts have been made on electrical stoves tailored for Areke production.

While commercial electric stills exist globally, they are: very expensive, Not tailored for areke production, and ignore culturally vital practices, like the use of traditional clay pots which are believed to influence the final taste and aroma.

The Gap: There is no documented research on a locally appropriate, affordable, and efficient electrically powered stove designed specifically for Ethiopian areke distillation.

1.4 Research Questions

Arising from the identified research gap, this study seeks to answer the following primary research questions:

- Can an electrically powered stove be designed and fabricated using locally available materials and skills that is compatible with the traditional clay pot distillation method used for areke?

- What is the thermal performance (i.e., thermal efficiency, energy consumption) of such a prototype, and how does it compare quantitatively to traditional biomass-fueled stoves?
- How does the use of electric heating with precise temperature control affect key product quality indicators, such as distillation time and final alcohol content (ABV), compared to traditional, uncontrolled methods?
- Is the proposed electrically powered stove a technically feasible and economically viable alternative for small-scale areke producers in Ethiopia?

1.5 Objectives

The general objective of this study is to design, manufacture and experimentally investigate electrically powered distillation stove for areke production.

Specific objectives:

- To design electrically powered areke distillation stove.
- To manufacture a functional prototype of the electrically powered distillation stove.
- To conduct a series of controlled experiments to assess the stove's performance.

1.6 Significance

This study on designing, building and testing an electric stove for areke distillation carries important health, environmental, technological, economic and policy significance.

Reducing indoor air pollution offers substantial health benefits. As stated in the problem statement section, according to the World Health Organization (WHO), indoor air pollution (IAP) resulting from biomass combustion ranks among the top ten global health risks (El-bayoumi & Albelbeisi, 2023). In 2020, household air pollution contributed to an estimated 3.2 million deaths annually, including over 237,000 deaths among children under five (*Household Air Pollution*, 2024). In Arsi Negele, over 3,500 households exclusively rely on traditional methods for areke production (Demissie et al., 2016). Transitioning to electric stoves has the potential to eliminate pollution-related illnesses and deaths within these households. Extrapolating these findings to the national level suggests a significant potential for saving lives across Ethiopia.

From an environmental perspective, transitioning away from biomass combustion for areke production offers significant potential for deforestation reduction. Given that each producer typically consumes 77 kg of firewood daily (Mohammed, 2008), and considering Ethiopia's alarming annual deforestation rate of 150,000 - 200,000 hectares (Mengistu, 2002), the environmental impact is substantial. In Arsi Negele, where over 3,500 households exclusively rely on traditional methods for areke production (Demissie et al., 2016), the annual wood consumption for areke production alone amounts to approximately 98,367.5 metric tons. The adoption of electric stoves would significantly mitigate this unsustainable environmental impact.

Technologically, precise temperature controls with electric stoves enable higher consistency between batches compared to traditional methods. Additionally, the development and experimental evaluation of an electric stove prototype tailored for areke distillation could establish proof-of-concept, performance benchmarks and design guidelines for further innovation in the future.

areke production plays a significant role in the local economies especially in regions known for its production, such as Debre Berhan and Arsi Negele. The municipality of Arsi Negele reports an annual tax revenue of approximately 1 million Birr exclusively from formal market transactions within the areke industry (Gezahegne, 2008), demonstrating its substantial economic impact on both distillers and the government. With the anticipated increase in production facilitated by electric stoves, this revenue stream is expected to grow significantly. Furthermore, this initiative aligns with global and national development vision of transitioning towards sustainable and renewable energy production.

Chapter 2

Literature Review

2.1 Traditional Areke Production

2.1.1 Traditional Areke Distillation Stoves

Two traditional stoves are employed in the distillation of areke: mud stoves and three-stone fire stoves. Mud stoves, constructed with a blend of mud, clay, and stone, feature a cavity to cradle the pot and are enclosed on all sides except for a front opening, providing insulation.

Three-stone fire stoves, on the other hand, involve arranging three stones in a triangle to support the cooking vessel. This straightforward and traditional method involves burning fuel, typically wood, between the three stones. Its open design results in lower efficiency compared to the mud stove, primarily due to heat loss as a result of lack of insulation.

Figure 2.1: (a) Multiple mud distillation stoves (Getachew et al., 2022); (b) Three stone fire areke distillation (*Areqie Local Alcohol Cutting Dreams*, 2022)

2.1.2 Preparation of Mash

Gesho leaves (scientifically known as Rhamnus Prinoides) and water are combined for three to four days, creating a mixture referred to as *tenses*. Following this, a *kita'*(whole-grain flour bread, typically made from *teff* or other cereals) and germinated barley or wheat known as *bikil* along with additional water, are incorporated. The resulting mixture

undergoes fermentation for five to six days in warm regions and twelve days in colder areas, transforming into what is termed *difdif* or mash. Subsequently, the fermented mash is subjected to the distillation process (Assefa & Adem, 2022; Gezahegne, 2008; Kassa, 2015; Selinus, 1971).

Figure 2.2: Difdif ready for distillation (Getachew et al., 2022)

2.1.3 Distillation Apparatus

The major apparatus needed for the setup of the distillation process include: pot and pot lid made of clay, condensation tube made of bamboo, a distillate collector flask, and condenser tub made of clay filled with cooling water. (Gezahegne, 2008; Kassa, 2015)

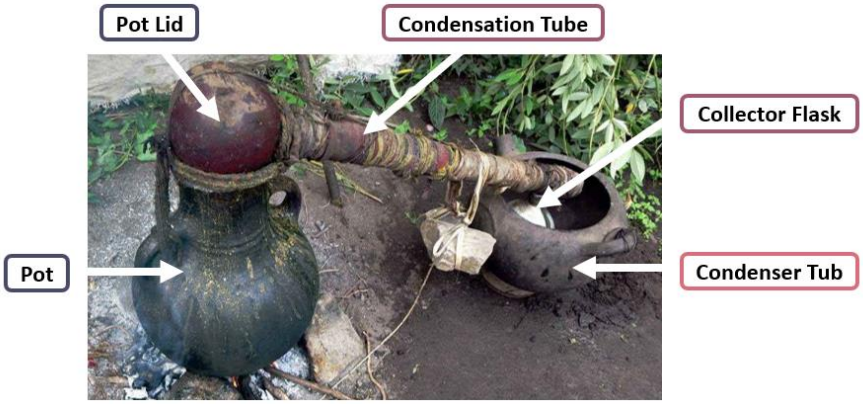

Figure 2.3: areke distillation apparatus (*Areqie Local Alcohol Cutting Dreams*, 2022)

The sturdy clay pot serves as the main vessel for holding difdif. Even heat distribution along the pot is crucial for consistent distillation. The pot lid, sealing the top of the pot, featuring a small opening that allows a bamboo tube to connect and channel alcohol vapors from the pot to the distillate collector flask (Getachew et al., 2022; Kassa, 2015).

The condensation tube with approximate internal diameter of 60mm connects the pot and the collecting flask. The flask, usually made of aluminum, is immersed in the cooling tub filled with water (Gezahegne, 2008). The tube has a small opening at one end which gets inserted in the distillate collector flask (Getachew et al., 2022; Kassa, 2015).

The condensation cooling tub is an open container filled with cooling water on which the distillate collector flask is immersed (Getachew et al., 2022). The water in the tub cools the flask to maintain low temperature region that facilitates condensation (Gezahegne, 2008). In the traditional method, the majority of the vapor undergoes condensation directly within the collector flask itself, effectively functioning as a condenser in addition to its primary role of collecting the distilled product. Maintaining the water temperature is essential for successful distillation.

2.1.4 Working Procedure (Distillation process)

Following the cleaning of the distillation pot, difdif is poured into it. The quantity of difdif added to the pot varies depends on the desired amount of areke required. In certain regions of the country, eight liters of difdif are added to yield one liter of distilled areke, whereas in other areas, twelve to fourteen liters of difdif are added to produce 1.5 to 2 liters of distilled areke.

Next, Firewood is ignited to initiate combustion, and the pot is placed on the stove. The fermented difdif mash inside the pot then undergoes constant stirring to facilitate even thermal exposure. A generous amount of fuelwood is supplied to the stove at this stage to rapidly bring the pot contents to a boil. This continues until alcohol evaporation visibly starts through the pot's opening (Assefa & Adem, 2022; Gezahegne, 2008; Kassa, 2015). Once the evaporation process commences, stirring stops, and a clay lid is placed over the pot opening. This lid is then sealed with either mud or a wet fabric soaked in difdif, effectively preventing the evaporate from escaping into the atmosphere (Kassa, 2015).

Condensate tube is then inserted to the lid opening and the other end of the collector tube is inserted to the collector flask which is immersed in to the condenser tub filled with water. The quantity of firewood is gradually decreased to achieve the optimal boiling temperature, which is then maintained for the duration of the entire distillation process.

The evaporate coming from the difdif in distillate pot flows through the condensate tube and enters into the collecting flask. The hot steam that enters into the flask cools by releasing the heat to the cooling water in the cooling tub. When the cooling water in the tub gets hot about (35 °C - 40 °C), it will be drained and replaced by cool water (Kassa, 2015)

The termination of the operation is determined by factors such as the frequency of replacing the cooling water, the presence of specific odors and/or distinctive knocking sounds (Assefa

and Adem, 2022). Subsequently, the remaining stillage, referred to as *atella*, is repurposed as feed for livestock (Assefa & Adem, 2022; Kassa, 2015).

In addition to having a well-prepared mash, the quality of the product depends on the performance of the cook. The areke distillation requires constant follow up and careful management of fire. The heat supply or fire is controlled by the amount of wood fed to the stove. Less fuelwood could cause slower operation while more fuelwood could cause scorching, which is the burning and sticking of mash to the bottom and sides of the pot, and overflow of the mash down the condensation tube spoiling everything.

2.1.5 Types of Areke

Traditionally areke is classified into two: *Terra-areke* and *Dagim-areke*. The term *dagim* in Amharic refers to *second time* and, indicates that it is distilled second time, whereas the term *terra* in Amharic refers to ordinary. Terra-areke is the initial batch of areke distilled from difdif, with an average alcohol content of about 34%. Dagim-areke is a stronger variant of Terra-areke, created by re-distilling Terra-areke, resulting in a higher alcohol content (*Areqie Local Alcohol Cutting Dreams, Lives Short*, 2022; Tafere, 2015; Wedajo Lemi, 2020).

2.2 Advancements in Areke Distillation

Traditional areke distillation methods utilize inefficient, polluting biomass-based distillation resulting in economic, health, quality and environmental issues. Seeking improvements, few researchers have dedicated efforts to enhance Ethiopian local areke distillation processes, with some technologies explored and findings published. Improved biomass stoves as well as solar and biogas solutions are explored.

The subsequent sections critically evaluate and analyze these findings by the form of energy employed. While emerging systems show potential, the research illustrates that further optimization is required before cleaner solutions are ready for widespread adoption.

2.2.1 Efficient Biomass Stoves for Areke Distillation

The reliance on biomass leads to indoor air pollution, energy wastage and deforestation (Mohammed, 2008). To address this, innovative stove designs have been explored. Three notable literatures stand out the most: the Berkeley-Darfur Stove, the Mirt Stove, and the

GTZ-SUN Project. Each literature brings unique advancements and insights, offering promising improvements to traditional biomass stoves.

The Berkeley-Darfur Stove

Bekele (2019) designed and tested an improved enclosed metal stove for areke distillation as an alternative to the prevalent three-stone fires. The improved stove was designed based on the Berkeley Darfur stove, a highly efficient wood-burning cookstove designed by engineers at Lawrence Berkeley National Lab using the knowledge and input of local Darfuri women (*Berkeley-Darfur Stove V.14*, 2014), was modified for distillation with a non-removable skirt, fiber glass insulation, and metal shielding.

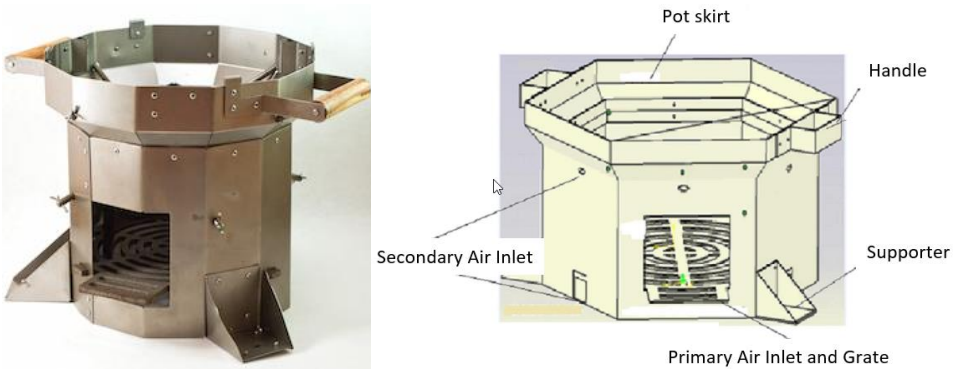

Figure 2.4: (a) the Darfur stove (*Berkeley-Darfur Stove V.14*, 2014) (b)Parts of Biomass Improved areke distillation Stove (Bekele, 2019)

A controlled cooking test (CCT) allowed comparative assessment of the traditional and improved stoves. Qualitative observations revealed the three-stone fire had highest smoke emissions during operation. Quantitative emissions testing was not undertaken.

Compared to the traditional biomass areke distillation stove, the improved biomass areke distillation stove improves the thermal efficiency by 14.4% (from 11.2 % to 25.6%), reduced specific fuelwood consumption by 45% (from 2.65 to 1.322 g/g) and decreased total distillation time by 50% (from 2 hours to 1 hour) to distillate 8 liter of difdif (Bekele, 2019).

During the areke distillation process, the new stove demonstrated better energy efficiency than the three-stone stove. The author concludes replacing traditional three-stone fires would conserve biomass resources and limit indoor pollution exposure from the crude stoves. Further work should optimize design elements like the pot skirt and mouth gap to maximize heat transfer efficiency.

Mirt stove for areke Distillation

Mirt stove is a fairly modernized cylindrical stove constructed with mortar and cement using mold. While primarily used for injera baking, it can also serve other purposes, such as areke distillation. Since Mirt injera stoves (injera is Ethiopian flat bread) have been under dissemination for quite a number of years, producers have become comfortable to make Mirt areke stove using similar approach (Assefa & Adem, 2022).

Figure 2.5: (a) Mirt injera stove (Manaye Demissie et al., 2022), (b) Mud stove (c) Mirt areke stove (Assefa & Adem, 2022)

Assefa and Adem (2022) compared the thermal and emissions performance of three different stoves used for distilling areke. Employing three-stone fire (uses three-stones to support the spherical round ceramic pot) as a baseline the stoves tested were, a traditional mud areke stove (which is locally made out of mud and finally painted with wet dung), and an improved and modified Mirt areke stove.

The tests conducted indicates that the Mirt areke stove outperformed both the traditional mud stove and the three-stone fire in terms of fuel efficiency, brewing time, and emissions. Specifically, compared to the three-stone fire, the Mirt stove reduced fuel consumption by 51%, decreased brewing time by 52% (1 hour and 4 minutes), and significantly lowered indoor air pollutants, including CO by 29% (from 14 to 10 ppm), PM2.5 by 53% (from 347 to 163 ppm), and PM10 by 52% (from 387 to 185 ppm). The measured CO levels were

below the WHO recommendation of less than 30 ppm for one hour of exposure, aligning with the strong recommendations set by world health organization (WHO) in 2014 (Assefa & Adem, 2022).

By contrast, the traditional mud stove only reduced fuel use by 36% and brewing time by 23% (29 min) compared to the three-stone fire. It also increased CO emissions by 14%, while modestly reducing PM emissions. Both PM2.5, and PM10 were reduced by 18%.

The paper summarized that, the Mirt areke stove has significantly better thermal performance and lower emissions. And suggested that, disseminating the Mirt areke stove with its mold for producers in the country will save a large amount of fuel and decreases indoor air pollution for those who are currently engaged in the distillation of areke around the country. (Assefa & Adem, 2022), which highlights the pressing nature of the issue, calling for accelerated measures to address it.

The GTZ-SUN project

The GTZ-SUN (The German Development Cooperation) project has developed an improved areke distilling stove that is designed to reduce indoor air pollution and specific fuel consumption. The stove, made of bricks, has a number of features that make it more efficient than traditional stoves, including separate inlets for the fuel and air, a closed combustion chamber, a chimney, and a heat-retention jacket. The closed combustion chamber helps to trap heat and prevent it from escaping up the chimney, while the chimney helps to draw smoke and fumes away from the user. The heat-retention jacket helps to keep the stove warm and efficient, even when it is not in use.

Figure 2.6: GTZ-SUN brick stoves (Gezahegne, 2008)

Gezahegne (2008) studied air pollutant emissions and stove performance by comparing traditional stoves with GTZ-SUN improved distilling stoves. The findings revealed significant reductions in air pollutant emissions with the improved stoves. Over the entire 12+

hour distillation process, average CO levels decreased by 52.6% (from 49.81 to 23.61 ppm), while average PM2.5 levels dropped by 57% (from 1.22 to 0.53 mg/m³). During the more intense first 8 hours of distillation, the improved stoves reduced average CO by 53.2% (from 52.25 to 24.44 ppm) and average PM2.5 by 63.3% (from 1.27 to 0.47 mg/m³).

Even though these sizable reductions in emissions of harmful pollutants like CO and PM2.5 demonstrate the meaningful benefits of the improved stove compared to traditional stove, the CO levels are still above the limits set in WHO AQGs standards (Gezahegne, 2008).

In terms of stove performance, the study found that fuelwood consumption decreased slightly, by only 1.6%, from 56.68 kg with traditional stoves to 55.79 kg with improved stoves per day for a complete distillation cycle. However, the improved stoves significantly reduced the total distillation time, cutting it by an average of 22%, from 760 minutes to 597 minutes.

The author highlights the importance of controlling the temperature as it is one of the main factors greatly influencing the end product. The task of controlling the fire is relatively easier with the traditional stoves than with the improved ones. (Gezahegne, 2008) The study suggested that Further optimization of the stove design and increased user experience may lead to additional gains in thermal efficiency of the stoves.

2.2.2 Biogas Stove for Areke Distillation

Demissie et al. (2016) designed, fabricated and tested a biogas stove specifically for areke distillation in Ethiopia, aiming to reduce dependence on fuelwood. The stove has a 2.5mm injector nozzle, 17mm throat diameter, 210mm mixing tube length, 3mm/62 burner ports, and 130mm burner manifold diameter based on analytical design calculations to meet on areke distillation energy requirement of 1.547kW.

Figure 2.7: Assembled biogas stove (Demissie et al., 2016)

Stove performance was evaluated via water boiling tests and a controlled cooking test distilling areke. The water boiling test achieved up to 54.8% efficiency on 8 liters of water at high flame intensity, and 43.6% on 10 liters at lower flame intensity - a significant improvement over traditional biomass stoves limited to 10% efficiency.

During tests comparing a biogas stove to a firewood stove for distilling alcohol, the biogas stove took nearly half the time to distill the same amount. Based on an experienced distiller's opinion, two rounds of distilling with the biogas stove took approximately the same amount of time as one round with the firewood stove. This demonstrated the biogas stove provided a reduction in distilling time.

The improved stove consumed only 0.998 m3 of biogas on average to distill one liter of areke. An economic analysis found a positive net present value and estimated payback period between 3-4 years to adopt biogas stoves and digesters.

The study concluded that despite high upfront costs, using biogas for areke distillation could be an environmentally and economically viable option.

2.2.3 Performance Comparison of Biomass and Biogas Stoves

The following table provides a comparative analysis of biomass-based and biogas-based stoves for areke distillation. The comparison focuses on key performance indicators, including thermal efficiency, distillation time. The objective is to highlight the strengths and limitations of each stove type based on data extracted from the literatures presented.

Table 2.1: Performance comparison for biomass and biogas areke distillation stoves.

Metrics	**Berkeley-Darfur Stove**	**Mirt stove**	**GTZ-SUN stove**	**Biogas stove**
Thermal Efficiency	14.4% increase (from 11.2 % to 25.6%)	-	-	54.8% on high flame (8L) and 43.6% on low flame intensity (10L)
Fuel Efficiency (SFC)	45% reduction (from 2.65 to 1.322 g/g)	51% reduction	1.6% reduction	-
Distillation time	50 % reduction (2 – 1 hr.) (8L)	52 % reduction (1 hr 4 min)	22% reduction	50% reduction (distiller's opinion)
Pollution	-	29% CO & 52% PM10 & PM2.5 reduction	53.8% CO & 59% PM2.5 reduction	-

Drawbacks	Complex design, High cost, and emission	less durable, and emission	Temperature control difficulty, emission above WHO limits and big, immobile, and bulky	Very high initial invesment (3-4y PBP), technical Complexity, and availability of Feedstock

2.2.4 Solar-Powered Solutions for Areke Distillation

Researchers have investigated using solar energy as the thermal energy source for areke distillation processes. Two different solar concentrator setups were tested - one method involved directly heating the distillation pot using solar energy, while the other used an indirect heating mechanism where the solar energy did not directly heat the pot.

Direct solar distillation

Kassa (2015) presents the design and testing of a direct parabolic solar dish areke distillation system. This arrangement heats the clay-pot (containing the mash) directly by the solar concentrator. A 1.2m diameter dish with a 0.3m focal length was used. An absorber pot made of clay with a 0.071 m^2 surface area and 4-liter capacity was positioned directly at the focal point.

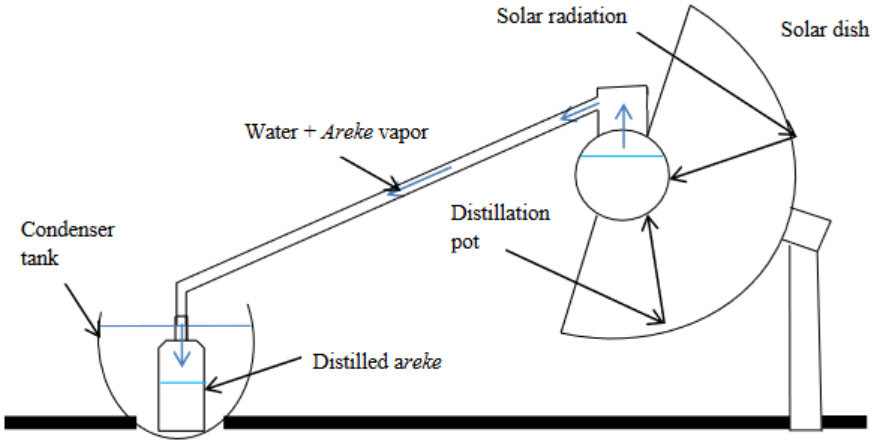

Figure 2.8: Schematic diagram of the experimental setup (Kassa, 2015)

In tests using 2.5 liters of areke mash (difdif), the system reached the ethanol boiling point of 70.4°C in 1 hour 15 minutes and it produced approximately 0.25 liters of areke with 44% alcohol content in 3 hours. This compares to 0.33 liters expected from traditional methods (Traditional distillation uses 8 liters of difedif to produce 1 liter of 40-45% alcohol content areke in 2.5-3 hours.)

By comparison the solar system using 2.5 liters of mash produced less areke (0.25 liters) when compared to 0.33 liters expected from traditional methods in approximately the same time, Meaning the solar system produced less areke than what is possible by the traditional system. The instantaneous thermal efficiency in this test only ranged from 35-38%.

Despite this the author draws positive conclusions given (the author says) this was an initial prototype test concluding further testing, optimization, and larger scale implementation will boot these shortcomings. The results demonstrate the solar dish system successfully produced areke.

Indirect solar Distillation

Getachew et al. (2022), has investigated an experimental performance analysis of using a solar parabolic dish concentrator for areke distillation in an indirect heating system.

In this experimental setup, a solar concentrator which uses an indirect heating setup with a 0.9m diameter parabolic dish reflector heats a water-filled receiver, causing the water to vaporize. The resulting water vapor circulates to a clay pot through natural or density-driven circulation due to elevation difference. The clay pot, enclosed by a helical copper tube, facilitates efficient heat transfer to the mash, effectively inducing boiling. Subsequently, ethanol (areke vapor) evaporates condenses, and is collected at the opposite end.

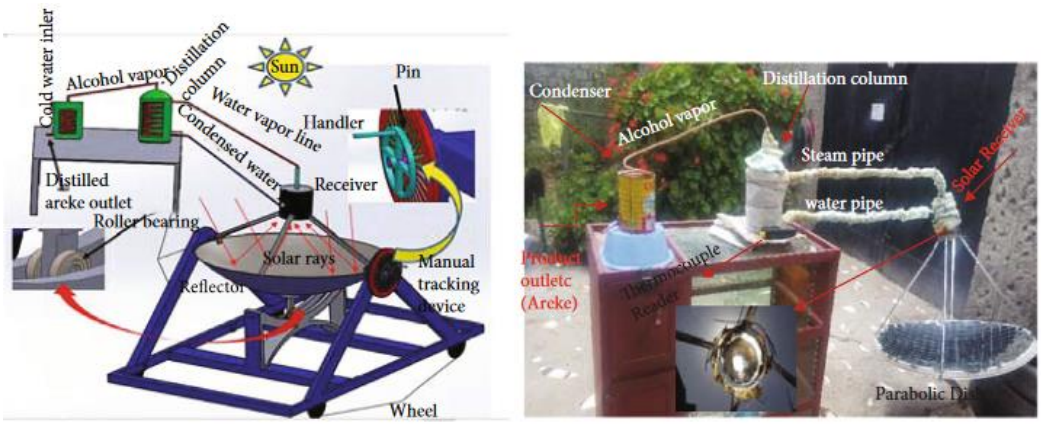

Figure 2.9: Schematic diagram and experimental setup of solar Distillation system. (Getachew et al., 2022)

Results showed the system increased areke distillation efficiency by 1.67% over the baseline firewood method. The receiver attained temperatures exceeding 300°C with a thermal efficiency of 54.6%. From an input of 2 liters of areke mash, one cycle of distillation with 0.2 liters of areke with 45% ethanol content could be produced in 65 minutes (0.185 l/h).

Heat losses were analyzed - the receiver had the most losses due to high temperatures and exposure.

The author generalized, the solar system demonstrates an insignificant 1.67% efficiency improvement over the firewood method but most of all it eliminates excessive biomass use and indoor pollution. The author recommends disseminating this technology to benefit rural households engaged in areke production by saving costs and reducing health impacts.

2.2.5 Performance Comparison of Solar Distillation Stoves

Table 2.2 Performance comparison for solar areke distillation stoves.

Metrics	**Indirect Solar Distillation (Getachew, Bekele and Pandey, 2022)**	**Direct Solar Distillation (Kassa, 2015)**
Efficiency (thermal)	1.67% increase over firewood (54.6% (receiver))	-
Distillation time	2L difdif take 65 min, to produce 0.2L of areke	2.5L of difdif in 3 hrs. to produce 0.25L of areke
Pollution	No	No
Drawbacks	High receiver heat loss, and complex	Inconsistent temperature distribution
	Hard to control temperature, requires further optimization, low production rate compared to traditional, and distillation restricted to only daytime.	

2.2.6 Exploring Electrical Distillation Systems

Modernizing Feni Distillation with Induction Stove: Indian traditional spirit

In searching for traditional alcoholic beverages produced elsewhere in the world that bear similarities to Ethiopia's areke, the *feni* liquor distilled in India was discovered. One study in particular examined the potential to adapt induction heating technology for modernizing feni's traditional distillation process with a satisfying result.

Feni, a traditional clear spirit from India, shares similarities with Ethiopia's areke in their distillation processes. Both involve heating fermented fruit juices to extract and condense ethanol vapor into liquor. The raw ingredients differ, with Feni originating from cashew fruit or coconut palm sap, while areke comes from enset, cereal grains, or gesho leaves. Though most Feni producers have shifted towards using copper pots, both traditionally use clay pots for boiling the fermented juice, and both traditionally use biomass fuels like

firewood to heat the fermented liquors. The basic arrangement of distillation pot, condenser tube leading to a collecting vessel is analogous. Cooling is achieved in both through collecting vessel sank into a water tank. And to seal gaps making the setup airtight, feni producers use mud from fine sand which is similar in application to the wheat dough areke distillers use. So, while raw ingredients differ between the Indian Feni and Ethiopian areke, their small-scale distillation processes employ comparable equipment and techniques.

Figure 2.10: Distillation setup for Feni using induction stove (Jalmi et al., 2018)

Jalmi et al. (2018) designed and prototyped a distillation apparatus shown in figure 2.10, with a capacity of approximately 8 liters for distilling cashew fruit or coconut palm juice feni mash. The system incorporates a condenser made of a helical copper tube, which is submerged in a circulating water tank to facilitate efficient cooling. The stainless-steel pot is heated by a highly efficient 2kW induction cooker with 80-84% efficiency.

In a test distilling 8 liters of fermented cashew juice using the induction heater at its 2kW setting, the system yielded 1,440 ml of distillate over a 170-minute period. An additional trial involved varying the power input to maintain a constant 80-90°C temperature in order to improve alcohol concentration in the distillate. This test produced 800 ml of distillate over 170 minutes.

Despite the lower alcohol concentrations of the distillate 15% compared to 16-17% of traditional, this 8-liter prototype unit achieved faster overall distillate production rates over shorter periods of time. And using induction stove the efficiency of the distillation process was improved substantially and the pollution emanating from using biomass was eliminated.

The paper suggested that the lack of insulation resulted in some heat losses from the system, so further optimizations like integrated induction heating coils could enhance the efficiency and performance.

Despite its hefty price the paper generalized that, the quantitative results clearly demonstrate the potential for this type of still to modernize and improve the productivity of traditional liquor production processes.

An electric still for the lab

Allen and Jacobs (1912) describes an externally-heated electric still adapted for difficult laboratory distillations. The still uses a custom electric heater made of heat-resistant materials like magnesia and asbestos, enclosing the distillation flask. Nickel-chromium alloy wires embedded in the heater allow precise control of temperatures up to 325°C under vacuum. This still was used to distill complex mixtures like crude oil containing up to 33% water and suspended solids.

The paper discusses reasons for using the electric heater instead of gas heating to be:

- Fluctuating flame temperature causes irregular distillation rates
- Uneven heating causes strains and cracks in the glassware
- Local overheating causes decomposition of compounds
- Upper parts of flask are not directly heated, causing vapors to drip back and slow distillation

After testing this apparatus, the key advantages of electric heating are then are outlined to be - provides steady, uniform heating not subject to fluctuations and Temperature control is always under the operator's control which improved repeatable results compared to gas heating.

2.2.7 Commercial Areke Distillation Products

In cities such as Arsi Negele and Debre Berhan, local manufacturers have introduced larger steel distillation stills capable of processing greater volumes of mash at once, which are currently being produced and sold, albeit in very limited quantities. These distilling setups, which operate using biomass fuel, are constructed by local manufacturers with little to no research backing their design. However, producers report that areke distilled in these stills lacks the aroma and taste quality of traditionally processed products. Furthermore, the steel stills require a constant stirring mechanism throughout the distillation process to prevent

scorching, adding to their cost and making them unaffordable for most distillers. Although these innovations signify progress, they have yet to achieve the product quality and consistency preferred by consumers and producers.

2.3 Temperature Controllers

One key advantage of utilizing electrical energy for areke distillation is the ease with which temperature control can be automated with relatively inexpensive temperature controllers. Temperature controllers are devices used to maintain the temperature of an object or environment within a specified range. They receive input from a temperature sensor, compare it to the desired setpoint, and provide an output to control the heating or cooling elements accordingly (Indmall Automation, 2024).

Digital temperature controllers are used in a variety of applications, ranging from industrial processes to consumer products. For example, industrial applications such as HVAC systems, food processing, and chemical processing often require precise temperature control in order to ensure quality and safety. On the other hand, consumer products such as refrigerator air conditioners and waer heaters also rely on temperature controllers to maintain a comfortable environment (OMEGA Engineering, n.d.-c).

2.3.1 Types of Temperature Controllers

The primary types of temperature controllers include On/Off controllers, Proportional controllers, and PID controllers. Each type of controller has its unique characteristics and is suited for different applications, ranging from simple home appliances to complex industrial systems (Indmall Automation, 2024).

On-Off Controllers

These are the simplest form of temperature control, switching the output fully on or off based on whether the temperature is above or below a setpoint. n on-off controller will switch the output only when the temperature crosses the setpoint. For heating control, the output is on when the temperature is below the setpoint, and off above setpoint. They are suitable for applications where precision is not critical. Since the temperature crosses the setpoint to change the output state, the process temperature will be cycling continually, going from below setpoint to above, and back below (OEM Heaters, n.d.).

Proportional Controllers

Proportional controls are designed to eliminate the cycling associated with on-off control. A proportional controller decreases the average power being supplied to the heater as the temperature approaches setpoint. This has the effect of slowing down the heater, so that it will not overshoot the setpoint but will approach the setpoint and maintain a stable temperature (OMEGA Engineering, n.d.-b).

PID Controllers

According to feng (2022), GoSwitchgear (2022) and New England Temperature Solutions (2023) Proportional-Integral-Derivative (PID) controllers are the most advanced type, combining proportional, integral, and derivative control actions to provide precise and stable temperature regulation. The proportional control looks at the temperature difference between the desired level and the actual measurement. It applies an output based on how big the difference is. If the difference is big, the controller applies a larger output. The integral control adds up the differences between the desired temperature and the actual measurement over time. This helps get rid of ongoing errors and adjusts the output accordingly. The derivative control predicts how the temperature will change based on how fast the error is changing. It helps keep the control process stable by reducing overshooting and adjusting the output based on how quickly the temperature is changing.

2.3.2 Components of PID Temperature Controller System

According to Instrumart, (n.d.) and Sinny (2024a, 2024b), in a PID temperature control system, the primary components include sensors, the PID controller, and actuators such as solid-state relays (SSRs). Sensors, like thermocouples or RTDs, measure the current temperature and provide real-time data to the PID controller. Both quality and placement being of the sensors plays great significance in regards to PID controller performance. The controller processes this data by calculating the error between the desired setpoint and the measured temperature, applying proportional, integral, and derivative calculations to determine the necessary corrective action. Actuators, such as SSRs, receive signals from the controller to adjust the process temperature accordingly. SSRs are electronic switching devices that control the power supplied to heating or cooling elements, enabling precise and rapid adjustments without the mechanical wear associated with traditional electromechanical relays. This coordinated operation ensures accurate and stable temperature control in various simple to industrial applications.

Together, these components work to automatically regulate temperature inside the pot and record data as follows: The desired temperature is set on the digital panel meter. Thermocouples continuously measure the actual temperature within the distillation system and sends the information to the PID controller and the data logger. The data logger reader interprets, records and stores the temperature data for comprehensive monitoring and analysis. The PID controller compares the set point (desired temperature) with the actual temperature. If the actual temperature deviates, the PID controller adjusts the heating element to bring it back to the set point. This feedback loop ensures the temperature inside the pot stays within the desired range, providing precise and predictable heating conditions.

2.3.3 Data Loggers

Data loggers are compact, battery-powered electronic devices designed to monitor and record data over time, making them invaluable tools in temperature monitoring applications. They typically consist of a microprocessor, internal memory for data storage, and sensors that collect data from the environment. When measuring temperature, a data logger interfaces with temperature sensors such as thermocouples or RTDs, capturing temperature readings at predefined intervals. The recorded data is stored in non-volatile memory, allowing for long-term monitoring without the need for continuous human intervention. Data loggers can operate as stand-alone devices or connect to computers for data analysis, providing insights into temperature trends and fluctuations over time (dewesoft, n.d.; OMEGA Engineering, n.d.-a).

2.4 Stove Efficiency: A Comparative Review

To assess the performance of the novel electric areke stove prototype, a comprehensive literature review was conducted to compile thermal efficiency values for diverse stove types. The findings are summarized in the following table.

Table 2.3: Thermal Efficiency of Various Stove Types

Stove Type	Thermal Efficiency	Measure Protocol	Reference
Traditional Open fire stove (Three stone fire)	9.55% Cold Start; 14.6% Hot Start	WBT	(Ikpambese et al., 2014)
	5-20%		(Koffi et al., 2014)
Traditional mud stove	14%	Possibly WBT	(Tesfay et al., 2024)
	15.4%	WBT	(Someswararao et al., 2012)
Mirt stove	16%	WBT	(Tesfay et al., 2024)
	22%	-	(Dagnew & Rzehak, 2015)
	18-23%	-	(GIZ Ethiopia, 2011)
Biogas areke Stove	54.8% (higher flame intensity); 43.6% (lower flame intensity)	WBT	(Demissie et al., 2016)
Resistance coil stove	49.1 %	WBT	(Muluken, 2020)
	51% Cold Start; 58.3% Hot Start	WBT	(Ikpambese et al., 2014)
	32.43% (300w)	WBT cold start	(Aisyah et al., 2021)
	42.02% (600w)	WBT cold start	(Aisyah et al., 2021)
	39.3 – 51.8%	WBT cold	(Karunanithy & Shafer, 2016)
	50-60%	-	(Chheti et al., 2015)
	59.4	-	(Adria & Bethge, n.d.)
Induction stove	81.78% (1800w)	WBT cold start	(Aisyah et al., 2021)
	70%-81	WBT cold start	(Karunanithy & Shafer, 2016)
	80.2%	-	(Adria & Bethge, n.d.)

Chapter 3

Design

3.1 Design Requirements and Considerations

The design process commenced with a comprehensive analysis of areke distillers' needs, observations of small-scale distillation setups, and an evaluation of best design practices. This foundational work informed the development of a set of design requirements and considerations to guide the project. These criteria ensure that the final design meets functional, economic, and environmental objectives.

Design Requirements:

1. Product Quality: The taste and aroma of the final areke product must closely match that produced by traditional methods.
2. Heating Efficiency: The stove must efficiently heat and maintain the temperatures required for the distillation process.
3. Safety: The system must incorporate appropriate thermal insulation and temperature controls to ensure safe operation.
4. Environmental Impact: The design should significantly reduce or eliminate pollution compared to traditional wood-fired stoves.

Design Considerations:

1. Power Consumption: The stove’s power consumption must not exceed 6.6 kW, which is the typical capacity of common Ethiopian electric meters.
2. Affordability: The price of the stove should be affordable for small-scale areke producers to encourage widespread adoption.
3. Local Materials: The design should incorporate locally available materials to reduce costs and improve maintainability.
4. Ease of Manufacture: The design should be simple and easy to manufacture, enabling local manufacturers to produce it without requiring specialized skills.

5. Compatibility with Traditional Practices: Where feasible, the design should allow the use of existing components from traditional distillation setups to facilitate a seamless transition and reduce entry costs.

3.2 Concept Generation and Selection.

Commercial and DIY distillation stills worldwide were studied to identify key variables that contribute to their design and differentiation. Three critical variables were identified: (1) the materials used for components such as the pot and condenser tube, (2) the type and placement of the heating element, and (3) the condensation or cooling system employed. These variables informed the development of design concepts aligned with the project's objectives and requirements.

Most commercial distillation stills are constructed from copper and stainless steel, which contribute to their high cost. To address the design requirement of cost reduction, the use of locally available materials was prioritized. Additionally, to facilitate a seamless transition from traditional distillation methods, components such as the pot and potlid were directly adopted from traditional setups. These components are made of clay, a material that is both affordable and readily available.

For the condensation tube, two primary condensation approaches were considered: Modified Traditional bamboo tube and a modernized condenser that is constructed from copper for efficient heat exchange. Both of which will be explained later.

Heating elements were another critical consideration. Immersion heating elements and coil-type heating elements, typically positioned at the bottom of the pot, are the most common types observed. Coil heaters are typically placed at the bottom of the pot, while immersion heaters require a specially designed hole in the pot for proper installation. Incorporating immersion heaters introduces additional complexity to the manufacturing process, as pots traditionally used in distillation cannot be directly sourced from the market and repurposed. Instead, they must be custom-made to accommodate this type of heating element. Both options were examined and considered for concept development.

3.2.1 Concept Generation

Based on the above decisions and in alignment with the design requirements and considerations, three concepts were developed.

Concept 1 utilizes a coil-type heating element, strategically placed within a groove in a clay bowl to promote even heat distribution. The clay pot is housed within this bowl, which is supported by a metal encasing to ensure structural integrity. Thermal insulation is implemented between the bowl and the metal encasing to minimize heat loss. A traditional bamboo tube connects the pot to an aluminum flask, which is part of the water bath condenser. The bamboo tube is modified by incorporating a shell-and-tube design, with the shell constructed from low-cost PVC.

The shell-and-tube design is added to study whether bamboo, a cheap and locally available material, can effectively function as a condenser tube and potentially replace the water bath condenser entirely. Given that the shell-and-tube design with a small pump is more efficient than the water bath condenser, this modification aims to evaluate its performance in terms of heat transfer efficiency, as well as its impact on the taste and aroma of the final product. If bamboo alone cannot fully replace the water bath condenser, the modified shell-and-tube design is expected to assist in handling the condensation load, particularly taking full responsibility during periods of low distillate flow rate. Additionally, this design has the advantage of preventing the bamboo from overheating, ensuring safer and more efficient operation.

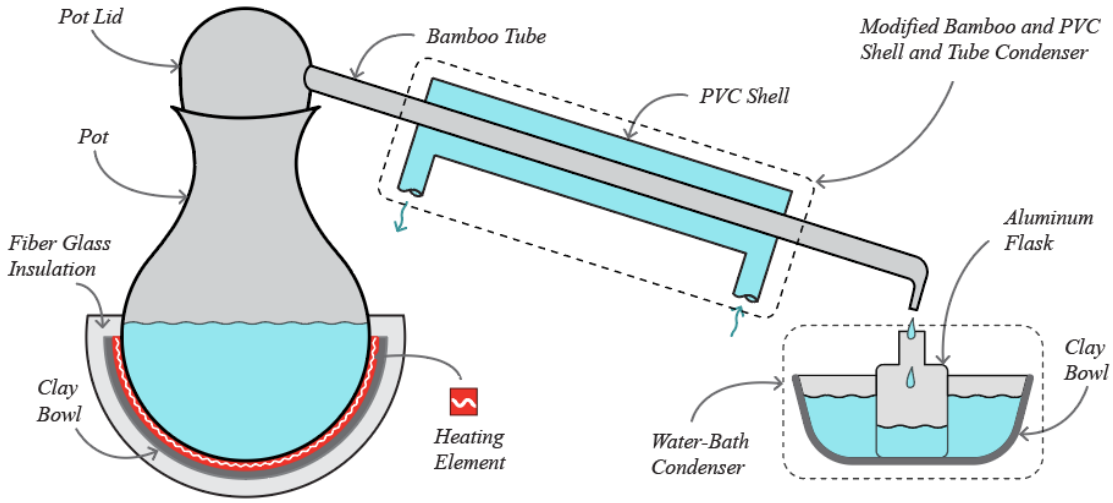

Figure 3.1: Concept 1

Concept 2 employs an immersion heater installed through an opening in the clay pot. The pot is insulated to reduce heat loss. This concept utilizes a modernized approach for condensation, incorporating an efficient shell-and-tube heat exchanger constructed from copper powered by a small pump, negating the need for a water bath condenser. This design also eliminates the need for an aluminum flask for product collection, allowing a any

collector like glass bottle to be used. As a result, the overall setup is simplified, requires a smaller footprint, and operates with greater efficiency.

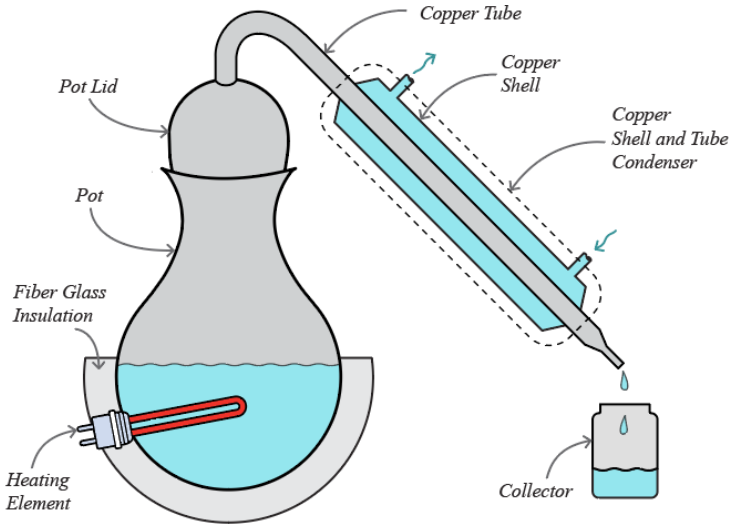

Figure 3.2: Concept 2

Concept 3 retains the immersion heater, pot, and insulation setup but replaces the shell-and-tube condenser with a copper coil condenser. This condenser can work with or without a pump, offering manual filling as an option. By avoiding the need for a pump, the system becomes cheaper and less complicated, while still delivering efficient performance.

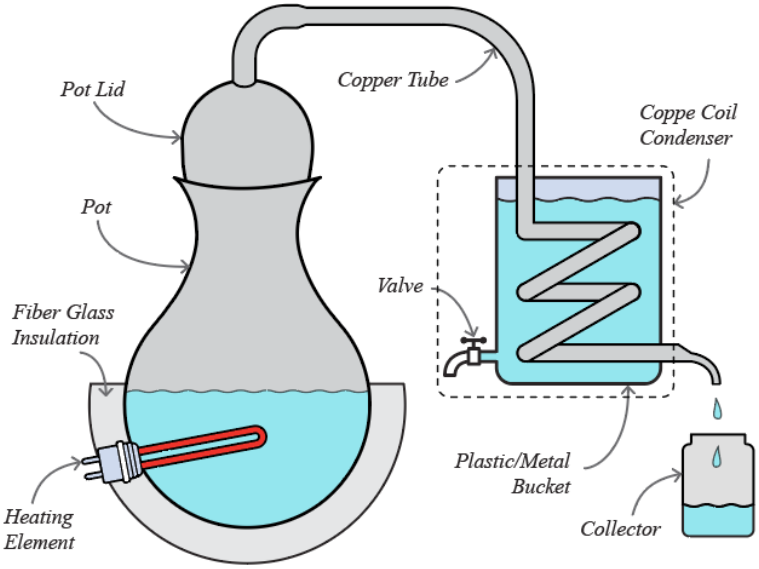

Figure 3.3: Concept 3

3.2.2 Concept Screening and Selection

The above concepts were evaluated against the key design requirements and considerations using a screening table below.

Table 3.1: Concept screening table.

Criteria	Concept 1, (C1)	Concept 2, (C2)	Concept 3, (C3)	Score (1-5)		
				C1	C2	C3
Cost	Lower material costs (clay, bamboo, PVC); Lower manufacturing complexity	Higher material costs (copper, immersion heater); Higher manufacturing complexity (pot modification and shell and tube construction)	Relatively less material and manufacturing cost than concept 2	5	2	3
Manufacturability	Easier to fabricate using local skills and less complex assembly	Requires specialized skills for immersion heater installation and copper condenser manufacturing; Requires specialized pot manufacturing	Requires specialized skill for manufacturing but relatively easier than concept 2	5	2	3
Maintainability / Repairability	Relatively harder to replace the heating element; Easier to clean and maintain the water bath condenser; Cheaper to replace condensation components like bamboo, aluminum flask.	Easier to replace the heating element; Harder to clean and maintain the shell and tube condenser; relatively harder and expensive to replace condensation components than concept 3.	Easier to replace the heating element; Harder to clean and maintain the shell and tube condenser; harder and expensive to replace condensation components.	4	3	2.5
Component failure and cost of replacement	Heating element Less prone to failure and less cost of replacing it.; Less durable but cheap bamboo construction	Higher risk of immersion heater failure and high cost of replacement; High durability of copper condenser;		4	2	2
Compatibility with Traditional Practices	Reuses traditional clay pot and lid; Incorporates familiar water bath condenser	Requires modification of traditional pot; Eliminates familiar water bath condenser		5	2	2
Heat Distribution/Surface Load	More uniform heat distribution due to controlled coil placement; Lower risk of scorching the mash	Potential for localized overheating due to high heat concentration from the immersion heater; Higher risk of scorching the mash if not properly positioned		4	3	3
Efficiency	Potential for lower efficiency due to heat loss through the clay bowl and insulation	Potentially higher efficiency due to direct heat transfer to the mash and efficient condenser.	Potentially higher efficiency due to direct heat transfer to the mash but slightly lower efficiency than concept 2 due to condenser.	3	5	4
Adoption Potential	Higher potential for adoption due to lower cost, ease of integration with traditional practices, and familiarity with existing components	Lower potential for immediate adoption due to higher cost, disruption of traditional practices, and requirement for specialized skills		5	2	2
			Total Score	35	21	21.5

Concept 1 scores highly in cost, manufacturability, compatibility with traditional practices, and adoption potential. It is the preferred choice mainly due to its affordability, ease of fabrication, and alignment with traditional methods. Concept 2 and 3, while they offer higher efficiency and easier maintenance for the heating element, these advantages are outweighed by their higher cost and complexity of condenser and heating element installation.

To further explore the trade-offs, a concept 2 style copper condenser will be designed to determine if the performance improvements justify the increased cost. This analysis will ensure that the final design optimally balances cost, performance, and ease of adoption.

3.3 Material Selection

The primary considerations for material selection are cost-effectiveness and minimizing deviations from traditional distillation systems to ensure a high adoption rate among areke producers.

3.3.1 Insulation Material

For the insulation material, after conducting comparative analysis of locally available insulation materials as tabulated in table 3.2, fiberglass was selected as the insulation material due to its optimal balance of low thermal conductivity, moderate cost, local availability, and adequate operating temperature range, while also minimizing health risks compared to alternative materials. Additionally, Tsegay (2011) employed fiberglass as insulation in a study on a solar-powered *injera* baking pan and achieved successful results, further validating its suitability for this project. The following table lists commonly available local materials being considered for insulation, along with their key properties.

Table 3.2: Comparison of Locally Available Insulation Materials.

Metric	**Fiberglass/Glass giber**	**Rock wool**	**Asbestos (loosely packed)**	**Wood Ash**
Thermal Conductivity (W/(m·K))	0.033 - 0.04	0.033 - 0.045	0.154	0.048 - 0.055
Density (kg/m³)	24 - 112	30 - 180	520	2970
Operating Temperature (°C)	-4 - 350	-100 - 750	Up to 1200	Up to 500 and above
Toxicity	Low (irritant)	Low (irritant)	High (carcinogenic)	Very Low

Cost	Moderately expensive	Moderate	Cheap	Very cheap
Local Availability	Widely available (imported)	Rarely Available (imported)	Widely available	Readily available (locally)
Reference	(Hung Anh & Pásztory, 2021)		(Edge & LLC, 2024; Testbook Edu Solutions Pvt. Ltd., 2023)	(Cetiner & Shea, 2018; Vu et al., 2019)

3.3.2 Distillation Pot and Potlid

As outlined in the concept generation section, to meet the design requirements of cost reduction, utilization of locally available materials, and ensuring a smooth transition from traditional distillation methods, components such as the pot and pot lid were directly sourced from traditional setups. These components, crafted from clay, offer an affordable and readily available material solution.

Significant deviations from the traditional design could hinder the adoption rate of the new stove. Historical examples, such as the slow adoption of modern injera baking stoves, illustrate the challenges of introducing innovations that differ significantly from traditional practices.

Additionally, the impact of clay pots on the taste and aroma of areke is not yet fully understood. Introducing new materials could complicate the process by adding too many variables, making it difficult to identify areas for improvement in the stove's performance.

3.3.3 Condenser Tube Material

Traditional distillation typically employs a water bath condenser as the primary condensation unit, with a bamboo tube serving as a connector between the distillation pot and the water bath condenser. The condenser setup consists of an aluminum flask acting as both the collector and condenser, submerged in a water bath contained within a large bowl.

As outlined in the concept generation section, a decision was made to upgrade the bamboo tube to a shell-and-tube condenser for evaluation as a potential condenser tube material. The primary role of the condenser tube is to effectively transfer heat from the vaporized areke spirit, ensuring efficient phase transition from gas to liquid. Therefore, the material's thermal conductivity is critical to the overall performance of the distillation process. Bamboo, however, has a significantly lower thermal conductivity of 0.39-0.43 W/m·K (Shah et

al., 2019), compared to widely used materials such as copper (110-401 W/m·K) and aluminum alloys (127-237 W/m·K) (Dewitt et al., 2017), resulting in a less efficient condensation process.

For this reason, the design of a copper shell and tube condenser will be performed. Copper is widely recognized in distillation practices for its superior performance. However, while copper offers high thermal conductivity and proven effectiveness, its cost is considerably higher. This study, by designing a copper condenser, aims to assess whether the performance improvements offered by a copper condenser tube justify its additional cost. Additionally, the adoption of a copper condenser would eliminate the need for a water bath condenser, potentially simplifying the system in addition to its performance gain.

3.3.4 Heating Element Material

The selection of an appropriate heating element material was based on a comparative review of the most common resistance heating alloys. While several options exist (Molybdenum Disilicide (MoSi2), Silicon Carbide (SiC), etc.), the primary contenders for this application were Nickel-Chromium (Nichrome) and Iron-Chromium-Aluminum (FeCrAl or Kanthal) alloys. While FeCrAl alloys offer higher maximum service temperatures, Nichrome's operating temperature of up to 1200°C is more than sufficient for the thermal requirements of *areke* distillation. More importantly, Nichrome exhibits superior mechanical strength and formability (ductility) at high temperatures, making more durable and easier to form into coils without becoming brittle. It also exhibits strong corrosion resistance, which contributes to a longer service life (Heanjia Super-Metals Co., Ltd, 2015; “Heating Element,” 2025; *Types and Properties of Heating Elements*, 2025; Thermcraft, Inc., 2016).

Ultimately, the decision was driven by the project's core design considerations. As the most widely used and readily available resistance wire in the local Ethiopian market, Nichrome was the most cost-effective and practical choice. This ensures the stove is not only functional but also easily maintainable and replicable by local producers. For these reasons, Nichrome 80/20 was selected as the optimal material.

Nichrome is a nickel-chromium alloy with non-magnetic properties. The alloy also sometimes includes some parts of iron as its constituents. The Nickel-Chrome alloys have been in use back to 1900 and these have been successfully employed in heating element applications. A well-known alloy combines 80% Nickel and 20% Chromium. This alloy is

known as Nichrome 80/20. There are however other alloy compositions which combine nickel, chromium and iron in different other ratios. (Heanjia Super-Metals Co., Ltd, 2015).

3.4 Pot Sizing and Capacity

The pots commonly used in traditional distillation have a capacity of 12–14 liters. To ensure ease of comparison and maintain consistency with traditional practices, a pot of the same capacity was selected for this project. Traditional pot on average has an internal radius ($r_{i,p}$) of 16 cm, a height of 50 cm, and a thickness (t) of 1.2 cm. According to Cengel & Ghajar (2019), the thermal conductivity of burned clay is 1 W/m.K.

Figure 3.4: Traditional clay distillation pot.

3.5 Thermal Analysis: Initial Heating Phase

The areke distillation process, as observed from traditional distillation methods, naturally progresses through two phases: the initial heating phase and the distillation phase. In the heating phase the fermented mash is loaded into the pot and heated at a high-power setting to raise its temperature from ambient to the desired distillation temperature as quickly as possible, without causing violent boiling or bubbling. During this phase, the mash inside the pot undergoes constant stirring to ensure even thermal exposure. This phase continues until visible alcohol evaporation commences through the pot's opening. The temperature of the mash changes over time, making this phase a transient heat transfer process.

The goal of the thermal analysis is to determine the power required to design the heating element. To achieve this, it is essential to identify which phase demands more power, as the heating element's power requirement is determined by the phase with the highest demand. Therefore, power requirements of both phases will be calculated and compared. This section focuses on the power requirement for the initial heating phase.

3.5.1 Power Requirement to Heat Mash

The power requirements of the mash can be estimated using the following equation (Cengel & Ghajar, 2019). The equation calculates the total sensible heat energy required to raise the temperature of the mash from ambient to the distillation temperature.

$$Q = mc_p\Delta T \tag{3.1}$$

Where Q is the amount of heat energy needed to heat up the mash(kJ), m is the mass of the mash (kg), c_p is the specific heat at constant pressure (kJ/kg°C), and ΔT is the temperature change of the system (°C).

The composition and properties of areke mash exhibit considerable variation across different regions of the country and can even differ within the same locality. Consequently, precise average values for specific heat capacity of the mash are not currently available. Additionally, there is no existing research or literature from which such data can be sourced.

Based on the conducted survey, a 262 kg areke mash (*difdif*) typically consists of 30 kg of germinated wheat, 2 kg of gesho (Rhamnus prinoides), 170 liters of water, and 60 kg of corn. The specific heat capacities of wheat, water, and corn are reported as 1.0792 to 5.5336 kJ/kg°C (Cao, Y et al., 2010), 4.2 kJ/kg°C, and 1.4868 to 2.4224 kJ/kg°C (İNCE et al., 2008), respectively. This wide range suggests that theoretical calculations of the specific heat capacity of the mash would yield significant variability.

However, given that water constitutes the majority of the mash and has the highest specific heat capacity, it is reasonable to assume that the specific heat capacity of the mixture will be closer to that of water. Therefore, given that $m = 12\ kg$ (obtained by measurement), $c_p = 4.2$ kJ/kg°C and $\Delta T = 60$°C (from 20°C, room temperature, to 80°C, where 80°C is the average temperature at which distillation starts in traditional areke production), the total sensible heat Q Can be calculated as $3024\ kJ$.

To determine the power requirement, the total heat energy, is divided by the desired heating time:

$$P_m = \frac{Q}{t} \tag{3.2}$$

Where P is power (W) and t is the desired time (s). Traditional distillation, based on observations, typically takes 45 minutes to 1 hour to reach the distillation temperature.

Assuming this time can be improved with efficient heating, the time (t) can be reduced and assumed to be 30 minutes (1800 seconds). Given $Q = 3024\ kJ$ and $t = 1800\ s,\ P_m = 1.68\ kW$.

3.5.2 Heat Loss Through Mash Surface

The heat loss through the mash surface due to convection is a significant factor during the heating phase. This loss happens during the heating phase when the mash is occasionally stirred and exposed to the ambient environment. This convective heat loss increases with the temperature of the mash, necessitating a transient heat analysis to accurately model the heat transfer dynamics throughout the heating process. However, since the heating element must be designed to accommodate the maximum heat loss, which occurs when the mash reaches its distillation temperature of 80°C, the power rating of the heating element should be based on this peak heat loss scenario, as the heating element must be capable of supplying sufficient power to counterbalance this peak loss. Consequently, the problem can be approximated as a steady-state heat transfer process at this critical temperature. Designing the heating system to meet this maximum thermal demand ensures operational reliability during the distillation process.

To calculate the heat loss through the mash surface due to convection, we use Newton's Law of Cooling (Cengel & Ghajar, 2019):

$$\dot{Q}_{conv} = hA(T_m - T_\infty) \tag{3.3}$$

Where $\dot{Q}_{conv}$ is the heat loss (W), h is the convective heat transfer coefficient (W/m²K), A is the surface area (m²), T_m is the temperature of the mash (°C), and T_∞ is the ambient temperature (°C). An ambient temperature (T_∞) of 20°C was taken for all calculations. This value represents a standard and widely accepted reference temperature for indoor thermal analysis in engineering calculations. It also closely reflects the typical daytime indoor temperature conditions in Debre Berhan, where the experiments were conducted, providing a realistic basis for the heat loss analysis.

The typical range for natural convection of air at room temperature is approximately 5–25 W/m²·K (Dassault Système, n.d.); However, the *areke* distillation process involves occasional manual stirring, which disrupts the boundary layer and induces periods of forced convection. To account for this enhanced heat transfer, a conservatively high value of h = 100 W/m²·K was selected. This value, which falls in the range of forced convection for air,

ensures that the heating element is designed to overcome the peak heat loss scenario, guaranteeing robust performance throughout the process.

Given $T_m = 80°\text{C}$, $T_\infty = 20°C$, $A = \pi r^2 = \pi(0.16)^2 = 0.0804m^2$, and $h = 100\text{W/m}^2 \cdot \text{K}$, the convective heat loss is calculated to be $\dot{Q}_{conv} = 482.4$ W.

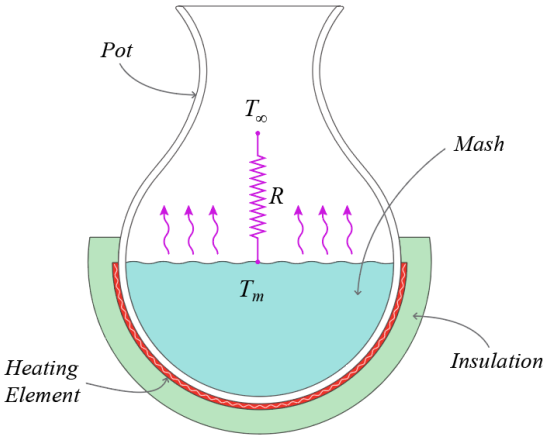

Figure 3.5: Heat loss from the mash surface via convection

3.5.3 Insulation Heat Loss and Insulation Thickness

Given that the heating elements maintain a constant temperature throughout the initial heating period, the system can be simplified to a steady-state heat transfer problem across the insulation layer. For this analysis, the effects of radiation are disregarded.

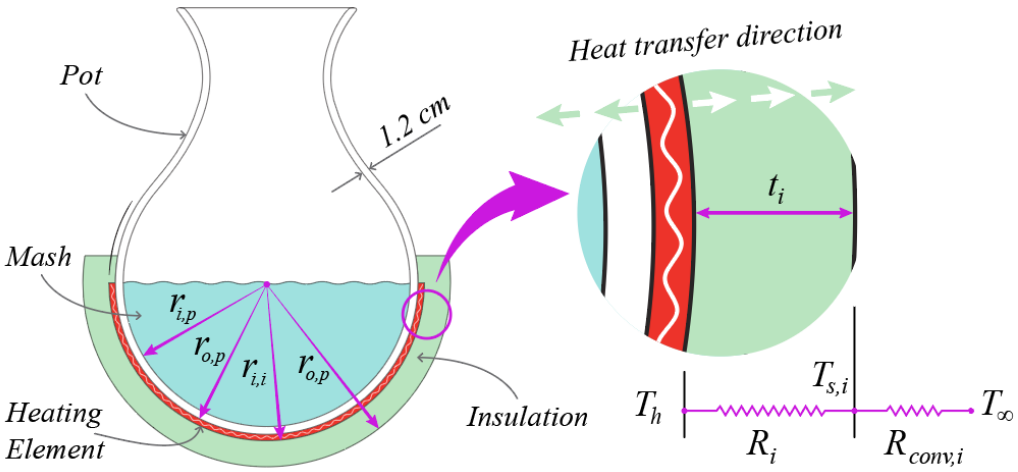

Figure 3.6: Thermal Resistance Network for Heat Loss through Insulation.

After an iterative calculation process, a design target of 100W maximum allowable heat loss through the insulated base was established. The iterative process involved assuming a heat loss value, calculating the corresponding insulation thickness and resulting outer

surface temperature, and adjusting the parameters repeatedly until a suitable balance was achieved. This value was selected because it offered an optimal compromise between competing design priorities: High Thermal Efficiency (Ensuring most of the electrical input directly heats the mash), User Safety (Keeping the external stove surface at a safe temperature, calculated at 33.65°C), and Cost and Practicality (Avoiding the need for excessively thick or expensive insulation materials).

The heat loss through the insulation, for steady state heat transfer, can be calculated using the thermal resistance network approach as:

$$\begin{pmatrix} rate\ of\ heat \\ conduction\ through \\ insulation \end{pmatrix} = \begin{pmatrix} rate\ of\ heat \\ convection\ from \\ insulation \end{pmatrix}$$

$$\dot{Q}_{i,loss} = \frac{T_h - T_{s,i}}{R_i} = \frac{T_{s,i} - T_\infty}{R_{conv.i}} \tag{3.4}$$

Adding the numerators and denominators yields:

$$\dot{Q}_{i,loss} = \frac{T_h - T_\infty}{R_i + R_{conv,i}} \tag{3.5}$$

Where $\dot{Q}_{i,loss}$ is heat loss rate through insulation, T_h is heating element temperature, $T_{s,i}$ is insulation surface temperature, T_∞ is ambient temperature, R_i is insulation thermal resistance and $R_{conv.i}$ is the convective thermal resistance at the insulation surface.

The thermal resistance of insulation R_{ins} and convection resistance $R_{conv,i}$ for a hemispherical setup can be calculated from (Cengel & Ghajar, 2019):

$$R_i = \frac{r_{o,i} - r_{i,i}}{2\pi r_{o,i} r_{i,i} k} \tag{3.6}$$

$$R_{conv,i} = \frac{1}{2\pi r_{o,i}^2 h} \tag{3.7}$$

Where $r_{i,i}$, $r_{o,i}$ are inner and outer radius of insulation respectively, k is thermal conductivity of insulation material (fiberglass), and h is convective heat transfer coefficient.

A heating element thickness (or coil diameter) of 0.6 cm was assumed based on the typical specifications of commercially available heating coils commonly sold in local markets. Thus, the inner radius of the insulation becomes 17.8 cm.

A convective heat transfer coefficient h of 25 W/m²·K, representing the typical maximum

value for natural convection in air at room temperature, as documented by Dassault Système (2025), is adopted in this analysis.

During the heating phase, a greater amount of heat should be applied to rapidly raise the mash temperature to the distillation level without inducing violent boiling. To achieve this, the mash is heated using the stove's high-power setting. While distillation stoves at their highest power setting generally operate within a temperature range of 100 to 400 °C, a conservative heating element temperature of $T_h = 500°C$ is selected for the insulation thickness design to incorporate an additional safety margin.

Given $r_{i,i} = 0.178\,m$, and $k = 0.038\,W/m.K$, $h = 25\text{W/m}^2\text{K}$, $T_h = 500°C$, $T_\infty = 20°C$, and $\dot{Q}_{i,loss} = 100\,W$, Using a trial-and-error method, the outer radius of the insulation was calculated to be approximately $r_{o,i} = 0.222$ m, resulting in an insulation thickness, t_i, of 4.4 cm.

The outer surface temperature of the insulation, $T_{s,i}$, can be calculated using Eq. (3.4). By rearranging the equation, the temperature is determined to be 33.65 °C.

3.5.4 Heating Phase Power Requirement

During the initial heating phase, the required power must both raise the mash temperature and compensate for heat losses. Therefore, the total power needed for this phase, $P_{heating}$, is the sum of the mash heating power P_m, the convective heat loss from the mash surface $\dot{Q}_{conv}$, and the insulation heat loss $\dot{Q}_{i,loss}$, expressed as:

$$P_{heating} = P_m + \dot{Q}_{conv} + \dot{Q}_{i,loss} \tag{3.8}$$

Given $P_m = 1680W$, $\dot{Q}_{conv} = 482.4W$, and $\dot{Q}_{i,loss} = 100W$, the total power requirement of the heating phase is calculated to be $P_{heating} = 2262.4\,W$.

3.6 Thermal Analysis: Distillation Phase

In this phase, the distillation of areke occurs by maintaining a constant distillation temperature for the mash. During this stage, the entire system can be effectively modeled as a steady-state heat transfer process, as there is no significant variation in the temperatures of the heating element and mash over time.

3.6.1 Power Required to Evaporate Distillate

In the distillation process, a significant amount of energy is required to vaporize the distillate. This section focuses on calculating the power needed to overcome the latent heat of vaporization and maintain steady evaporation during the distillation phase. The energy required for vaporization is directly proportional to the mass flow rate of the distillate and its latent heat of vaporization, as described by the formula:

$$\dot{Q}_{vap} = \dot{m} \cdot h_{fg} \tag{3.9}$$

Where Q_{vap} is heat transfer rate required for vaporization (kW), $\dot{m}$ is the mass flow rate (kg/s) and h_{fg} is the latent heat of vaporization of the distillate mixture (kJ/kg).

Once the mash reaches a specific boiling point, additional heat input directly influences vapor generation. Thus, to calculate the necessary power, a desired evaporation rate must be established, ensuring the system can efficiently produce the required amount of vapor. Based on the conducted survey, 1.5 liters of areke can be distilled in 2 hours from 12 liters of mash when production speed is prioritized. To accommodate for a higher throughput in the new stove, the stove design assumes a production rate of 1.5 liters (equivalent to 1.4025 kg) in 1 hour. Taking the density of 40% ethanol by volume as 935 kg/m³ (The Engineering Toolbox, n.d.), this translates to a mass flow rate of 0.0003896 kg/s.

Areke is primarily composed of water and ethanol, on average 37.22% ethanol by volume and the remaining portion predominantly water (Tafere, 2015). To convert these volume fractions to mass fractions, the respective densities of ethanol (789 kg/m³) and water (997 kg/m³) were used. Assuming a 100 mL mixture, the mass of ethanol becomes 31.56 g (40 mL × 0.789 g/mL), and the mass of water becomes 59.82 g (60 mL × 0.997 g/mL), resulting in a total mass of 91.38 g. From this, the mass fractions were calculated to be approximately 34.5% ethanol and 65.5% water. These values were then used in a weighted average method to estimate the enthalpy of vaporization (h_{fg}) of the mixture using,

$$h_{fg} = x * h_{fg,water} + y * h_{fg,ethanol} \tag{3.10}$$

Where x is the mass fraction of water, y is the mass fraction of ethanol, and $h_{fg,water}$ and $h_{fg,ethanol}$ are the enthalpy of vaporization for water and ethanol at their respective boiling points at standard atmospheric pressure (1 atm), respectively.

Given $x = 0.655$, $y = 0.345$, $h_{fg,water} = 2256\ kJ/kg$ and $h_{fg,ethanol} = 846\ kJ/kg$, the

enthalpy of vaporization for areke was calculated as $h_{fg} = 1769.5\ kJ/kg$. And given $\dot{m} = 0.0003896$ kg/s, the heat transfer rate required for vaporization utilizing Eq. (3.9) is calculated as, $\dot{Q}_{vap} = 0.6894\ kW = 689.4\ W$.

Note that this approximation assumes ideal behavior of the mixture (no significant interactions between water and ethanol molecules). In reality, water-ethanol mixtures exhibit non-ideal behavior due to hydrogen bonding, so the actual enthalpy of vaporization may differ slightly.

3.6.2 Heat Loss Through Distillation Pot

Heat flows from the inner section of the pot to the surroundings through conduction across the clay surface of the pot. The temperature of the air and vapor inside the illustrated system, as depicted in figure 3.7, is assumed to be approximately $80°C$ (average distillation temperature), similar to that of the mash.

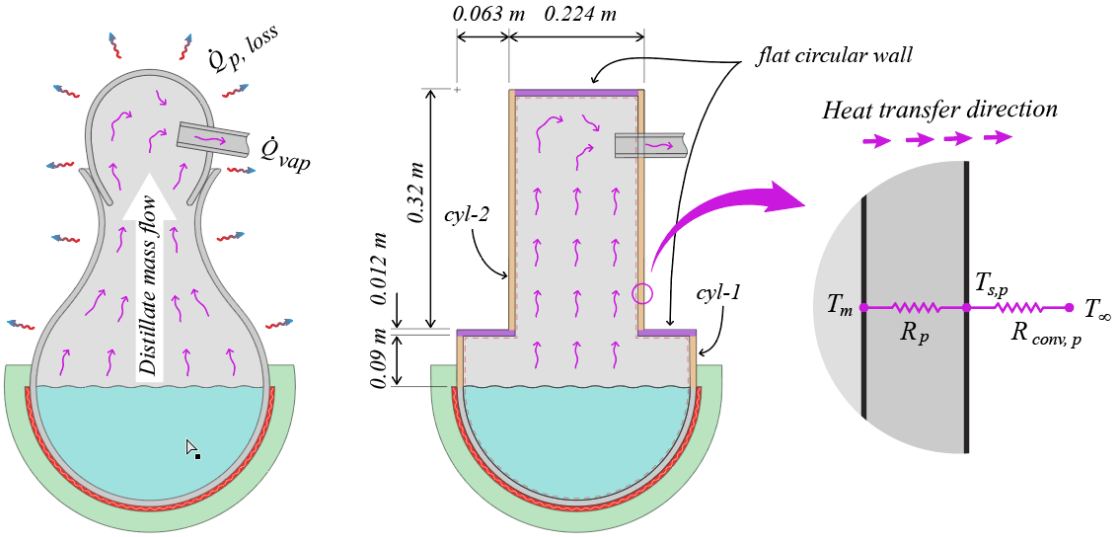

Figure 3.7: Geometric Simplification and thermal resistance network for distillation pot heat loss.

Due to the intricate design of the pot, accurately calculating heat transfer rates is challenging. To simplify the analysis, the pot's structure is approximated as a basic cylindrical shape, as depicted in figure 3.7. By modeling the pot in CAD software and measuring its surface area, the dimensions of the cylindrical approximation were adjusted to match this value, providing an estimated representation for subsequent calculations.

The simplified cylindrical model consists of three primary elements: a short, wide cylinder (cylinder-1), a long, narrow cylinder (cylinder-2), and a circular flat wall (formed by

projecting the bottom flat ring upwards). Consequently, the overall heat loss is determined by summing the heat losses from these three components.

Heat loss through flat circular pot wall

The heat loss through the flat circular wall can be obtained by equation:

$$\begin{pmatrix} rate\ of\ heat \\ conduction\ through \\ clay\ pot \end{pmatrix} = \begin{pmatrix} rate\ of\ heat \\ convection\ from \\ clay\ pot \end{pmatrix}$$

$$\dot{Q}_{p,f} = \frac{T_m - T_{s,p}}{R_{p,f}} = \frac{T_{s,p} - T_\infty}{R_{conv.p,f}} \tag{3.11}$$

Adding the numerators and denominators yields:

$$\dot{Q}_{p,f} = \frac{T_m - T_\infty}{R_{p,f} + R_{conv.p,f}} \tag{3.12}$$

Where $\dot{Q}_{p,f}$ is conduction heat transfer rate through flat clay pot, T_m is mash temperature, $T_{s,p}$ is clay pot surface temperature, T_∞ is ambient temperature, $R_{p,f}$ is clay pot thermal resistance, and $R_{conv.p,f}$ is the convective thermal resistance at the pot surface.

The conduction resistance of the pot $R_{p,f}$ and convection resistance $R_{conv,p,f}$ can be calculated from:

$$R_{p,f} = \frac{L}{kA} \tag{3.13}$$

$$R_{conv,p,f} = \frac{1}{hA_s} \tag{3.14}$$

Where L is thickness of circular wall, A is conduction surface area, A_s is convection surface area, k is thermal conductivity of clay pot and h is convective heat transfer coefficient.

Given, $h = 25\ W/m^2K$ (typical value for natural convection in air at room temperature (Dassault Système, 2025)), $A = A_s = \pi r^2 = \pi * 0.172^2 = 0.093\ m^2$, $L = 0.012\ m$ and $k = 1\ W/m.K$, the thermal resistances are calculated as: $R_{p,f} = 0.13\ °C/W$ and $R_{conv,p,f} = 0.43\ °C/W$.

And given $T_m = 80°C$ and $T_\infty = 20°C$, heat loss via the circular wall is $\dot{Q}_{p,f} = 107.14\ W$.

Heat loss through cylinders

The heat loss through the cylinder walls can be obtained by Eq (3.11) and Eq (3.12) with the exception of the conduction resistance of the cylindrical pot $R_{p,c}$ and convection

resistance $R_{conv,p,c}$ which can be calculated from:

$$R_{p,c} = \frac{\ln(r_o/r_i)}{2\pi Lk} \tag{3.15}$$

$$R_{conv,p,c} = \frac{1}{2\pi r_o h} \tag{3.16}$$

Where L is length of cylindrical wall, r_o, r_i are inner and outer diameters of the cylinders respectively, k is thermal conductivity of clay pot and h is convective heat transfer coefficient.

For cylinder-1: Given $r_o = 0.172\ m$, $r_i = 0.16\ m$, $h = 25\ W/m^2K$, $L = 0.09\ m$ and $k = 1\ W/m.K$, the thermal resistances are calculated as: $R_{p,c1} = 0.128\ °C/W$ and $R_{conv,p,c1} = 0.037\ °C/W$.

For cylinder-2: Given $r_o = 0.112\ m$, $r_i = 0.1\ m$ and $L = 0.32\ m$ the thermal resistances are calculated as: $R_{p,c2} = 0.056\ °C/W$ and $R_{conv,p,c2} = 0.056\ °C/W$.

And given $T_m = 80°C$ and $T_\infty = 20°C$, heat loss via the cylindrical wall utilizing Eq. (3.12) is $\dot{Q}_{p,c1} = 363.6\ W$ for cylinder-1 and $\dot{Q}_{p,c2} = 535.7\ W$ for cylinder-2.

Total Distillation Pot Heat Loss

The total distillation pot heat loss thus becomes the addition of the above three component heat losses which becomes, $\dot{Q}_{p,loss} = \dot{Q}_{p,f} + \dot{Q}_{p,c1} + \dot{Q}_{p,c2} = 1006.4\ W$

3.6.3 Insulation Heat Loss

As is well understood, the heating element operates at a lower temperature during distillation phase compared to the initial heating phase. With the designed insulation thickness of 4.4 cm in the heating phase, this lower operating temperature naturally results in reduced heat loss compared to the 100W loss of the heating phase. However, since distillers may adjust the heating element's temperature to control the distillation rate, the maximum heat loss of $\dot{Q}_{i,loss} = 100W$ is conservatively taken as insulation heat loss during this phase.

3.6.4 Distillation Phase Power Requirement

During the distillation phase, the required power must both supply power to evaporate the distillate (areke vapor) and compensate for heat losses. Therefore, the total power needed for this phase, $P_{distillation}$, is the sum of the power requirement to evaporate the distillate

$\dot{Q}_{vap}$, the heat loss through distillation pot $\dot{Q}_{p,loss}$, and heat loss through insulation $\dot{Q}_{i,loss}$, expressed as:

$$P_{distillation} = \dot{Q}_{vap} + \dot{Q}_{p,loss} + \dot{Q}_{i,loss} \quad (3.17)$$

Given $\dot{Q}_{vap} = 689.4\,W$, $\dot{Q}_{p,loss} = 1006.4\,W$, and $\dot{Q}_{i,loss} = 100\,W$, the total power requirement of the distillation phase is calculated to be $P_{distillation} = 1795.8\,W$.

3.7 Heating Element Design

The heating phase, requiring 2262.4 W, demands more power than the distillation phase, which needs 1795.8 W. As a result, the heating element must be capable of handling at least 2262.4 W to accommodate peak demand during the initial heating phase. To ensure reliability and account for safety margins, operational variability, and power fluctuations on the grid (a common phenomenon in Ethiopia where the voltage often falls below the stated 220 V) the heating element will be designed with a 3kW power rating. This ensures consistent performance even under suboptimal grid conditions. This 3 kW for heating the mash during the initial heating phase falls within the typical capacity (6.6 kW) of residential electrical meters in Ethiopia, indicating the feasibility of the design.

3.7.1 Wire Diameter and Length

As described by Hegbom (1997), a common method for determining wire diameter involves calculating the ratio of surface area to cold resistance (S/R_o). This ratio can then be used to find the corresponding wire diameter from a reference table.

$$\frac{S}{R_o} = \frac{C_t P^2}{U^2 p} \quad (3.18)$$

Where S represents the wire surface area (cm^2), R_o is the cold resistance or resistance at room temperature (Ω), C_t is dimensionless resistance temperature factor, P is power (W), U is voltage, and p is surface load of wire (w/cm^2).

Table A8 in the Appendix of Hegbom (1997) provides the S/R_o ratio as a function of wire diameter for nichrome 80 alloy (80 Ni, 20 Cr), a widely used heating element material composed of 80% nickel and 20% chromium. This alloy, selected as the heating element material for this project, has a resistivity of 1.09 $\Omega\,mm^2/m$ (Kanthal AB, 2019) and a density

of 8.3 g/cm³ (VZPS, n.d.). The Nichrome 80 properties table, sourced from Kanthal AB (2019), is included in Appendix A-1 for reference.

Surface load, also known as surface watt density, refers to the amount of power (in watts) dissipated per unit area of the heating element's surface area. At a higher surface load, less material is needed to build the heating element, but the durability and life expectancy of the heating element is reduced (AGH University, 2012; *Design Calculations for Heating Elements — Kanthal®*, n.d.). For a heating element in grooves or sandwiched in between, the recommended surface load is 4 W/cm^2 (Kanthal AB, 2018, 2019).

The dimensionless resistance temperature factor (C_t) for Nichrome 80 at 500 °C, as taken from the Nichrome 80 properties table provided by Kanthal AB (2019), is 1.05.

Given $C_t = 1.05$, $P = 3000W$, $U = 220V$, and $p = 4\ W/cm^2$, surface area to cold resistance ratio is calculated to be $S/R_o = 48.8\ cm^2/\Omega$. Based on the calculated S/R_o ratio, the corresponding wire diameter was determined by referencing the table and choosing the closest value, resulting in a diameter of 1.291 mm. Approximating this value to the nearest standard on the local market value we have, $d = 1.2\ mm$.

The wire length can be calculated by dividing the resistance (R_o) by the resistance per unit length (R_{unit}) of the material as expressed by the formula:

$$l = R_o/R_{unit} \tag{3.19}$$

Where l is length of the wire (m), R_o is total resistance of the wire (Ω), and R_{unit} is resistance per unit length of the material (Ω/m).

The resistance (R_o) can be calculated using the formula:

$$R_o = \frac{U^2}{P} \tag{3.20}$$

Where U is voltage (V), and P is power (W). Given $P = 3000W$ and $U = 220V$, The resistance is calculated to be 16.13 Ω.

For a wire diameter of 1.2 mm, nichrome 80 (Nikrothal 80) has a resistance per meter value of 0.964 Ω/m (Kanthal AB, 2018). Using this value and the calculated resistance of 16.13 Ω, the required wire length is determined as: $l = 16.13\ \Omega/0.964\ \Omega/m = 16.7\ m$.

3.7.2 Diameter, Pitch, Number of Turns and Length of Coil

The outer diameter D of the spiral heating element is related to the wire diameter d by the ratio D/d, which is recommended to be between 5 and 12 (Kanthal AB, 2019). This means D can range from 6 mm to 14.4 mm. Since a 6 mm coil diameter is locally available, this minimum value has been selected.

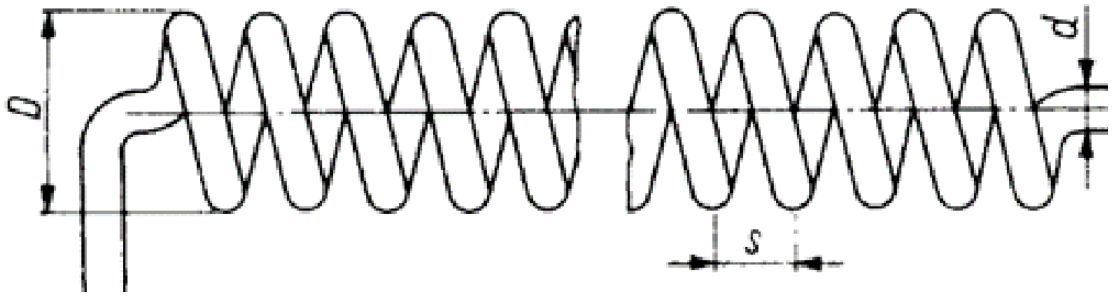

Figure 3.8: Schematics for heating coil

When the coil length and diameter are known, the coil pitch, s, can be estimated. According to Kanthal AB (2019), the coil pitch s is typically 2 to 4 times the wire diameter d (1.2mm). Using the average value of three, the coil pitch is calculated to be 3.6 mm:

$$s = 3 * d \tag{3.21}$$

The number n of the turns of the spiral heating element is determined to be $1259.9 \approx 1260$ turns from equation:

$$n = \frac{l}{\pi(D - d)} \tag{3.22}$$

where $\pi(D - d)$ is the average length (circumference) of one turn of the spiral heating element.

The Un-stretched length of coil is $1512\ mm \approx 1.5\ m$ from equation:

$$l_{unstrached} = d * n \tag{3.23}$$

The stretched spiral heating element length l_s is $4536\ mm \approx 4.6\ m$ from equation:

$$l_s = s * n \tag{3.24}$$

3.8 Condenser Design

The objective of this heat exchanger design is to determine the optimum coolant mass flow rate and the required heat transfer surface area (length of the distillation tube hence the diameter is known) to effectively condense the distillate vapor.

The log mean temperature difference (LMTD) method is used for this analysis. The LMTD method is very suitable for determining the size of a heat exchanger to achieve prescribed outlet temperatures when the mass flow rates and the inlet and outlet temperatures of the hot and cold fluids are specified (Cengel & Ghajar, 2019).

To find optimum heat transfer surface areas, size the condenser, the following procedure from Cengel & Ghajar (2019) are used.

First, select the type of heat exchanger suitable for the application. A simple counter-flow double-pipe heat exchanger configuration as illustrated in figure 3.9 is selected for this application. This type of heat exchanger is chosen because it compatible with the existing traditional distillation tube, minimizing modifications to the traditional process. The double-pipe heat exchanger is a cost-effective and straightforward design, making it a practical choice for this application.

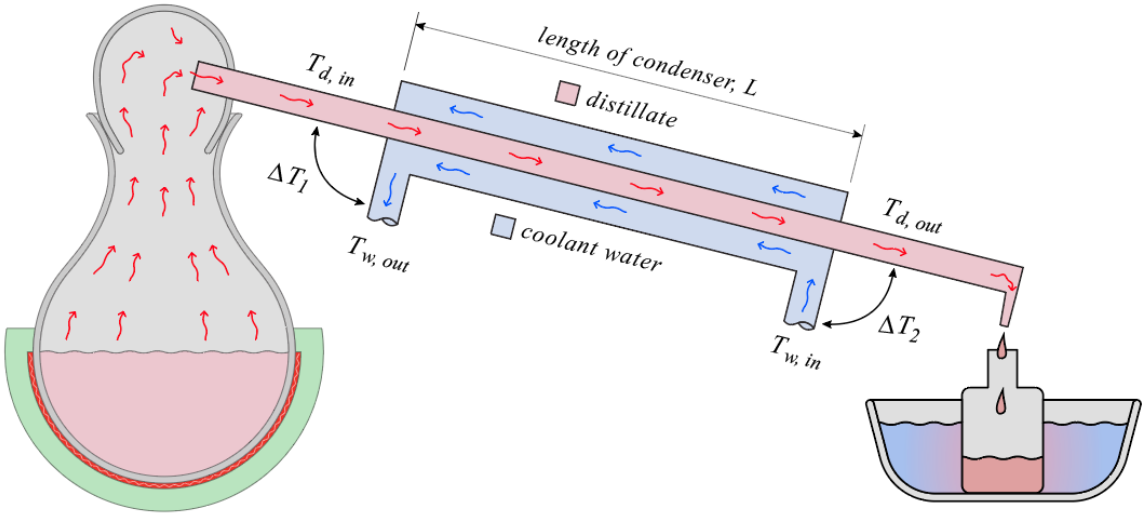

Figure 3.9: Schematics of Simple counter-flow double-pipe areke condenser

Second, assuming a reasonable temperature difference between the coolant inlet and outlet, determine the required coolant mass flow rate necessary to dissipate the heat load using an energy balance.

Third, calculate the log mean temperature difference ΔT_{lm}. The log mean temperature difference is the suitable form of the average temperature difference between the hot and cold fluids, which varies along the heat exchangers length, for use in the analysis of heat exchangers.

Then, select from a tabulated data sheet, the value of the overall heat transfer coefficient, U, that is suitable for alcohol condensers. And finally calculate the heat transfer surface area A_s.

3.8.1 Coolant Mass Flow Rate

The total load on the condenser is calculated in section 3.7.2 as distillate's evaporation heat flow rate to be $\dot{Q}_{vap} = \dot{Q}_{load} = \dot{Q}_{distillate} = 689.4\ W$.

Assuming the outer surface of the heat exchanger is perfectly insulated, so that there is no heat loss to the surrounding medium, and any heat transfer occurs between the two fluids only, the first law of thermodynamics requires that the rate of heat transfer from the distillate fluid be equal to the rate of heat transfer to the coolant water. That is,

$$\dot{Q}_{water} = \dot{Q}_{distillate}$$

$$\dot{m}_w c_{pw}\left(T_{w,out} - T_{w,in}\right) = \dot{m} h_{fg} \tag{3.25}$$

Where $\dot{Q}_{water}$ is the heat transferred to the coolant water, c_{pw} is the specific heat capacity of water, $T_{w,out}$ is the outlet temperature of water, and $T_{w,in}$ is the inlet temperature of water.

Assuming a coolant temperature increase of 2°C ($T_{w,out} - T_{w,in}$), and given the specific heat capacity of water (c_{pw}) as 4186 J/kg°C and the distillate heat load ($\dot{Q}_{distillate} = \dot{m} h_{fg}$) of 689.4 W, the required coolant mass flow rate ($\dot{m}_w$) is calculated as 0.08 kg/s.

3.8.2 The Log Mean Temperature Difference

The log mean temperature difference can be calculated from (Cengel & Ghajar, 2019):

$$\Delta T_{lm} = \frac{\Delta T_1 - \Delta T_2}{\ln\left(\Delta T_1 / \Delta T_2\right)} \tag{3.26}$$

Where 〖ΔT〗_1=T_(d,in)-T_(w,out) and 〖ΔT〗_2=T_(d,out)-T_(w,in) represent the temperature difference between the distillate and coolant water at the two ends (inlet and outlet) of the heat exchanger as illustrated in figure 3.9.

Since the phase change can be assumed to occurs at a constant temperature of 80°C for the condenser, $T_{d,in} = T_{d,out} = 80$ ℃. Given a room temperature inlet coolant temperature of $T_{w,in} = 20$℃ and an assumed 2°C temperature rise to $T_{w,out} = 22$℃, the inlet and outlet temperature differences are calculated as $\Delta T_1 = 58$℃ and $\Delta T_2 = 60$℃. Consequently, the log mean temperature difference (LMTD) is determined to be $\Delta T_{lm} = 58.9°C$.

3.8.3 Length of Condenser

According to Cengel (2019), a heat exchanger typically involves two flowing fluids separated by a solid wall. Heat transfer occurs in three stages: (1) convection from the hot fluid to the wall, (2) conduction through the wall, and (3) convection from the wall to the cold fluid. The thermal resistance network associated with this process consists of two convection resistances and one conduction resistance, as illustrated in Figure 3.10. The total thermal resistance (R_{total}) is expressed as:

$$R_{total} = R_i + R_{wall} + R_o = \frac{1}{h_i A_i} + \frac{\ln(D_i/D_o)}{2\pi kL} + \frac{1}{h_o A_o} \tag{3.27}$$

Where k is the thermal conductivity of the wall material, L is the length of the tube, A_i is the inner surface area of the wall, A_o is the outer surface area of the wall, and h_i and h_o are the convection heat transfer coefficients for the inner and outer fluids, respectively.

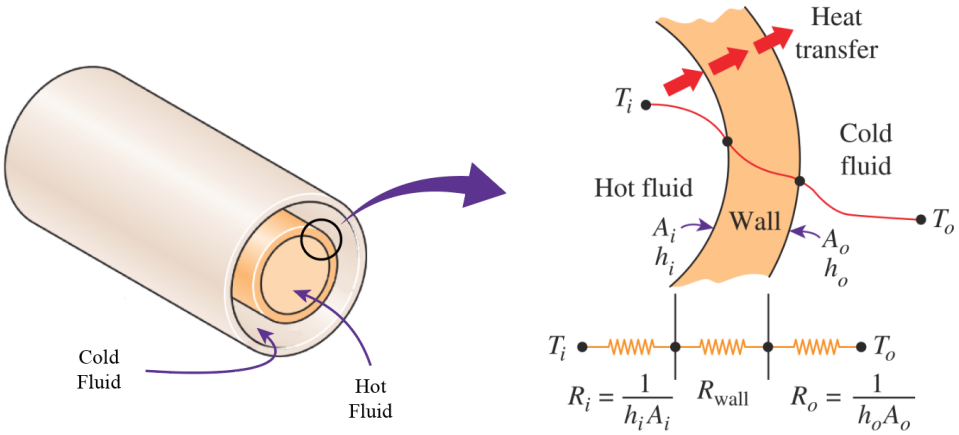

Figure 3.10: Thermal resistance network associated with heat transfer in a double-pipe heat exchanger (Cengel & Ghajar, 2019).

In heat exchanger analysis, it is often convenient to use the overall heat transfer coefficient (U), which simplifies the calculation of heat transfer rates. The overall heat transfer coefficient accounts for all resistances in the system and is defined as:

$$\frac{1}{UA_s} = \frac{1}{U_iA_i} = \frac{1}{U_oA_o} = R_{total} = \frac{1}{h_iA_i} + R_{wall} + \frac{1}{h_oA_o} \tag{3.28}$$

where U is the overall heat transfer coefficient, and U_i and U_o are the overall heat transfer coefficients based on the inner and outer surface areas, respectively.

For the condenser tube design, copper is selected as the material due to its high thermal conductivity. When the tube wall thickness is small and the thermal conductivity is high, common conditions in heat exchangers, the thermal resistance of the tube wall becomes negligible ($R_{wall} \approx 0$). Additionally, the inner and outer surface areas of the tube are nearly identical ($A_i \approx A_o \approx A_s$). These criteria simplify the equation for the overall heat transfer coefficient to:

$$\frac{1}{U} \approx \frac{1}{h_i} + \frac{1}{h_o} \tag{3.29}$$

For heat exchangers or condensers meeting these criteria, which is the case for this design, the overall heat transfer coefficient (U) can be selected from tabulated data. Such tables are prepared based on experimental and empirical data for various fluid combinations and operating conditions. A relevant table can be found in Cengel (2019), and a copy of this table is attached in Appendix A-2 for reference. According to Cengel & Ghajar (2019), the typical U-value range for water-cooled alcohol condensers is 250 to 700 W/m²K. To ensure robust performance, a conservative value of 300 W/m²K is chosen. This results in a larger heat transfer area, ensuring that the designed condenser will exceed performance requirements even under sub-optimal conditions.

Once the log-mean temperature difference (ΔT_{lm}), the mass flow rates, and the overall heat transfer coefficient are available, the heat transfer surface area of the heat exchanger, A_s, can be determined from equation:

$$\dot{Q} = UA_s\Delta T_{lm} \tag{3.30}$$

Where $\dot{Q}$ is the heat load (W), U is the overall heat transfer coefficient (W/m²K), A_s is the heat transfer surface area (m²), and ΔT_{lm} is the log mean temperature difference (°C).

Given the heat load $\dot{Q} = 689.4\ W$, $U = 300\ \mathrm{W/m^2K}$ and $\Delta T_{lm} = 58.9°C$, the surface area is calculated to be $A_s = 0.039\ m^2$.

Based on measurements, traditional bamboo tubes typically have an average diameter of 3

cm. However, to ensure sufficient surface area for effective heat transfer, the diameter can be reduced to 2 cm. By fixing the condenser radius, r, at 1 cm, the required condenser length, L, is calculated to be $L = A_s/2\pi r \approx 0.621\ m\ (or\ 62.1\ cm)$. To connect the heat condenser to the pot and a distillate collector, an additional 20 cm of copper tube is required at each end, bringing the total copper tube length to 102.1 cm.

3.9 Temperature Control Design

3.9.1 Why PID Controller?

For this project, two primary temperature control options were considered: PID and on/off. despite its steeper cost, a PID controller was ultimately chosen over an on/off controller due its superior ability to maintain precise temperature levels which is crucial for producing high quality areke product.

As shown in the figure 3.11, the PID controller maintains a much more stable temperature compared to the on/off controller. The on/off controller's graph exhibits significant temperature fluctuations around the setpoint (SP), repeatedly overshooting and undershooting the target temperature (TT), which is undesirable for a distillation system. In contrast, the PID controller's graph demonstrates a smooth response that quickly reaches and closely maintains the target temperature. This results in several key benefits, including greater energy efficiency as the PID controller makes small, continuous adjustments, avoiding the frequent cycling between full power and no power characteristic of the on/off controller. Additionally, the smooth operation of the PID controller reduces stress on heating elements and other components, potentially extending the lifespan of the distillation equipment.

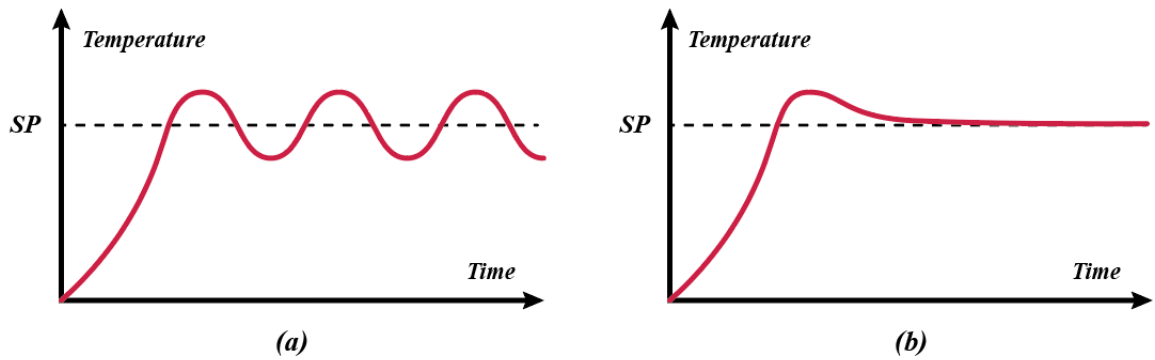

Figure 3.11: Temperature vs Time graph for (a) on/off controller and (b) PID controller.

3.9.2 System Components and Connections

The areke distillation stove's temperature control system consists of several key components working in conjunction. The main control components are thermocouple (k-type), PID controller and Solid-State Relay (SSR). The connection between those components (control design) is presented in the diagram below.

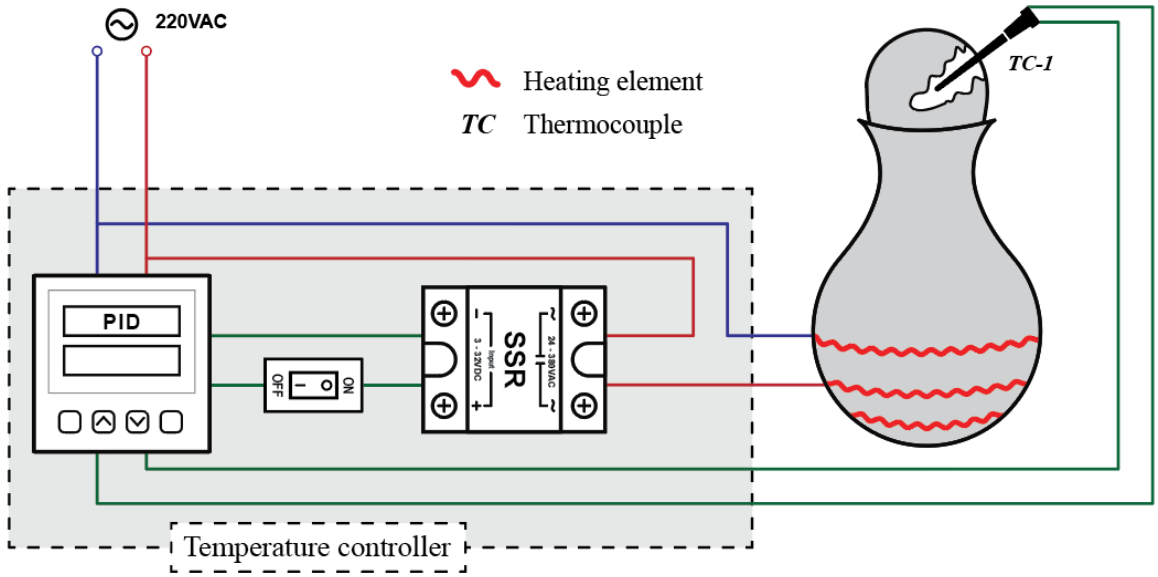

Figure 3.12: Temperature control system diagram.

The control loop operates as follows: The thermocouple TC-1 continuously measures the temperature of the vapor leaving the pot and entering the condenser tube at the point of no return (as soon as it is about to enter the tube). This temperature data is sent to the PID controller, which compares the measured temperature with the setpoint and calculates the necessary control output. The control signal is then sent to the SSR (Solid State Relay), which switches the power of the heating element on or off as needed based on the control signal, bringing it closer to the setpoint temperature.

For the control cooking test (CCT), additional components such as a watt meter and data logger are required to monitor power consumption and record temperature data over time. These additional components are integrated into the distillation setup, as illustrated in figure 3.13.

The data logger records temperature measurements over time at five locations: vapor temperature entering the condenser tube (TC-2), heating element temperature (TC-3), shell and tube condenser temperature (TC-4), water bath condenser temperature (TC-5), and ambient temperature (TC-6).

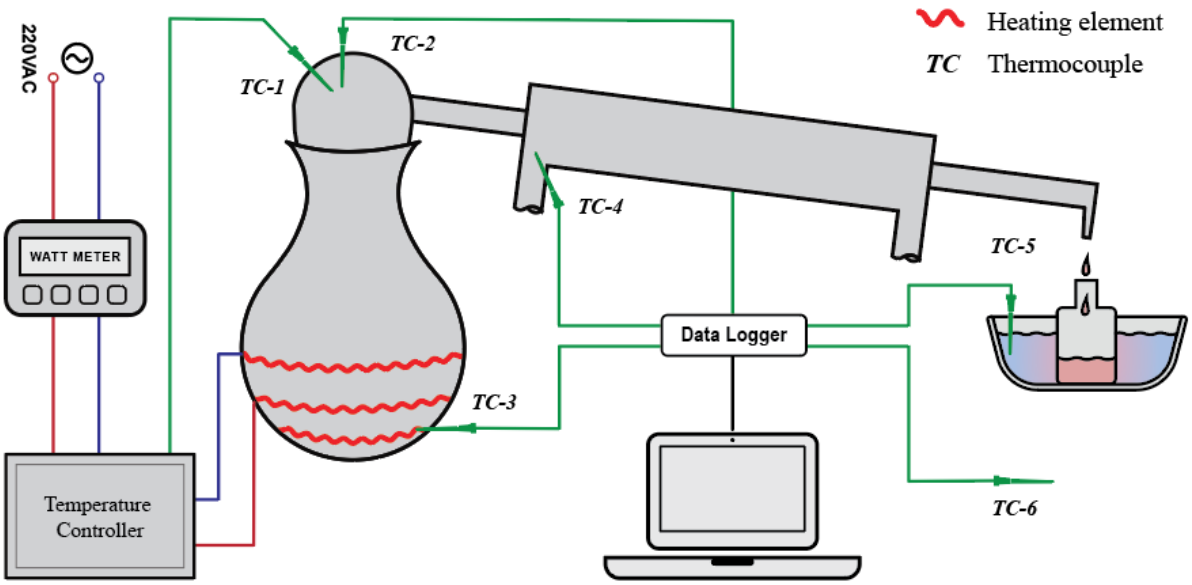

Figure 3.13: Temperature control system with CCT components.

Chapter 4

Manufacturing

4.1 Materials and Tools used

This section provides a comprehensive overview of the materials, components, and tools utilized during the manufacturing process of the electrically powered distillation stove prototype. The selection of materials and tools was guided by the design requirements, availability, and the need to ensure safety, durability, and functionality. The tables below categorize and detail the base materials, thermal control and electrical components, fabrication and measurement tools, consumables, and safety equipment used throughout the project.

Table 4.1: Base Materials

Name	Specification	Quantity	Price, Br
Clay pot	Locally made; average thickness: 1.2 cm	1	600
Clay pot lid	Locally made; average thickness: 1.2 cm	1	200
Clay bowl	Locally made; average thickness: 2 cm	1	400
Aluminum pot	Internal diameter: 34 cm; thickness 2 mm	1	4700
Aluminum flask	2-liter capacity	1	600
Bamboo tube	Diameter: 3 cm; length: 80 cm	1	120
PVC tube	Internal diameter: 8 cm; length: 60 cm	1	100
End caps for PVC tube	8 cm PVC tube end caps	2	120
Aluminum sheet metal	72 x 60 cm; Thickness: 1 mm	2	400
Fiber glass insulation	2 kg	1	500
Ply wood	1.22 x 1m; 1cm thickness	1	300
		Total Price	**8,040.00**

Table 4.2: Thermal Control and Electrical Components

Name	Specification	Quantity	Price, Br
PID Controller	Pixsys ATR243-20ABC (1 relay + 1Ssr/V/mA)	1	6000
Temperature Sensors	PT100 RTD	1	(DBU)
Thermocouples	K - type	5	(AAiT)
Heating Element	Nichrome alloy; Wire diameter: 1.2 mm; Coil diameter 0.6 mm; Coil length: 70 cm; resistance 32 ohm	2	340
Twisted resistor wire (*weraj*)	1 meter	1	80
Electrical wire	Copper wire; diameter:4 mm; length: 10 meters	1	300
Solid State Relay (SSR)	Celduc SC862110; 25 A Load; output 25 – 520 Vac; input 5 – 30 Vdc	1	2000
ON/OFF Switch	-	1	200
plug (male connector)	25 Ampere	1	70
socket (female connector)	25 Ampere	1	100
Screw terminal block	Material: Copper	2	300
		Total Price	**9,390.00**

(DBU), (AAiT) = Freely rented from Debre Berhan University and Addis Ababa Institute of Technology respectively.

Table 4.3: Fabrication and Measurement Tools and Equipment

Name	Specification	Quantity	Price, Br
Combination plier, Utility knife, Measuring Tape, Tin Snips, Rubber Mallet, Metal hammer, Table saw, Cordless drill, and Jig saw	-	-	5000*
Multimeter	Metrahit 2+ Universal True RMS Multimeter	1	(DBU)
Data logger	cDAQ-9172 Chassis equipped with NI9211(A) thermocouple module	1	(AAiT)
Power Clamp	Extech 382075 3ϕ/1ϕ Power Clamp	1	(AAiT)
Infrared Thermometer	Fluke 868 IR Thermometer	1	(AAiT)
		Total Price	**5,000.00**

(DBU), (AAiT) = Freely rented from Debre Berhan University and Addis Ababa Institute of Technology respectively.

* Rented from local woodworking and metal working shops at specified amount.

Table 4.4: Consumables, Safety Equipment and other expenses

Name	Specification	Quantity	Price, Br
Two-part epoxy	-	1	400
Super glue	-	1	50
Wood screws	Size; 3 cm	30	30
Protective Gloves	-	1	100
Safety Goggles	-	1	80
Mask	-	3	30
Ear Plug	-	1	100
Transport	-	-	1000
Labor	-	1	3000
		Total Price	**4,790.00**

4.1.1 Manufacturing Cost Analysis

The total cost of manufacturing the prototype amounts to 27,220 birr, which includes all expenses related to materials, labor, and production. By eliminating costs associated with labor, transport, tools, and machine rentals, since these expenses are accounted for within the profit margin. and opting for more affordable alternatives, such as replacing the aluminum pot with a clay pot typically priced at 500 birr and using a more affordable commercially available PID controller priced at 3,500 birr, the overall material cost is significantly reduced. As a result, brings the total material cost down to 11,520 birr.

If the prototype were to be sold to consumers, a 50% profit margin would be added to the material cost. This 50% profit margin is a generous estimate, determined through a study of the profit margins typically observed among local machine producers, furniture manufacturers, and metal workers. With this markup, the final selling price would be set at 17,280 birr, balancing competitive pricing with fair profitability for the manufacturer.

4.2 Fabrication Process

This section provides a detailed account of the step-by-step process involved in the fabrication of the prototype. The areke distillation stove prototype was fabricated with a focus on local manufacturing and readily available resources.

4.2.1 Production of Clay Components

The clay components, including the distillation pot, pot lid, and heating element bowl, were outsourced to a local artisan. The pot and pot-lid are those utilized in traditional distillation processes, while the bowl serves as an additional clay component designed to house the heating element. It features grooves slightly wider than the diameter of the heating element (resistor wire) and holes at the end of those grooves for ease of connecting the heating element to a power source. After the bowl structure was made by the local artesian (1), grooves were created in the clay using a homemade compass with a rod tip (2). The rod tip is slightly larger than the heating element diameter. The groove was made while the clay bowl was still wet (approximately 1 day old). Once the grooves were completed, the clay components were fired and finished by the artisan following standard practices (3). Finally, the pot is prepared for distillation by first firing the pot and its lid (4). Then, water is boiled inside the pot, and Urtica simensis (a locally grown plant known as samma) is added (5), boiled for about 30 minutes, and the pot is thoroughly washed. This entire process is traditionally referred to as *mamuashet*.

Figure 4.1: Bowl fabrication process

Figure 4.2. Traditional process of pot preparation (*mamuashet*)

Figure 4.3: (a) Homemade compass, (b) Finished clay pot and pot lid

4.2.2 Heating Elements Installation

With the clay bowl ready, the next step was the installation of the heating elements. To ensure proper connection, the ends of the heating element were straightened to a length of 10 cm and then twisted together using a pre-twisted heating element wire purchased locally (1). This reduces resistance preventing overheating at the ends of the heating element wire.

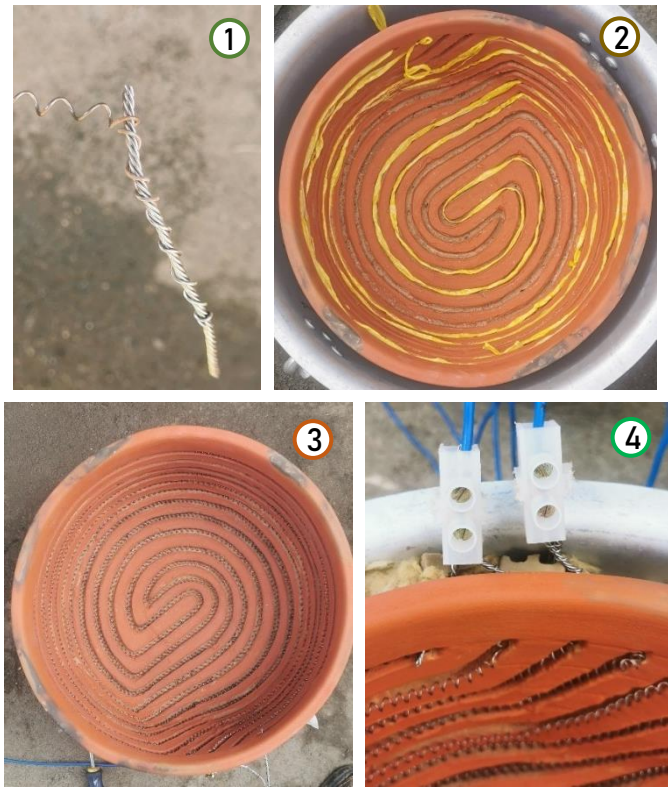

Figure 4.4: Heating Elements Installation

Then, the length of the groove for the heating element was measured with a rope (2), and the element was stretched to match this length, ensuring a precise fit. Two heating elements

purchased in the local market, each with a resistance of approximately 30 ohms, were then installed in parallel within the grooves of the clay bowl (3). This arrangement was selected to reduce the overall resistance and increase the wattage of the stove. The heating elements were purchased locally to avoid complications and additional costs that would arise from sourcing them elsewhere.

Once positioned, the ends of the element were connected to a #4 electrical conductor wire using a screw terminal block (4). The ends of the conductor wire were fitted with a plug (male connector) for connection to the temperature control box.

4.2.3 Stove Assembly and Insulation

The clay bowl was then positioned inside an aluminum pot, which functioned as both structural support and housing for insulation and the clay bowl itself. The aluminum pot is a standard cooking pot purchased from the local market, and the bowl was specifically designed to fit this pot leaving a 4 cm gap around the bowl for insulation.

Figure 4.5: Distillation prototype stove assembly

Metal scraps, 4 cm in height, were placed at the bottom of the aluminum pot to elevate the bowl, ensuring its top edge aligned with the rim of the metal pot (1). Fiberglass insulation was then placed at the bottom of the aluminum pot and around the sides of the clay bowl, filling the gap between the bowl and the aluminum walls (2).

To cover the insulation, a metal pot lid was cut into a ring shape using a 1 mm thick aluminum sheet (3&4). The inner diameter of the ring is slightly larger than that of the clay pot, allowing for easy insertion and removal of the pot. Finally, the heating element embedded in the grooves was securely sealed with a thin layer of gypsum (5).

4.2.4 Bamboo Shell and Tube Condenser Fabrication

Copper tubes required for building a shell-and-tube condenser were difficult to source and expensive, which would significantly increase the overall cost and hinder early adoption. As a result, a bamboo tube purchased from the local market, already prepared for traditional distillation use, was utilized for the prototype due to its low cost and local availability (1). It should be noted that as outlined in the design chapter, the bamboo shell-and-tube design is intended to complement the water bath condenser.

The traditional bamboo is typically wrapped with rope, which is wetted with cold water to help lower the temperature during operation. The manufacturing process begins with unwrapping and removing the rope (2).

Next, PVC end caps were drilled to a diameter slightly smaller than that of the bamboo to ensure a snug fit (3). One end cap, positioned to the product collection side, was heated until it softened and then inserted onto the bamboo (4). The cap and bamboo were then secured with epoxy from both sides. Prioritizing the insertion of the cap on the collector side is crucial. During operation, the condenser tube is tilted towards the collector, resulting in higher pressure at that end. By starting with the collector side, both the inner and outer openings can be effectively sealed.

Then the PVC tube was cut to length and its end was heated and the remaining end cap was inserted (5). The end cap was then heated and the entire sub assembly was fitted to the other end of the bamboo tube.

After allowing the epoxy to harden for approximately one hour, the remaining PVC end was heated and attached to the first end cap (6). This connection was then sealed with epoxy from the outside (6).

A small, conical-shaped plastic piece (from a light bulb) was then inserted into a hole drilled at the top (pot-side) of the PVC pipe to facilitated water filling. During operation, water is added at the start of the distillation process, and when it becomes warm, cold water is poured by syphoning out the hot water to create space.

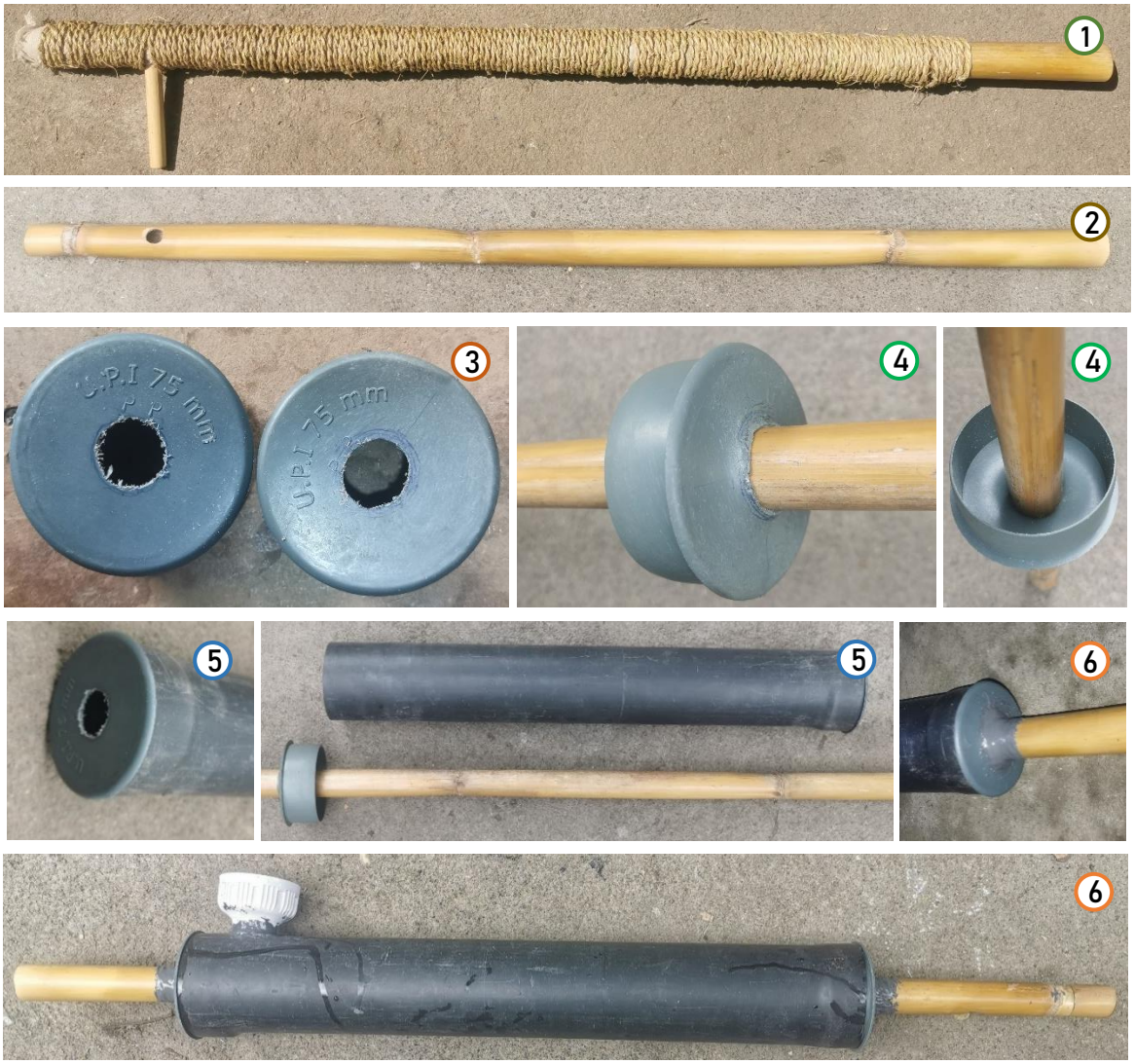

Figure 4.6: Fabrication of bamboo shell and tube type condenser

4.2.5 Temperature Controller Box Construction

Plywood was chosen for the box due to already rented and available woodworking tools, although sheet metal or plastic could be used as well.

The box was first modeled in Fusion360 3D modeling software. Plywood panels (1 cm thick) were cut to the required dimensions using a table saw, and openings were drilled and cut for the PID controller, switch, SSR and electrical socket using a cordless drill and jig-saw. The box was then assembled using wood screws of various sizes (1.5, 3, and 5). The SSR, PID, switch, and socket were then screwed or fixed into their designated spot. Electrical connections were then made using terminal connectors, following the wiring diagram detailed in the design section.

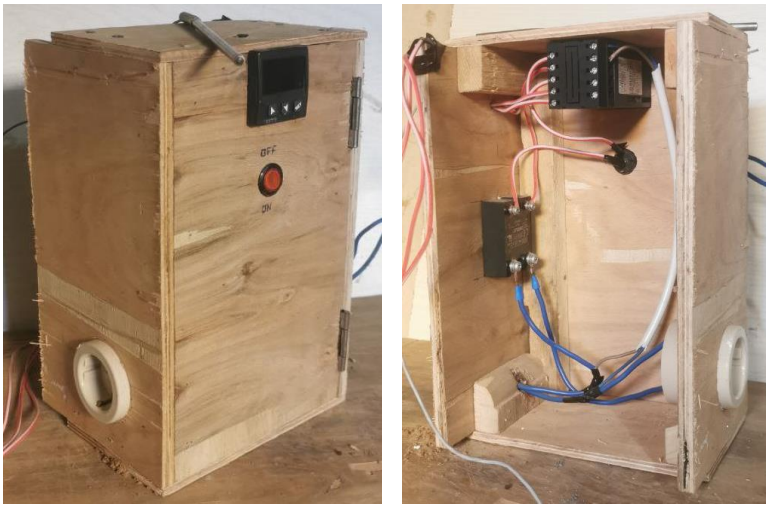

Figure 4.7: Temperature control box

4.2.6 Final Assembly and Initial Testing

With the stove, condenser assembly, and temperature control box complete, the prototype was ready for initial testing. Before full-scale testing, the temperature control box was initially checked for functionality using a commercial stove. The PID controller was then tuned (using its autotune function) under conditions similar to the distillation process. The heating element was subsequently turned on and tested. Finally, the shell and tube condenser were inspected for leaks.

Note that the clay pot to potlid and potlid to condenser connections were sealed using dough to prevent leaks during the distillation process. An aluminum flask placed within a water bath will serve as the product collector, with the aluminum flask and water bath together forming the water bath condenser. The complete setup is shown in Figure 5.2.

Chapter 5

Material and Method

5.1 Introduction

This chapter outlines the materials, equipment, and methodologies employed in the experimental investigation of the electrically powered stove prototype designed and constructed for areke distillation in previous chapters. It provides a detailed description of the experimental setup, the procedures followed during testing, and the methods used for data collection and analysis. The goal of this chapter is to ensure the replicability of the experiment and offer clarity on how the performance of the stove was evaluated.

The primary objective of the test is to assess the stove's ability to efficiently distill areke while ensuring optimal product quality and minimizing energy consumption. Two distinct testing protocols were employed: the Water Boiling Test (WBT), to assess the stove's energy efficiency, and the Controlled Cooking Test (CCT) to assess the stove and condensers performance in distilling areke under controlled conditions, simulating real-world usage scenarios. Two distinct experimental setups were employed, each corresponding to a specific testing protocol, with three trials conducted for each method.

5.2 Experimental Setup for Water Boiling Test

The WBT followed the Ethiopian Standards Agency (2018) guidelines for testing. As per the standard, an aluminum pot containing 5 liters of water was placed on the stove. The WBT experimental setup, illustrated in Figure 5.1, consisted of:

- Stove Prototype: The electrically powered areke distillation stove prototype.
- Aluminum Pot: An aluminum pot size of 33 cm internal diameter, and 21 cm height, as specified by Ethiopian Standards Agency (2018), was chosen to match the heating area.

- Temperature Measurement: A PID controller and a data logger (connected to a PC) were used to monitor water temperature. A PT100 RTD sensor (connected to the PID controller) and a K-type thermocouple (connected to the data logger) were positioned at the center of the pot, midway between the bottom and water surface, secured with a wooden fixture.
- Power Measurement: A power clamp-on meter (Extech 382075 3φ/1¢) was used to measure grid voltage, current, and active power.
- Stopwatch: A stopwatch was used to measure time.

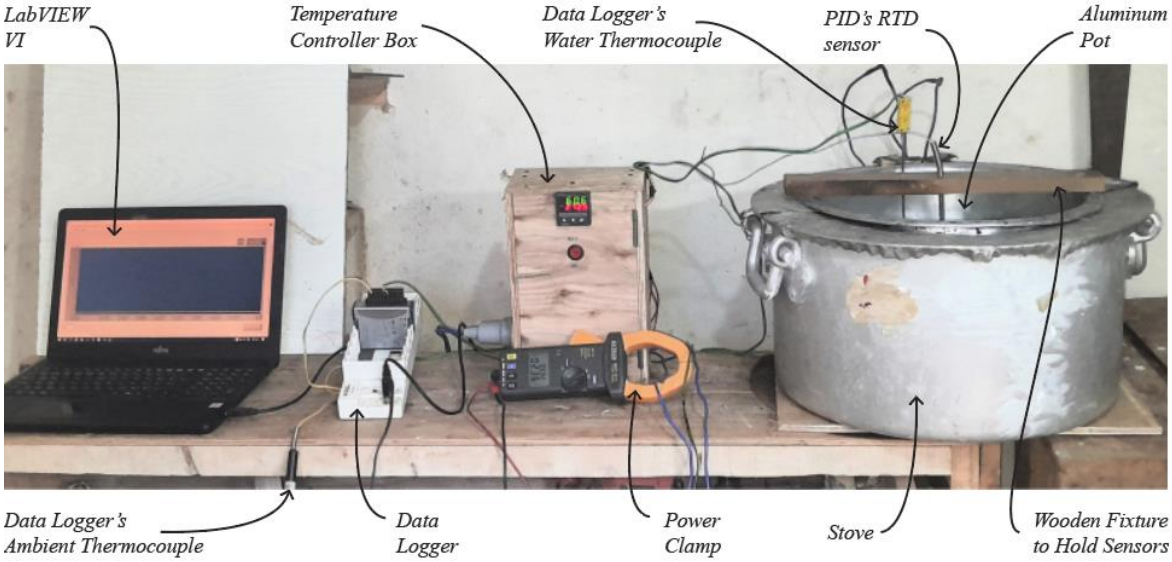

Figure 5.1: Water Boiling Test (WBT) experimental setup

5.3 Testing Methodology for WBT

The Water Boiling Test (WBT) is conducted under two conditions: the cold start and the hot start. In the cold start, both the stove and the water begin at room temperature, this test strictly follows the Ethiopian Standards Agency (2018) protocol. The hot start test begins immediately after completing the cold start test, using a fresh batch of room-temperature water while the stove remains hot from the previous test. Distillers typically carry out 4 to 5 consecutive distillations each day, with only the first distillation starting from a cold state, while all subsequent batches begin under hot start conditions. To provide a more thorough evaluation of the stove's performance across varying operating conditions and better represent real-world usage, the hot start test was included in the assessment.

Prior to the test, the local boiling temperature of water was determined experimentally by bringing water to a boil and measuring the temperature using a PID controller and a PT100 temperature sensor. The measured boiling temperature was found to be 90.1°C. This result can be cross-checked using the known formula (Eq. 5.1), which estimates boiling temperature based on altitude. For the reported altitude of 2805 m for Debre Berhan, the formula predicts a boiling temperature of 90.5°C.

$$Boiling\ Point = (100 - \frac{Altitude}{300}) \quad (5.1)$$

The tests begin by filling the saucepan (Aluminum pot) with 5 kg of water, ensuring that both the stove and saucepan are at ambient temperature. The saucepan, without a lid, is then placed centrally on the cooking zone. The thermocouples are inserted at the center of the pot secured with a fixture as shown in figure 5.1. Once all preparations are complete and testing setup checked, the test commences by activating the stove and all measurement instruments. Data collection then begins.

5.4 Data Collection and Analysis for WBT

Time, energy reading, and water temperature were recorded at the start and when the water reached boiling point. The final water weight was measured to account for evaporation. The full set of data recorded at the start and upon reaching the boiling temperature is presented in the table below. The table is applicable for both cold and hot start tests.

Table 5.1: Test Data Collection Format (Ethiopian Standards Agency, 2018)

	Cold Start			Hot Start		
Parameters	Test - 1	Test - 2	Test - 3	Test - 1	Test - 2	Test - 3
Date						
Stove Rated Power, P (kW)						
Initial Readings						
Initial Ambient Air Temperature, $T_{am,i}$ (°C)						
Initial Water Temperature, T_1 (°C)						
Initial Weight of Water, W_1 (g)						
Starting Time, t_1 (H:M:S)						

Final Readings and Initial Analysis						
Final Ambient Air Temperature, $T_{am,f}$ (°C)						
Final Weight of water, W_2 (g)						
Boiling Temperature, T_b (°C)						
Time for Boiling ($t_2 - t_1$), t (min)						
Energy Input/Consumed ($E_2 - E_1$), E (kWh)						

*Where t_1, t_2 and E_1, E_2 are time and energy (kWh) readings at the start and end of the test.

The test was repeated at least three times for both cold and hot start tests for consistency, with any inconsistent data being discarded due to external interference. Then, the test results are analyzed based on the following formulas.

Table 5.2: Formula for WBT result analysis (Ethiopian Standards Agency, 2018)

Parameter	Formula	Equation no.
Temperature corrected Time to Boil (min)	$Time\ to\ Boil * 75/(T_b - T_1)$	(5.2)
Energy Output (kWh)	$\left(\frac{W_1}{1000} * 4.186(T_2 - T_1) + 2.26 * (W_1 - W_2)\right)/3600$	(5.3)
Power Input (kW)	$\frac{Energy\ Input}{(Time\ to\ Boil/60)}$	(5.4)
Power Output (kW)	$\frac{Energy\ Output}{(Time\ to\ Boil/60)}$	(5.5)
Efficiency (%)	$\left(\frac{Energy\ Output}{Energy\ Input}\right) * 100\%$	(5.6)
Temperature corrected Time to Boil (min/kg)	$\frac{Time\ to\ Boil}{(W_1 * 1000)}$	(5.7)
Specific Energy Consumption (kWh/kg)	$\frac{Energy\ Input}{(W_1 * 1000)}$	(5.8)

5.5 Experimental Setup for Controlled Cooking Test

The Control Cooking Test (CCT) setup consists of the distillation prototype stove, a clay pot with lid, and the condenser assembly. During distillation, the clay pot, pot lid, and condenser are sealed together using dough. The clay pot has a capacity to hold 12 liters of mash. An aluminum bottle is used to collect the areke product.

The stove assembly includes a bowl housing the heating element and fiberglass insulation,

all fit inside an aluminum pot (providing support). The stove is connected to a PID temperature controller box to regulates the power based on the set temperature of the vapor entering the condenser. This box, detailed in the manufacturing chapter, incorporates a PID controller, solid-state relay (SSR), socket, RTD (PT100), and a switch.

The RTD (Pt100) sensor is positioned at the pot lid, specifically at the entry point where the areke vapor enters the condenser. This placement is crucial to make sure the PID controller measures the vapor temperature that will be condensed to areke.

During the test, temperature data tracking occurs at Four points along the distillation setup using the data logger (NI Cdaq-9172 Chassis with NI9211(A) thermocouple module) with K-type thermocouples. The sensors were placed: inside the stove to measure heating element temperature, at the pot lid alongside the PID's RTD to measure vapor temperature, suspended in air to measure ambient temperature and inside the shell and tube condenser or water bath condenser to measure condenser liquid (water) temperature over time.

The setup employs a traditional water bath condenser, where the aluminum collection bottle is immersed in a water bath. To modernize the system, the traditional bamboo tube, traditionally used as vapor channel instead of condenser, is modified to a shell and tube condenser. This upgrade aims to modernize the system and evaluate whether the bamboo shell-and-tube condenser alone is adequate for effective condensation. A power meter and power clamp-on meter are utilized to measure energy consumption and active power.

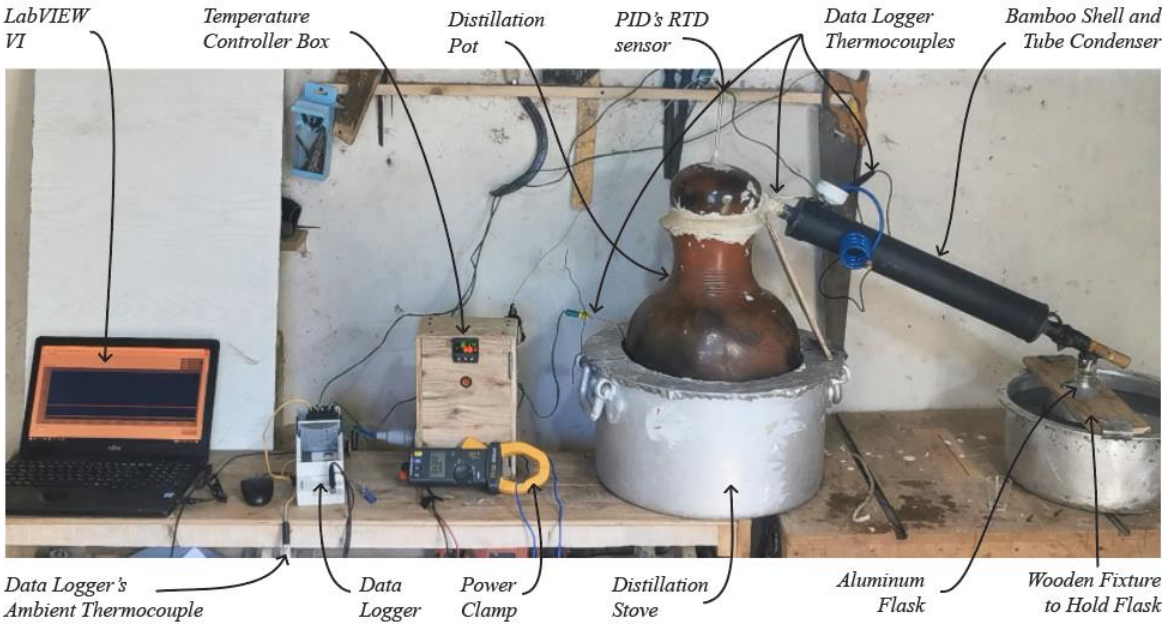

Figure 5.2: Control Cooking Test (CCT) experimental setup.

5.6 Testing Methodology for CCT

The distillation process begins by filling the clay pot with 12 liters of mash. The pot is placed on the stove, and a temperature sensor is attached to monitor the stove temperature throughout the operation. The data logger is initiated, and the stove is powered on with the PID controller set to 60°C.

During the initial heating phase, the pot lid is secured and sealed with dough. Two temperature sensors are inserted through the lid and sealed with dough: a PT100 sensor for the PID controller and a K-type thermocouple for the data logger.

The shell and tube condenser are then attached and sealed to the pot lid with dough. An aluminum bottle collector is positioned at the condenser's outlet and submerged in a water-filled bowl, serving as a secondary water bath condenser. Temperature sensors are then installed on the condensers. Water is added to the condensers at the start, with periodic replacement of warm water with cold water through a siphoning system to maintain effective cooling.

The distillation process is monitored using both PID controller and data logger. When the vapor temperature reaches the initial set point of 60°C, the PID temperature is increased to 70°C. The actual distillation begins once the vapor temperature reaches around 70°C. The temperature is then gradually increased by 2-3 degrees based on monitoring the product flow rate. As the flow rate decreases, the set temperature is incrementally raised. The process is terminated when either the vapor temperature reaches 90°C or the collected product volume reaches 1.5 liters. Finally, the alcohol samples were sent to the Debre Berhan University Chemical Laboratory for alcohol content analysis.

5.7 Data Collection and Analysis for CCT

To gain insights into traditional areke distillation practices, local distillers were interviewed. Data on biomass consumption, monthly production and sales, frequency and extent of product loss, and other relevant operational details were collected. Additionally, direct process observation enabled close monitoring of traditional distillation, capturing key parameters such as total distillation time, product volume, and temperature progression with time. Due to the absence of electrical infrastructure, temperature data was manually recorded at one-minute intervals using a Fluke 568 IR Thermometer with a K-type

thermocouple extension, allowing for comprehensive documentation of the temperature profile throughout the distillation process.

During the test, data acquisition was performed using a National Instruments cDAQ-9172 Chassis equipped with an NI9211(A) thermocouple module. The data logging system was programmed using LabVIEW 2017, running the NI-DAQmx 17.0 driver, which is the final version compatible with this specific hardware configuration. The data was collected at intervals of 10 seconds. For reference and reproducibility, the LabVIEW Virtual Instrument (VI) developed for this setup has been included in the appendix B.

Three consecutive Control Cooking Tests (CCTs) were conducted, with modifications made to the setup and components after each iteration to refine the process and achieve a high-quality product. A detailed overview of these modifications and their corresponding results is presented in the Results and Discussion chapter. The collected data was analyzed using Microsoft Excel.

Chapter 6

Result and Discussion

6.1 Water Boiling Test Result

The Water Boiling Test (WBT), as briefly described in the Materials and Methods chapter, includes cold and hot start phases. In cold start, both stove and water begin at room temperature. The cold start test strictly adheres to Ethiopian standard ES 6053:2018. Hot start follows immediately after the cold start test, using fresh room-temperature water while the stove remains hot.

During the tests, the grid voltage was on the lower side, fluctuating between 165-190 volts, while the grid was supposed to deliver 200-240 volts. As a result, the stove could not operate at its designed power of 3 kW. Presented below are two graphs displaying the power consumption over time during the first cold and hot start Water Boiling Tests (WBT).

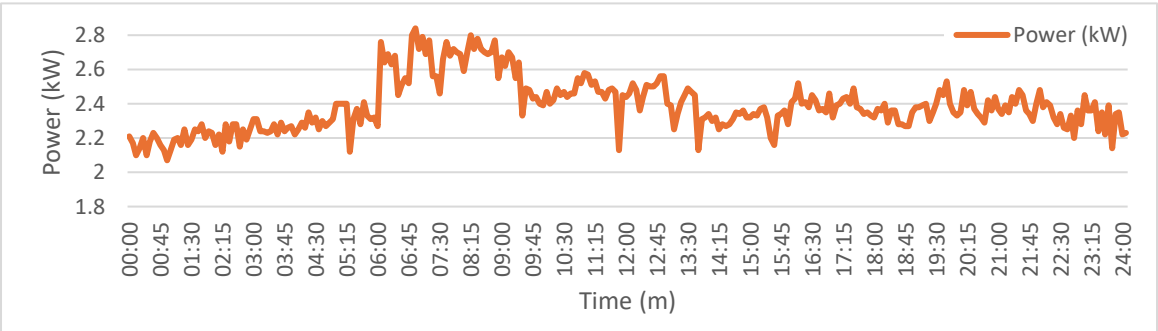

Figure 6.1: Power consumption over time for cold start WBT

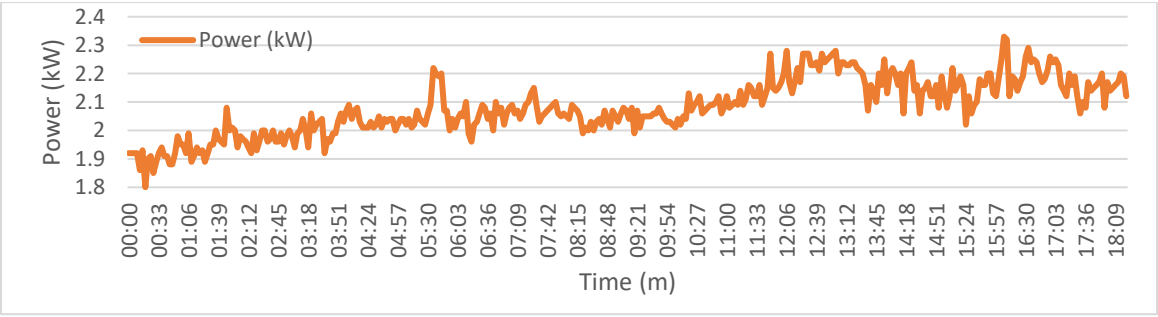

Figure 6.2: Power consumption over time for hot start WBT

The total electrical energy consumed during each test was determined by calculating the area under the corresponding power-time curve (Figures 6.1 and 6.2). This was achieved through numerical integration using the trapezoidal rule, a standard method for approximating the area under a curve from a set of discrete data points.

The calculation was performed in Microsoft Excel. With power readings (P) taken every 1 seconds (Δt), the energy for each small-time step was calculated as:

$$Energy\ step\ (kWh) = \left(\frac{P_i + P_{(i+1)}}{2}\right)\left(\frac{\Delta t}{3600}\right) \quad (6.1)$$

Where P_i is the power reading at the beginning of a time interval, $P_{(i+1)}$ is the power reading at the end of that time interval, and Δt is the 10-second interval converted to hours. The total energy consumed for the entire test was then found by summing the energy values from all the individual time steps. As a result, the cold start test used 0.92 kWh, 0.88 kWh, and 0.91 kWh for the first, second, and third tests, respectively. In contrast, the hot start test consumed 0.6 kWh, 0.62 kWh, and 0.59 kWh for the corresponding tests. The table below presents the initial and final readings for the water boiling tests.

Table 6.1: Cold and hot start water boiling test readings

	Cold Start				**Hot Start**			
Parameters	Test - 1	Test - 2	Test - 3	Avg.	Test - 1	Test - 2	Test - 3	Avg.
Date	21/10/24	24/11/24	25/11/24	-	21/10/24	24/11/24	25/11/24	-
Stove Rated Power, P (kW)	3							
Initial Readings								
Starting Time, t_1 (H:M:S)	3:39:54 PM	3:41:25 PM	3:20:14 PM	-	4:36:43 PM	4:07:38 PM	3:47:24 PM	-
Initial Ambient Air Temperature, $T_{am,i}$ (°C)	16.3	16.7	16.6	-	18.2	18.1	18.2	-
Initial Water Temperature, T_1 (°C)	16.6	16.8	16.9	16.77	19.3	18.9	18.5	18.9
Initial Weight of Water, W_1 (g)	5000							
Final Readings and Initial Analysis								
Final Ambient Air Temperature, $T_{am,f}$ (°C)	17.7	17.9	18.2	-	19.2	19.5	18.9	-
Final Weight of water, W_2 (g)	4940	4930	4920	4930	4915	4910	4920	4915
Boiling Temperature, T_b (°C)	90							
Time for Boiling ($t_2 - t_1$), t (mm:ss)	24:14	24:01	24:25	24:13	19:15	19:00	18:40	18:58

Energy Input/Consumed ($E_2 - E_1$), E (kWh)	0.92	0.88	0.91	0.9	0.62	0.62	0.59	0.61

By analyzing the recorded readings and applying equations from 5.2 to 5.8, the performance of the stove was evaluated and tabulated in table 6.2.

Table 6.2: Test result analysis

Parameter	**Cold Start**	**Hot Start**
Temperature corrected Time to Boil (mm: ss)	24:48	20:01
Efficiency	52.22 %	75.8 %
Temperature corrected Time to Boil	4.84 min/kg	3.79 min/kg
Specific Energy Consumption	0.18 kWh/kg	0.12 kWh/kg
Energy Input	0.9 kWh	0.61 kWh
Energy Output	0.47 kWh	0.47 kWh
Power Input	2.23 kW	1.93 kW
Power Output	1.16 kW	1.49 kW

* Specific heat capacity of water = 4.186 kJ/kg, Latent heat of vaporization = 2.26 kJ/g

The following graphs illustrate the temperature progression over time for the first cold and hot start tests. This graph serves to highlight the typical heating pattern observed during tests.

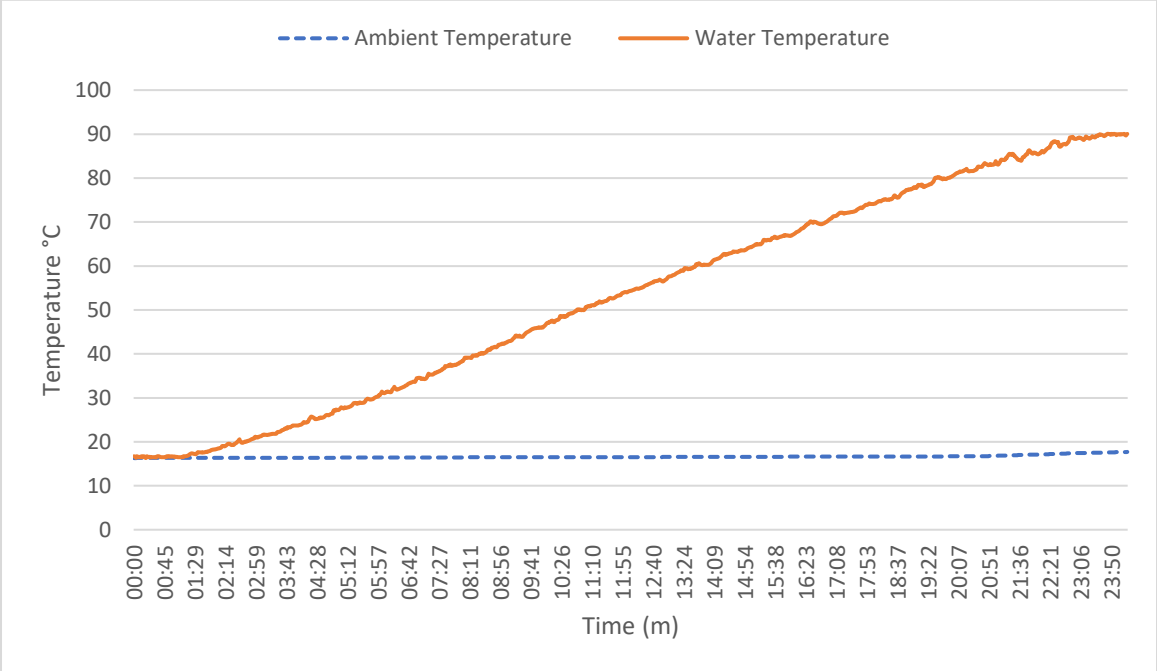

Figure 6.3: Temperature vs. Time for Cold Start Water Boiling Test

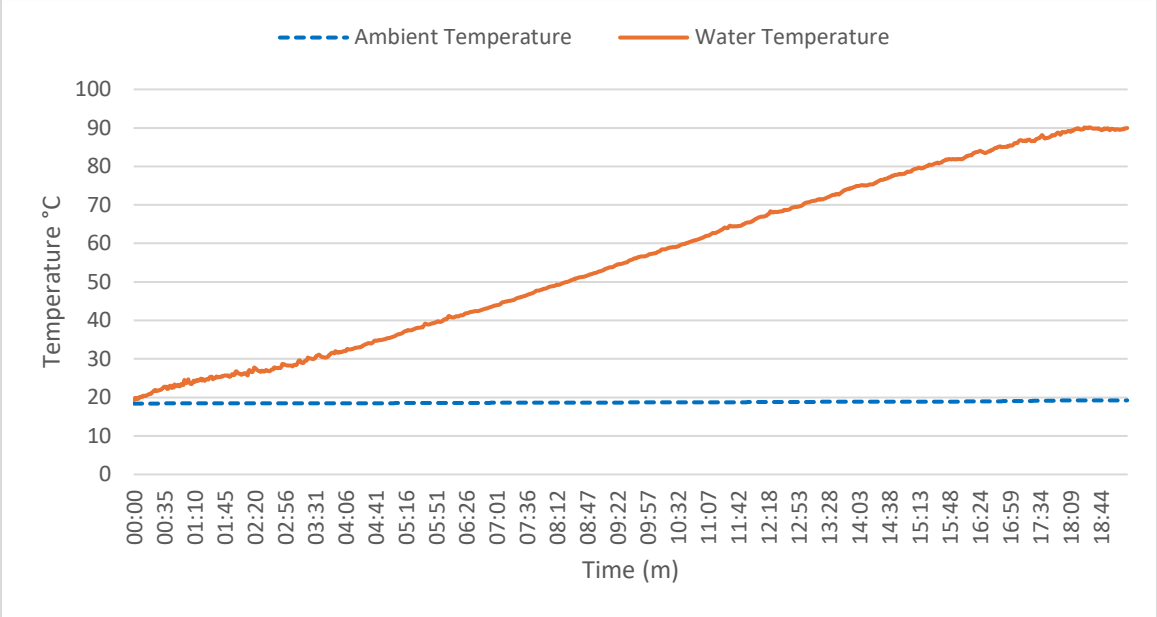

Figure 6.4: Temperature vs. Time for hot Start Water Boiling Test

The temperature-time graph for both the cold and hot Start WBT demonstrates a linear progression, indicating a steady rate of temperature increase as the water approaches its boiling point. This implies that the energy supplied to the water is being used efficiently to raise its temperature without significant losses or changes in the heating rate. The linearity also implies minimal temperature fluctuations, reinforcing the stove's efficiency and predictability in achieving boiling under similar conditions.

The custom designed and fabricated areke distillation stove demonstrated a thermal efficiency of 52.2% during cold start conditions. During hot start conditions, the efficiency further increased to 75.8%. This substantial improvement can be attributed to the thermal properties of the stove's clay construction material. during cold start, the clay initially absorbs substantial thermal energy to reach operational temperature, reducing efficiency. This effect diminishes during hot start operation.

These efficiency values exceed the minimum 40% efficiency set by the Ethiopian Standards Agency (2018) and considerably surpass biomass areke stoves like three stone fire (10-20% efficiency), mud stoves (14-15.4% efficiency) and mirt stoves (16-23% efficiency), as well as outperforming typical commercial modern resistance coil cookstoves (39.3-60% efficiency) as illustrated in the thermal efficiency comparison chart (Figure 6.5). The enhanced efficiency compared to commercial resistance coil stoves can be attributed to the stove's tailored design and fit to the distillation pot and adequate insulation, as these stoves lack

insulation and are designed to accommodate a variety of pot designs. The thermal efficiency of various stove types is summarized in Section 2.4 of the literature review chapter.

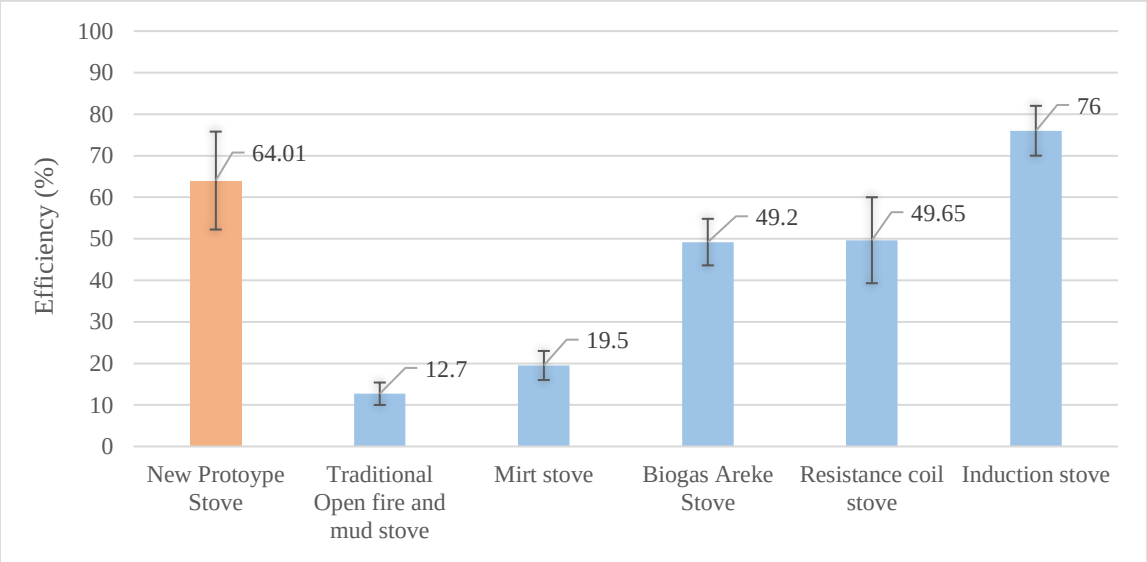

Figure 6.5: Thermal efficiency comparison chart

Considering that distillers often perform 4 to 5 consecutive distillations daily, with only the first distillation operating under cold start conditions, subsequent batches benefit from the hot start efficiency of 75.8%. Consequently, the overall daily operational efficiency of the stove is predominantly governed by its superior hot start performance.

It is important to note that differences in research methods (efficiency calculation methods), testing conditions, and other factors can make it challenging to directly compare the efficiency of stoves across various studies. While this comparison provides valuable insights into stove performance, it was essential to consider these limitations when interpreting the results.

6.2 Energy Usage analysis of the Traditional Areke Distillation Stove

In this section the energy consumption of a traditional distillation stoves (in the study area of Debre Berhan) per 1.5 liters of areke is calculated for the purpose of comparing it with the performance of the prototype.

The thermal efficiency of open fire stoves typically ranges from 10-20% (Ikpambese et al., 2014; Koffi et al., 2014; Someswararao et al., 2012; Tesfay et al., 2024). Traditional

cookstoves, locally made from mud or metal, are slightly more fuel-efficient than the three-stone fire (Koffi et al., 2014). The commonly used mud stoves in the study area, as depicted in figure 6.6, are mud stoves. Given the design and performance characteristics of such stoves a conservative 20% efficiency is assumed for the analysis.

The stove consumed 68 kg of dry eucalyptus wood to distill 20 liters of areke, as measured during the study. The calorific value of dry eucalyptus wood is taken as 18,000 kJ/kg (Sibongiseni et al., 2024; Biomass Connect, n.d.; The SHORTFOR research project, n.d.).

Figure 6.6: Traditional distillation mud stove taken at (a) location 1, and (b) location 2.

6.2.1 Total Energy Calculation

The total energy released by the biomass is calculated using the formula:

$$E_{total} = W * CV \tag{6.2}$$

The total energy released by the biomass (E_{total}) is calculated based on the weight of the biomass (W) and the calorific value of eucalyptus wood biomass (CV), both measured in kilojoules. Substituting the values into the formula, with W = 68 kg and CV = 18,000 kJ/kg, the total energy released by 68 kg of eucalyptus wood biomass is E_{total} = 1,224,000 kJ.

6.2.2 Usable Energy Calculation

The usable energy accounts for the stove's thermal efficiency. It is calculated using:

$$E_{usable} = E_{total} * \eta \tag{6.3}$$

The usable energy (E_{usable}) represents the portion of the total energy effectively utilized by the stove, calculated by factoring in the thermal efficiency (η) of the stove, which is 20%

or 0.20. Substituting the values into the formula, the usable energy for the system is E_{usable} = 244,800 kJ.

6.2.3 Energy Usage per Batch

Since 60 kg of biomass is used to distill 20 liters of areke, the energy usage for one batch of 1.5 liters can be calculated as:

$$E_{batch\ total} = \left(\frac{E_{total}}{V}\right) * V_{batch} \tag{6.4}$$

$$E_{batch\ usable} = \left(\frac{E_{usable}}{V}\right) * V_{batch} \tag{6.5}$$

Where V represents the total volume of areke produced (20 liters) and V_{batch} denotes the batch volume (1.5 liters). Substituting these values, the total energy required for one batch of 1.5 liters is $E_{batch\ total}$ = 91,800 kJ, while the usable energy for the same batch is $E_{batch\ usable}$ = 18,360 kJ.

To compare with electrical energy, converting the energy values to kilowatt-hours (kWh), where 1 kWh=3,600kJ, $E_{batch\ total}$ (kWh) = 25.5 kWh and $E_{batch\ usable}$ (kWh) = 5.1 kWh.

These values will serve as a benchmark for evaluating the energy performance of the electric distillation stove discussed in subsequent sections.

6.3 Control Cooking Test Result

The Control Cooking Test (CCT) evaluates the performance of the stove and condenser during distillation under controlled conditions, simulating real-world usage scenarios. The mash used in the distillation is sourced from local producers. A total of three tests have been conducted. After each test, certain aspects of the setup and components were modified to achieve a desired and high-quality product in the final test.

6.3.1 Initial Test Results

For the first test heating element coil configuration shown in Figure 4.5 were employed. In this arrangement, the stove's heating element coil was wrapped around the clay bowl, allowing heat transfer to the distillation pot from both its lateral sides and base. This design was chosen to ensure more uniform heat distribution and maximize the heating surface area in contact with the distillation pot.

Temperature Profiles and Condensation Behavior:

Temperature variations during CCT-1 of vapor, condenser and ambient temperature are illustrated in Figure 6.7. Cooling water was applied to both the shell and tube condenser and a water bath condenser. Due to the slower distillation rate and consequently reduced vapor flow, condensation primarily occurred in the shell and tube condenser rather than in the water bath condenser - a deviation from traditional patterns. The temperature curve in Figure 6.7 reflects the shell and tube condenser's water temperature. The water bath condenser's temperature remained relatively stable throughout this test. Periodic replacement of the condenser water maintained efficient condensation as shown in the condenser temperature profile of figure 6.7. For this initial test, the condenser water was pre-chilled in a freezer to ensure maximum vapor condensation, although subsequent tests demonstrated room temperature water was equally effective.

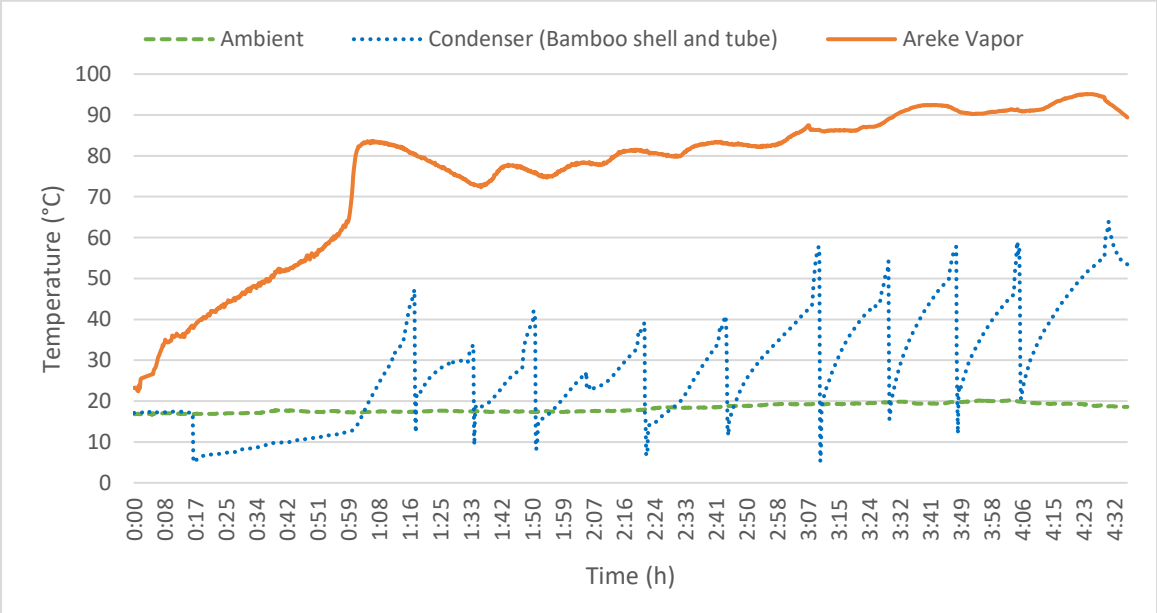

Figure 6.7: Temperature profiles at key locations during initial test.

Temperature Profile Comparison with Traditional Method:

To evaluate the prototype's performance against traditional methods, the vapor temperature progression curve from CCT-1 was plotted alongside data collected from local traditional distillers, as shown in Figure 6.8. This curve acts as a baseline for evaluating the performance of the electrical stove prototype.

This comparison reveals comparable durations for both the prototype and traditional methods to reach the distillation commencement temperature of approximately 80°C, indicating similar heating characteristics and thermal response.

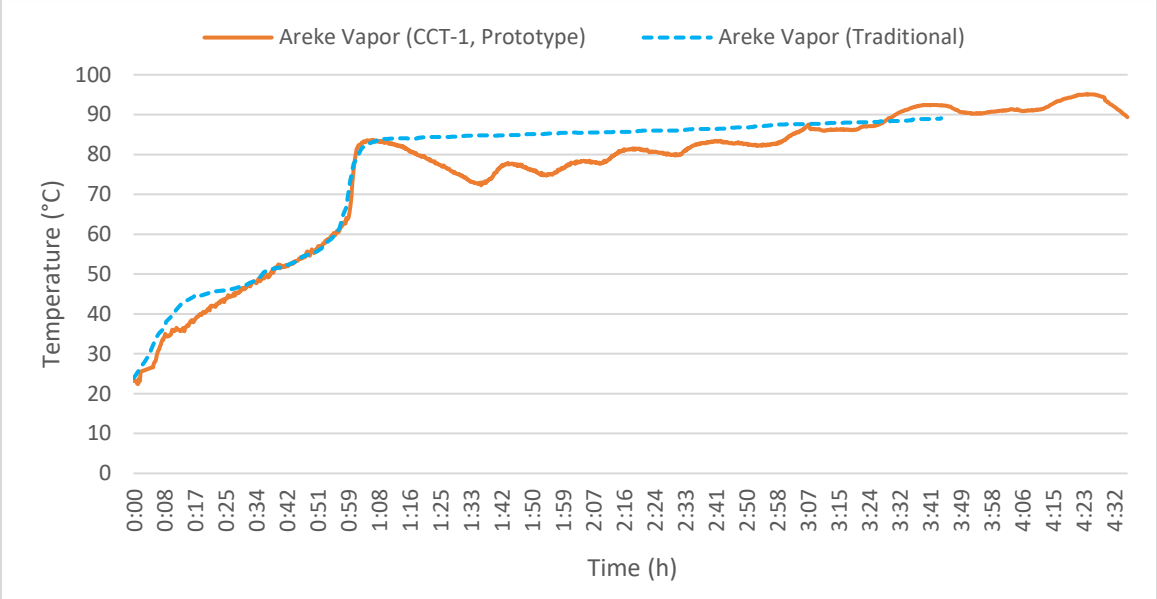

Figure 6.8: Temperature profile comparison: new (Initial test) vs. traditional method

In both prototype and traditional distillation, the vapor temperature rises rapidly from around 60–80°C but naturally slows after approximately 82°C, suggesting that this behavior could be an inherent characteristic of areke vapor during distillation. A separate test in Debre Berhan showed areke vapor begins boiling at ~70°C, where ethanol concentration is highest. In the traditional temperature curve (with no precise temperature controller), distillation (dripping) started at about 81–82°C and continue to ~89°C, whereas the prototype, despite an initial rise to ~80°C, was able to control the temperature down to ~72°C, capturing high-ethanol vapor (70–82°C) and continuing distillation to ~91°C.

Although distillation was carried out up to 91°C, compared to the traditional 89°C, this approach produced a higher-alcohol-content areke but extended the distillation time relative to traditional methods. Local distillers recognize slow distillation improves quality but often prioritize speed for business practicality. The rapid 60–80°C rise was likely due to the clay stove's thermal inertia and it made it challenging for effective PID temperature control.

Heating Element Temperature Profile:

The heating element temperature profile over time during CCT-1 is presented in Figure 6.9, illustrating the thermal behavior of the heating system. This data is presented independently due to its significantly higher temperature range. The heating element temperature data is essential for analyzing and comparing heating profiles. Examining how each test manages heating temperature over time helps identify differences in response times, stability, power

consumption, and energy efficiency. This comparison provides valuable insights into the impact of heating temperature on product quality, enabling informed decisions to optimize cooking methods for improved outcomes.

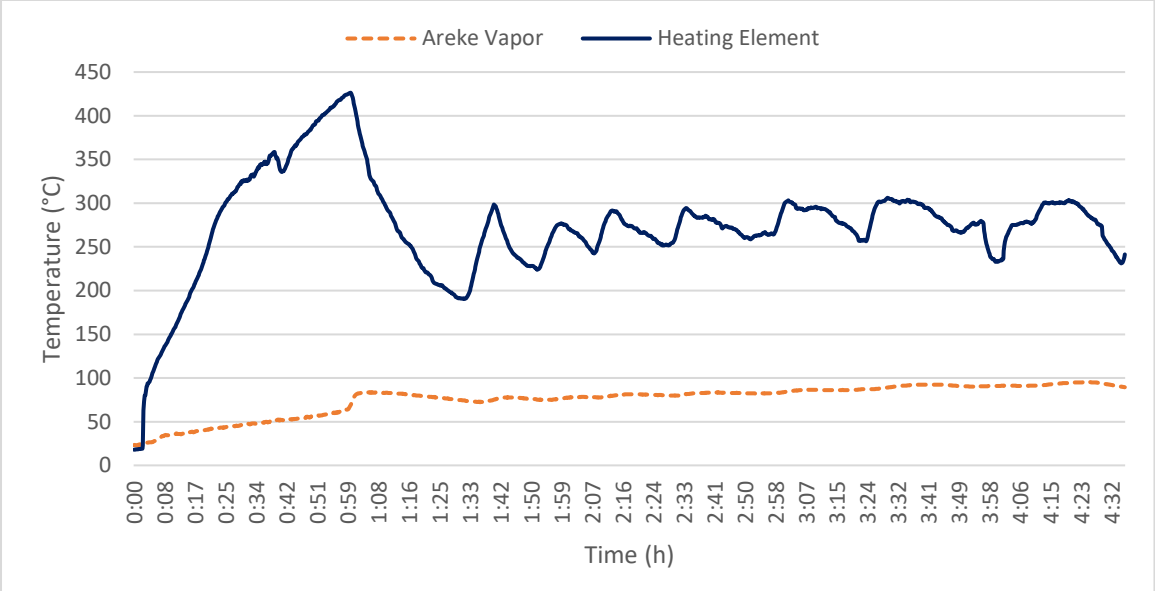

Figure 6.9: Initial test heating element temperature profile

Test Performance Summary:

The first test consumed 8.3 kWh of energy and yielded 1.55 liters of areke from 12 liters of mash. This yield slightly exceeded the expected 1.5 liters from traditional processes. However, the product exhibited an undesirable red tint, a quality issue targeted for improvement in subsequent tests. CCT-1 distillation time was 4 hours and 35 minutes, longer than the traditional 3 hours and 44 minutes.

6.3.2 Modifications and Second Test (CCT - 2)

Following the initial test (CCT-1), an investigation was conducted to address the undesirable red tint observed in the areke product. Consultation with a local areke producer involved in the project identified two potential causes: mash scorching due to excessive heat on the pot sides and potential coloration contribution from the new clay pot and bamboo tube. Further investigation indicated that traditional distillation methods primarily concentrate heat at the pot's bottom, with minimal heat distribution along the sides.

Modifications:

To reduce mash scorching and coloration in CCT-2, the heating element coil was rearranged to concentrate heat at the bottom of the pot, mimicking traditional methods.

Additionally, the new pot and bamboo were thoroughly cleaned by a local distiller to eliminate any potential contribution to the coloration.

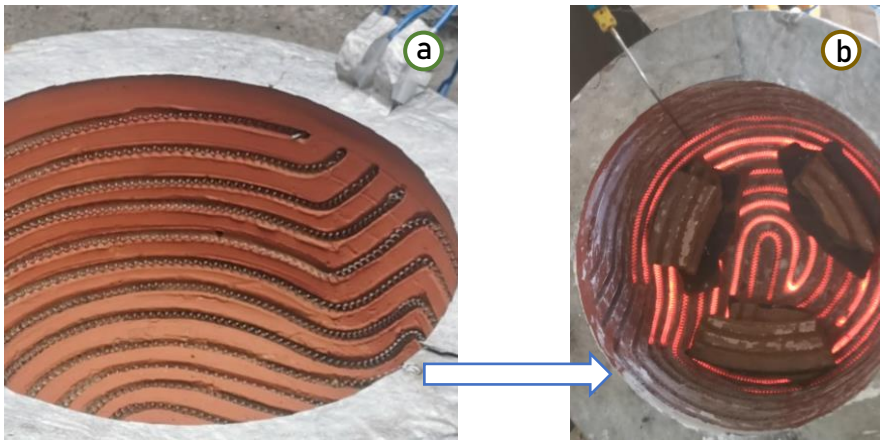

Figure 6.10: Heating element coil arrangement modification: (a) old, (b) modified.

Temperature Profiles and Condensation Behavior:

Figure 6.11 illustrates the temperature variations at key locations during CCT-2. The condenser temperature curve in Figure 6.11 reflects the performance of the shell and tube condenser. However, in contrast to CCT-1, the water bath condenser in CCT-2 reached a slightly higher temperature of 50°C by the end of the distillation process.

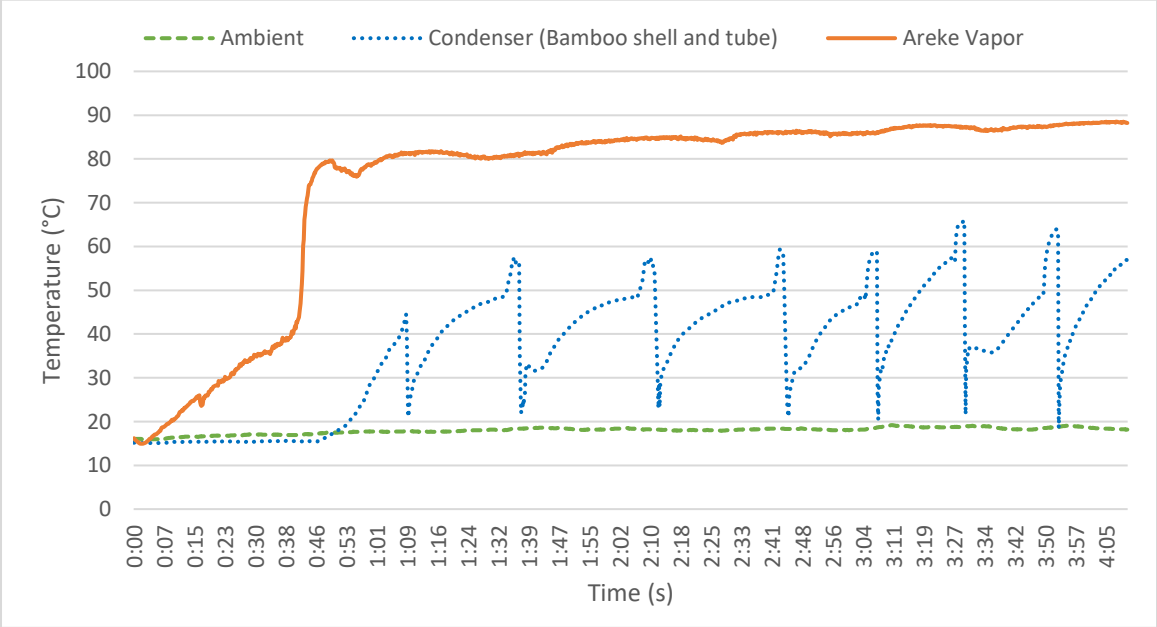

Figure 6.11: Temperature profiles at key locations during second test.

Temperature Profile Comparison with Traditional Method:

Instead of initiating distillation at lower temperatures between (70-80°C), this test aimed to replicate the traditional distillation method as depicted in figure 6.12.

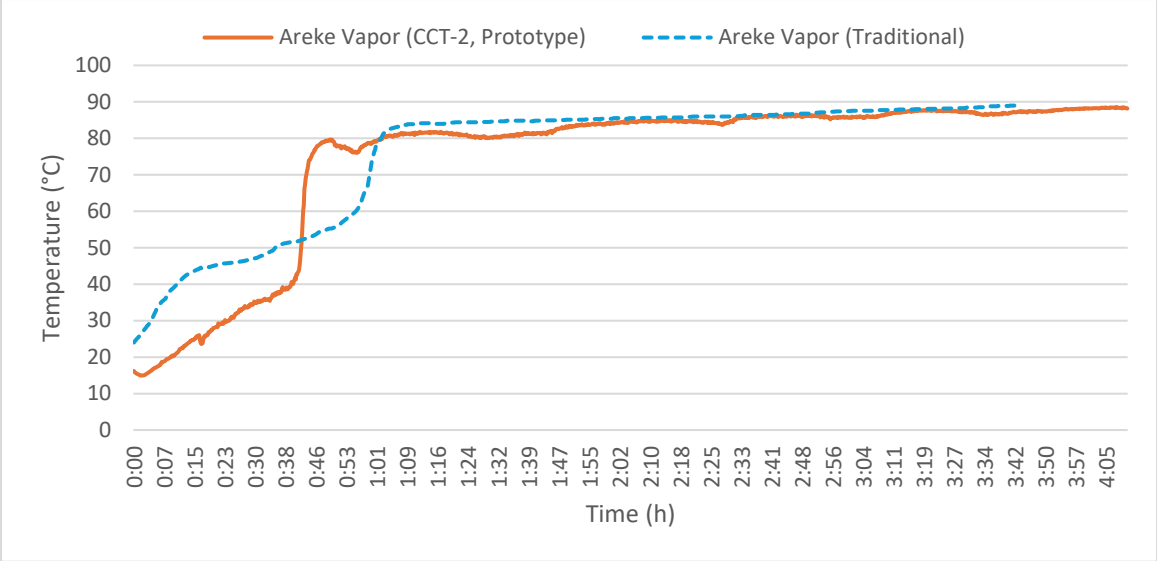

Figure 6.12: Temperature profile comparison: new (second test) vs. traditional method

While the overall distillation time remained comparable, the initial heating phase (time until distillation began) was shorter for the prototype in CCT-2 compared to traditional methods. Conversely, the distillation phase itself took longer to produce the same amount of areke, resulting in a product with a slightly higher alcohol content than traditional areke.

Heating Element Temperature Profile:

Figure 6.13 illustrate the thermal behavior of the heating system with the modified coil arrangement. As shown in Figure 6.13, the heating element temperature remained, on average, at 325°C during most of the distillation phase. This test utilized a higher average temperature compared to the previous test (CCT-1), which was around 275°C, resulting in a reduction of the distillation time by 8.36%.

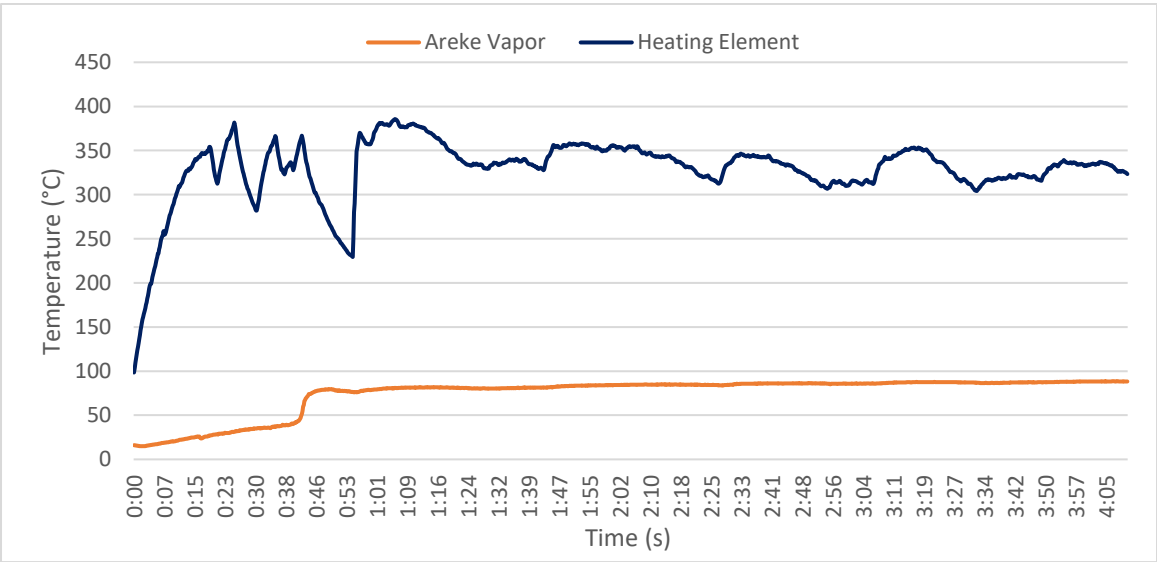

Figure 6.13: Second test heating element temperature profile

Test Performance Summary:

CCT-2 consumed 7.8 kWh of energy and took 4 hours and 12 minutes to distill 1.5 liters of areke. The coloration of the areke product was reduced but not entirely eliminated in CCT-2.

6.3.3 Final Process Optimization and Third Test

Despite the process modifications implemented for CCT-2, the areke product still exhibited some coloration, although much reduced compared to CCT-1. Upon inspection, mash scorching was still observed on the mash surface, indicating heat exposure to the pot sides despite repositioning the heating element to focus primarily on the bottom, as the insulation directed heat upward, causing it to escape at the stove top and warm the pot's sides along the way.

Setup Modifications:

To further minimize heat exposure to the pot sides and eliminate mash scorching, a final process optimization was introduced for the third Control Cooking Test (CCT-3): pot elevation. As illustrated in Figure 6.14, the clay pot was elevated by placing clay fragment supports underneath it. Clay fragments were also used to seal the gap created between the stove and the pot, providing additional insulation and preventing heat from reaching the pot sides.

Figure 6.14: Pot placement modification

The temperature variations of vapor, condenser and ambient temperature during the third test are illustrated in the following graph.

Temperature Profiles and Condensation Behavior:

In contrast to the previous two tests, the condenser temperature curve in Figure 6.15 reflects the performance of the water bath condenser. Due to an increased vapor flow rate in CCT-3, the shell and tube condenser alone became ineffective. Consequently, both condenser types were used, with the water bath condenser acting as the primary condensation unit. This shift is attributed to the superior heat transfer properties of the aluminum collector flask in the water bath condenser compared to the bamboo tubes in the shell and tube condenser under higher vapor load conditions.

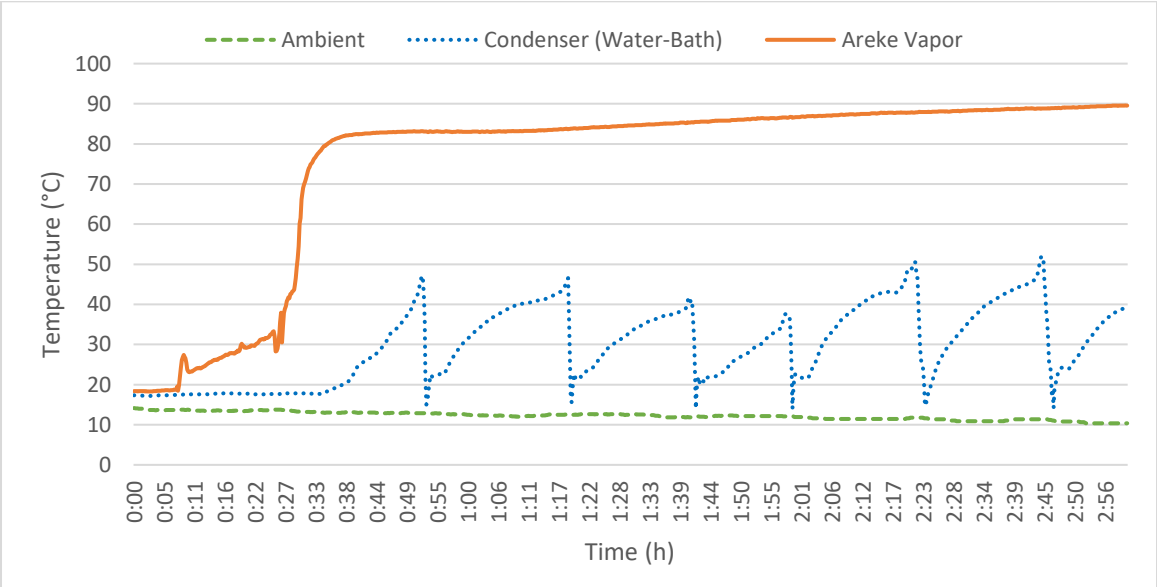

Figure 6.15: Temperature profiles at key locations during final test.

Temperature Profile Comparison with Traditional Method:

Figure 6.16 compares the vapor temperature profile of the prototype during CCT-3 against that of traditional distillation methods. The primary distillation phase in CCT-3, similar to traditional methods, occurred within the 80-90°C temperature range. However, the distillation process in CCT-3 was notably quicker, resulting, as expected, in a slightly lower alcohol content in the final areke product compared to traditionally distilled areke from the same mash. The initial heating phase, time up to the start of distillation, in CCT-3 was nearly halved compared to traditional methods, partially attributable to hot start conditions as CCT-3 followed immediately after CCT-2. Overall, the complete distillation process in CCT-3 finished 19.64% faster than the traditional method.

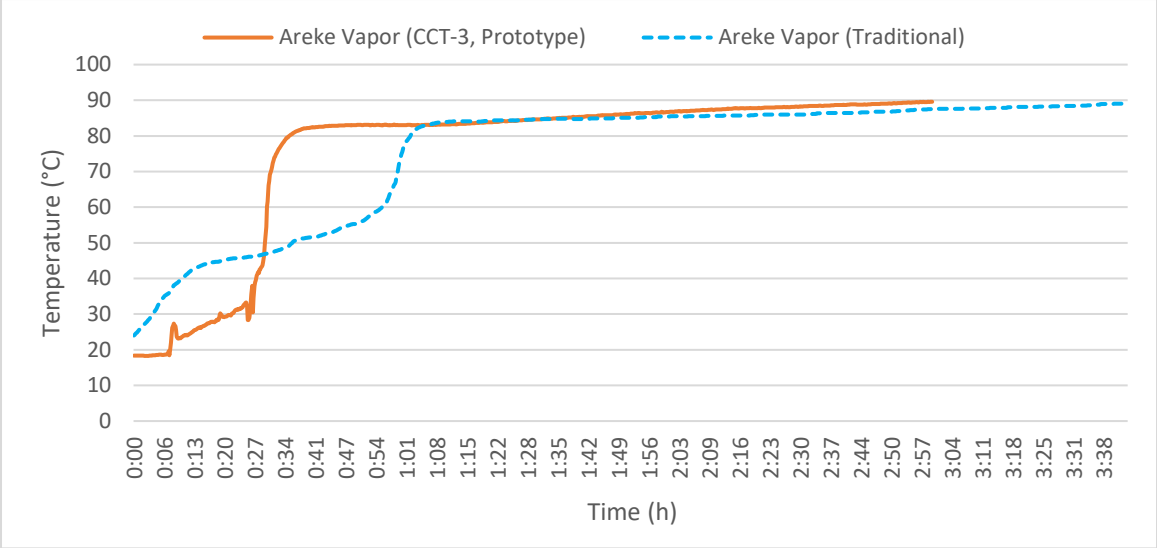

Figure 6.16: Temperature profile comparison: new (Final test) vs. traditional method

Heating Element Temperature Profile:

During the distillation phase of CCT-3, the heating element temperature was significantly elevated, fluctuating between 400-500°C, compared to previous tests. This elevated heating element temperature is considered a contributing factor to the shorter distillation time achieved in CCT-3.

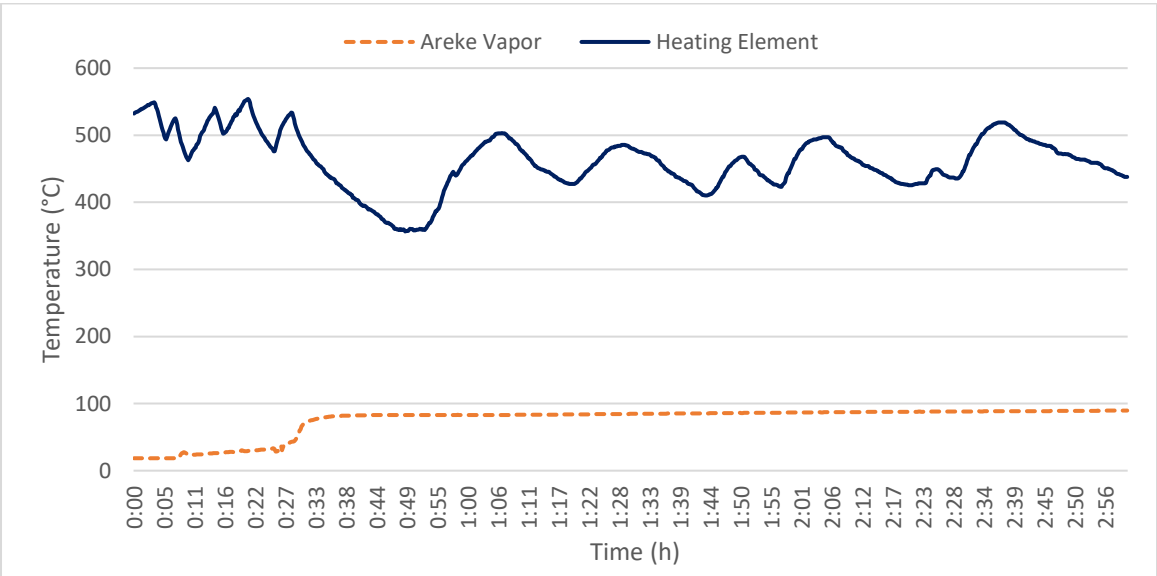

Figure 6.17: Final test heating element temperature profile

Test Performance Summary:

The areke product from CCT-3 was completely free of coloration, resulting in a pure, colorless, and ready-for-consumption product. CCT-3 consumed 7.6 kWh of energy and took 3 hours to distill 1.6 liters of areke.

6.4 Comparative Analysis of Distillation Methods

This section provides a comparative analysis of the electric distillation method against traditional methods and literature values, focusing on key performance indicators: alcohol content, distillation time, and energy cost.

6.4.1 Alcohol Content Comparison

The alcohol content of the areke produced by the prototype across the three Control Cooking Tests (CCTs) and a traditional distillation sample were measured at the Chemical Engineering Laboratory of Debre Berhan University using an Alcoolometer Cent. Gay Lussac hydrometer, calibrated at 20°C. At the time of testing, sample temperatures ranged from 19.8 to 20.1°C, closely matching the calibration temperature. Figure 6.18 visually compares the alcohol content (by volume percentage - ABV) achieved in each CCT and traditional distillation, produced from the same mash, alongside a reference literature value taken from Yohannes et al. (2013).

The electrical distillation method produced areke with alcohol content both higher and lower than that of the traditional method, varying across the three CCTs. CCT-1 yielded the highest ABV at 49%, while CCT-3 had the lowest at 42.5%. Traditional areke from the same mash measured 45% ABV. Yohannes et al. (2013) reported a lower average ABV (37.22%) for areke samples from Addis Ababa, likely due to variations in mash ABV and regional distillation processes. As observed in the three control cooking tests, the alcohol content is directly influenced by the duration of the distillation phase and the temperature at which this phase begins. The results demonstrate the prototype's capability to modulate alcohol content based on operator control of these parameters.

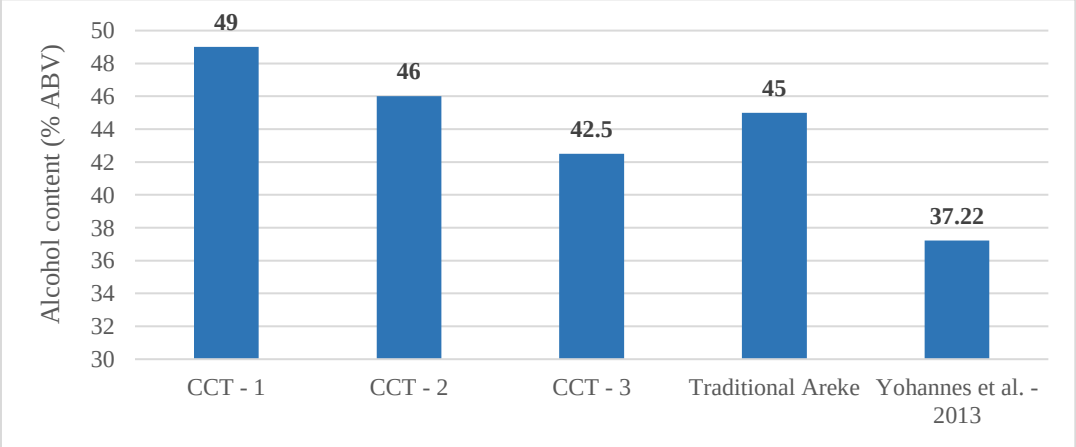

Figure 6.18: Alcohol Content Comparison: Prototype vs. Traditional

6.4.2 Distillation Time Comparison

The control cooking tests (CCTs) demonstrated the electrical stove prototype's ability to adjust distillation time to suit distiller preferences and production goals. The results indicate that the electric prototype can achieve distillation times comparable to or even shorter than traditional methods, while also offering the flexibility to extend distillation time for potentially higher alcohol content as observed in CCT-1.

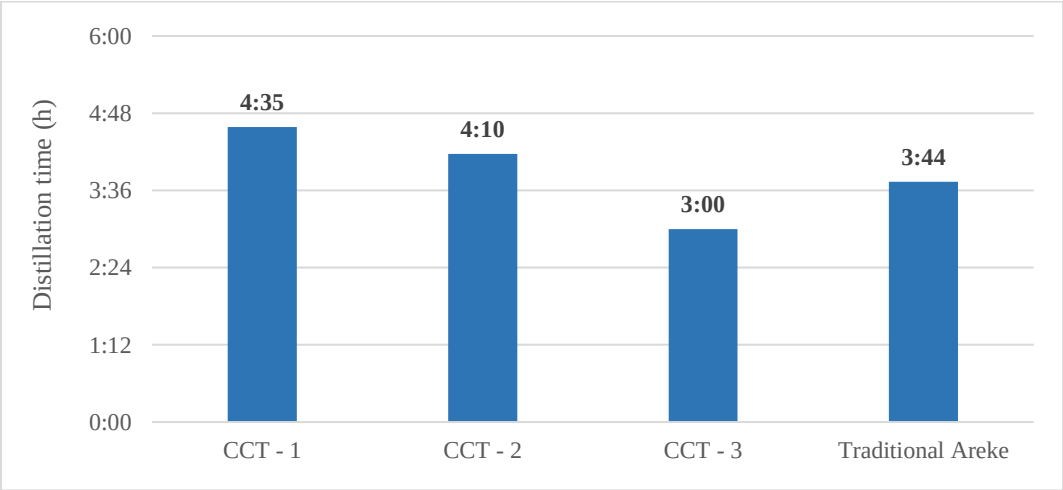

Figure 6.19: Distillation Time Comparison: Prototype vs. Traditional

6.4.3 Energy Cost Comparison

The energy consumption data from the controlled tests (CCTs) revealed an average energy consumption of 7.9 kWh to produce 1.5 liters of areke. Based on the current Ethiopian Electric Utility rate of 2.92 Birr per kWh, this translates to an electricity cost of 15.3 Birr per liter of areke. In contrast, a survey of traditional distillation practices indicated an average biomass cost of 600 Birr to produce 20 liters of areke, equivalent to 30 Birr per liter.

This comparison demonstrates a significant energy cost reduction of 49% per liter of areke with the electric prototype compared to traditional biomass-based methods. This translates to potential savings of 14.7 Birr per liter. For a typical distiller producing 200 liters of areke per month, this could result in substantial savings of 2,940 Birr per month and 35,280 Birr per year, significantly enhancing profitability.

6.5 Summary of Findings and Discussion

The Control Cooking Tests (CCTs) and Water Boiling Tests (WBTs) provided valuable insights into the performance of the electric areke distillation stove prototype. Key findings

and discussion points are summarized below:

Mash Scorching and Product Quality: Mash scorching, resulting in an undesirable red tint in the areke, was initially observed and identified as primarily occurring due to excessive heat application to the sides of the distillation pot. Modifying the heating element to focus heat at the pot's bottom and minimizing side heating effectively resolved this issue and improved product quality. This challenge is also faced by traditional distillers, as noted during discussions with local producers, who indicated that scorching is common among novice distillers and occasionally affects experienced ones as well, impacting both product consistency and profitability.

Bamboo Condenser Performance and Potential Enhancements: Bamboo was selected for the shell-and-tube condenser tubing instead of aluminum or copper, not only because of cost and sourcing challenges but also due to concerns about its potential impact on the flavor and aroma of the distilled areke. There was uncertainty about where the majority of the vapor condensed during the process. Testing traditional methods revealed that while the bamboo tube effectively transported vapor, the majority of condensation occurred within the aluminum collector flask of the water bath condenser. This finding demonstrates that the bamboo tubing does not contribute any discernible flavor or aroma to the areke product. Therefore, replacing bamboo with aluminum or copper for the condenser tube appears feasible without affecting the product’s flavor or aroma. Additionally, While the bamboo shell and tube condenser proved functional for low vapor flow rates and extended distillation durations, as the flow rate increases, bamboo struggles to condense the vapor efficiently. Thus, switching to copper or aluminum is necessary to accommodate higher flow rates.

Distillation Duration and Alcohol Content: The Control Cooking Test (CCT) provided strong evidence that the duration of the distillation process (the rate of distillation) significantly impacts the alcohol content of the final areke product. A longer distillation time generally resulted in a higher alcohol concentration in the final areke. This relationship suggests that careful control over the distillation duration is crucial for achieving the desired alcoholic strength in the final product.

areke Vapor Temperature Behavior: A distinct characteristic of areke vapor was observed in both CCTs and traditional distillation: a rapid temperature rise between 60°C and 80°C, followed by stabilization above 80–82°C, where distillation (product drip) naturally begins. In Debre Berhan, ethanol boils at approximately 70°C, and Starting distillation at this

temperature and proceeding from there may result in a higher alcohol content, as the vapor at lower temperatures contains a greater concentration of ethanol. While it was possible to force distillation at a lower temperature, doing so required a temperature controller to precisely control power.

6.6 Significance and Implications of Results

The electric areke distillation stove prototype offers significant advantages and implications for areke production and beyond:

Pollution Elimination and Health Benefits: The most significant and immediate implication of the electric distillation stove prototype is the elimination of pollution associated with traditional biomass-based areke distillation. As discussed in the literature review, the combustion of biomass fuels for distillation is a major source of harmful air pollutants that can lead to various health issues. Exposure to pollutants such as particulate matter, carbon monoxide, and other toxic emissions from traditional biomass-fired stoves has been linked to respiratory diseases, cardiovascular problems, and other serious health conditions. By adopting the electric stove and removing this source of pollution, it has the potential to significantly improve the health and well-being of areke distillers, who often operate in confined spaces with limited ventilation, carrying profound public health and environmental benefits.

Enhanced Process Control and Product Consistency: The prototype provides distillers with greater control over the distillation process, allowing for adjustments like distillation time to influence alcohol content and tailor product characteristics to market demands. This control also promotes batch-to-batch consistency, minimizing the risk of ruined batches, further maximizing profitability. Additionally, the ability to consistently stop distillation based on vapor temperature monitoring further enhances product uniformity compared to traditional methods which rely on less precise indicators like volume of product and/or the number of times the condenser water has changed. This feature of the electric stove prototype empowers distillers to achieve a level of process control and product consistency that is extremely challenging to attain with conventional biomass-fired stoves.

Energy Efficiency and Cost Reduction: The prototype's high energy efficiency, achieving 52.2% in cold start and 75.8% in hot start conditions, far surpasses traditional biomass stoves (10-23% efficiency). This translates to significant energy cost reductions for areke

distillers, potentially saving around 35,280 Birr annually for typical distillers and contributing to a more sustainable and environmentally friendly production model.

Widespread Adoption Potential: The electric stove prototype exhibits strong potential for widespread adoption due to its affordability (Priced at 17,280 Birr or less), ease of construction using locally available materials, and compatibility with traditional distillation practices. Its design seamlessly integrates with familiar clay pots, easing the transition for distillers to electric technology while preserving established methods. These factors, combined with the promise of improved efficiency, quality, and profitability, make the stove an accessible and appealing option for the areke distilling community.

Contribution to Research: This study addresses a notable research gap regarding thermal data for areke distillation. The findings contribute valuable insights into the thermal aspects of areke distillation and offer a foundational basis for future research in this area.

Chapter 7

Conclusion and Recommendation

7.1 Conclusion

This study successfully demonstrated the design, fabrication, and testing of a custom-designed electric areke distillation stove, offering a sustainable and efficient alternative to traditional biomass-based methods. The prototype directly addresses critical challenges within the local areke distillation sector, including environmental pollution, inconsistent product quality, and the high energy costs associated with biomass fuel. The custom-designed stove achieved thermal efficiencies of 52.2% during cold starts and 75.8% during hot starts, exceeding the Ethiopian standard requirement of 40% and far surpassing traditional stoves operating at 10–23% efficiency. This improved efficiency resulted in considerable energy savings, with the prototype consuming an average of only 7.9 kWh to produce 1.5 liters of areke, compared to 25.5 kWh required by the traditional method, representing a 69% reduction in energy use. This notable decrease in energy consumption also translated into a 49% reduction in operating costs when compared to traditional biomass-based distillation methods.

The integration of a PID temperature controller enabled precise regulation of temperature, distillation rate and duration. By controlling distillation rate and duration, the prototype was able to control alcohol content, ensuring consistent product quality. The prototype also completely eliminated harmful emissions from biomass combustion.

The performance metrics were compared with traditional biomass stoves (10-23% efficiency) and commercial resistance coil cookstoves (39.3-60% efficiency), confirming the prototype's superior performance. Energy cost analysis revealed average savings of 2,940 Birr per month which translates to 35,280 Birr per year for small production volumes. The inclusion of local materials for manufacturing and alignment with traditional practices further validated the stove’s compatibility and practicality for Ethiopian areke producers. The

prototype demonstrates that electric areke distillation is technically feasible, economically viable, and environmentally sustainable. The findings also provide valuable thermal data for areke distillation, addressing a significant gap in existing research.

Future studies should explore optimizing the design for mass production, integrating alternative materials like copper and aluminum for improved durability and efficiency, and scaling the prototype for larger production capacities. Economic and lifecycle analyses will also provide deeper insights into the stove's practical adoption and environmental impact.

References

Adria, O., & Bethge, J. (n.d.). Reviewer Dr. Stefan Thomas (WI) Antoine Durand (WI) Dr. Claus Barthel (WI) Heike Volkmer (GIZ HERA - Poverty-oriented Basic Energy Services) Stefan Salow (GIZ HERA - Poverty-oriented Basic Energy Services). *Environment and Energy*.

AGH University. (2012). *Design of Medium Temperature Spiral Resistance Heating Elements for a 3-phase Resistance Furnace*. AGH University of Science and Technology, Department of Power Electronics and Energy Control Systems. https://home.agh.edu.pl/~waradzyn/Instruction%20-%20resistance%20heating%20element%20project.pdf

Aisyah, S., Triani, M., & Rasgianti, R. (2021). Energy efficency analysis for various type of electric cooker. *Journal of Physics: Conference Series, 1869*(1), 012175. https://doi.org/10.1088/1742-6596/1869/1/012175

Alemayehu Zeleke Urge & Motuma Tolera Feyisa. (2019). Estimation of Households Fuelwood Consumption and Its Carbon Dioxide Emission: A Case Study on Adaba District South East Ethiopia. *Journal of Energy and Natural Resources, 7*(4), 92–102. https://doi.org/10.11648/j.jenr.20180704.11

Allen, I. C., & Jacobs, W. A. (1912, May). *An Electric Still Adapted for Difficult Distillations.* (world) [Research-article]. ACS Publications; American Chemical Society. https://doi.org/10.1021/ie50038a011

Areqie Local Alcohol Cutting Dreams, Lives Short. (2022, April). https://ethiopianbusinessreview.net/areqie-local-alcohol-cutting-dreams-lives-short/

Assefa, T., & Adem, K. (2022). *Comparison of Thermal and Emissions Performance on Three Stoves for Distilling Areke, A Traditional Ethiopian Beverage* (pp. 480–491). https://doi.org/10.1007/978-3-030-93712-6_32

Bekele, D. (2019). *DESIGN, FABRICATION AND EXPERIMENTAL INVESTIGATION OF IMPROVED BIOMASS AREKE DISTILLATION STOVE*.

Berkeley-Darfur Stove V.14. (2014, June 28). Engineering For Change. https://www.engineeringforchange.org/solutions/product/berkeley-darfur-stove-v-14/

Biomass Connect. (n.d.). *Eucalyptus (Eucalyptus spp.)*. Biomass Connect. Retrieved December 8, 2024, from https://www.biomassconnect.org/wp-

content/uploads/2023/03/Crop-information-factsheet-Eucalyptus-1.pdf

Cao, Y, Li, G, Zhang, Z., Chen, L, Li, Y., & Zhang, T. (2010). The specific heat of wheat. *Julius-Kühn-Archiv*, *425*, 243–249. https://doi.org/10.5073/jka.2010.425.202

Cengel, Y., & Ghajar, A. (2019). *Heat and Mass Transfer: Fundamentals and Applications*. https://www.mheducation.com/highered/product/heat-mass-transfer-fundamentals-applications-cengel-ghajar/M9780073398198.html

Cetiner, I., & Shea, A. (2018). Wood waste as an alternative thermal insulation building material solution. *Energy and Buildings*, *168*. https://doi.org/10.1016/j.enbuild.2018.03.019

Chheti, R., Chhoedron, D., Sunwar, T., & Robinson, D. A. (2015). *Analysis on Integrated LPG Cook Stove and Induction Cooktop for Cooking Purposes in Bhutan*.

Dagnew, D., & Rzehak, N. (2015, October). *Energising Development Ethiopia Improved Cook Stoves*. Energising Development (EnDev) Ethiopia, Deutsche Gesellschaft für internationale Zusammenarbeit (GIZ) GmbH. https://energypedia.info/images/9/92/EnDev_ET_ICS_Factsheet_Oct_2015_en.pdf

Dassault Système. (2025). *Convection Heat Coefficient*. https://help.solidworks.com/2015/english/SolidWorks/cworks/c_convection_heat_coefficient.htm?format=P&value=

Demissie, S., Ramayya, V., & Tekestebrihan, D. (2016). Design, Fabrication and Testing of Biogas Stove for "Areke" Distillation:The case of Arsi Negele, Ethiopia, Targeting Reduction of Fuel-Wood Dependence. *International Journal of Engineering Research*, *5*.

Design calculations for heating elements—Kanthal®. (n.d.). Retrieved March 31, 2024, from https://www.kanthal.com/en/knowledge-hub/heating-material-knowledge/design-calculations-for-heating-elements/

dewesoft. (n.d.). *What Is a Data Logger—The Ultimate Guide*. Data Acquisition | Test and Measurement Solutions. Retrieved December 29, 2024, from https://dewesoft.com/blog/what-is-data-logger

Dewitt, D. P., Bergman, T. L., & Lavine, A. S. (2017). *Fundamentals of Heat And Mass Transfer* (F. P. Incropera, Ed.).

Edge, E., & LLC, E. E. (2024). *Thermal Properties of Non-Metals*. https://www.engineersedge.com/heat_transfer/thermal_properties_of_nonmetals_13967.htm

Elbayoumi, M., & Albelbeisi, A. H. (2023). Biomass use and its health effects among the vulnerable and marginalized refugee families in the Gaza Strip. *Frontiers in Public Health*, *11*. https://www.frontiersin.org/articles/10.3389/fpubh.2023.1129985

Ethiopian Standards Agency. (2018). *Electric Power Supply System and Machines—Technical and Performance Requirements For Household Open Resistor Based Electric Stove*. Ethiopian Standards Agency. https://rise.esmap.org/data/files/library/ethiopia/Clean%20Cooking/Ethiopia_1-Electric%20Stove%20Standard%202020.pdf

feng niu. (2022, September 5). PID Digital Temperature Controller. *OMCH*. https://www.omchsmps.com/pid-temperature-controller/

Fullerton, D. G., Bruce, N., & Gordon, S. B. (2008). Indoor air pollution from biomass fuel smoke is a major health concern in the developing world. *Transactions of The Royal Society of Tropical Medicine and Hygiene, 102*(9), 843–851. https://doi.org/10.1016/j.trstmh.2008.05.028

Getachew, S., Bekele, A., & Pandey, V. (2022). Performance Investigation of Ethiopian Local Drinking Alcohol Distillation System Using Solar Dish Concentrator. *Journal of Energy, 2022*, e8478276. https://doi.org/10.1155/2022/8478276

Gezahegne, G. (2008). *DISTILLING STOVE BY MEASURING THE INDOOR AIR EMISSION*.

GIZ Ethiopia. (2011, November). *Mirt Stove*. Deutsche Gesellschaft für Internationale Zusammenarbeit (GIZ) GmbH. https://energypedia.info/images/a/a0/GIZ_HERA_2012_Mirt_stove.pdf

Goldemberg, J., United Nations Development Programme, United Nations, & World Energy Council (Eds.). (2000). *World energy assessment: Energy and the challenge of sustainability*. United Nations Development Programme.

GoSwitchgear. (2022, October 12). *On-off Vs PID Temperature Controller—GoSwitchgear*. https://goswitchgear.com/on-off-vs-pid-temperature-controller/

Heanjia Super-Metals Co., Ltd. (2015). *Nichrome Alloys for Heating*. https://super-metals.com/wp-content/uploads/2015/04/Nichrome-Alloys-for-Heating.pdf

Heating element. (2025). In *Wikipedia*. https://en.wikipedia.org/w/index.php?title=Heating_element&oldid=1295112930#Ni-Cr(Fe)_alloys_(AKA_nichrome,_Chromel)

Hegbom, T. (1997). *Integrating Electrical Heating Elements in Product Design*. CRC Press.

Household air pollution. (2024, October 16). https://www.who.int/news-room/fact-sheets/detail/household-air-pollution-and-health

Hung Anh, L. D., & Pásztory, Z. (2021). An overview of factors influencing thermal conductivity of building insulation materials. *Journal of Building Engineering, 44*, 102604. https://doi.org/10.1016/j.jobe.2021.102604

Ikpambese, K., Ager, P., & Daniel, I. (2014). *COMPARATIVE STUDY OF ENERGY PERFORMANCE OF KEROSENE, ELECTRIC, WOOD AND CHARCOAL STOVES*. *3*.

İNCE, R., GÜZEL, E., & İNCE, A. (2008). Thermal Properties of Some Oily Seeds. *Journal of Agricultural Machinery Science*, *4*(4), 399–405.

Indmall Automation. (2024, November 11). *Types of Temperature Controllers? | Explained*. https://www.indmall.in/faq/how-many-types-of-temperature-controllers-are-there/

Instrumart. (n.d.). *Temperature Controller Basics Handbook | Instrumart*. Retrieved December 29, 2024, from https://www.instrumart.com/pages/283/temperature-controller-basics-handbook

Jalmi, A. S., Chari, B. L., Bokar, V. D., Furtado, D. P., Naik, S. R., Chalwadi, D. P., Pawar, P. M., & Phaldesai, G. (2018). *Distillation for Liquor Using Electrical Induction Heating*. *9*(7).

Kanthal AB. (2018). *Resistance Heating Alloys And Systems for Industrial Furnaces*. KANTHAL AB. https://www.google.com/url?sa=i&url=https%3A%2F%2Fwww.kanthal.de%2Fglobalassets%2Fkanthal-global%2Fdownloads%2Fresistance-heating-alloys-and-systems-for-industrial-furnaces_b_eng_lr.pdf&psig=AOvVaw2FbOV5Fa3QSeXIWv8toztH&ust=1718688590312000&source=images&cd=vfe&opi=89978449&ved=0CAQQn5wMahcKEwjgo5-J9OGGAxUAAAAAHQAAAAAQBA

Kanthal AB. (2019). *Kanthal Handbook: Resistance Heating Alloys For Electric Appliances Handbook*. KANTHAL AB. https://www.kanthal.de/globalassets/kanthal-global/downloads/resistance-heating-alloys-for-electric-appliances-handbook_b_eng_lr.pdf

Karunanithy, C., & Shafer, K. (2016). Heat transfer characteristics and cooking efficiency of different sauce pans on various cooktops. *Applied Thermal Engineering*, *93*, 1202–1215. https://doi.org/10.1016/j.applthermaleng.2015.10.061

Kassa, A. (2015). *INVESTIGATION OF PARABOLIC DISH SOLAR CONCENTRATOR FOR LOCAL AREKE DISTILLATION*. 62.

Koffi, E., Kate, F., & Rushi, S. (2014, July). *Understanding the Differences between Cookstoves*. World Bank Group. https://documents1.worldbank.org/curated/zh/355711468165565579/pdf/88058-REVISED-LW7-fin-logo-OKR.pdf#:~:text=Across%20much%20of%20the%20world%2C%20the%20traditional,as%20much%20as%2015%20percent%20fuel%20savings.

Manaye Demissie, A., Amaha, S., Gufi, Y., Zeratsion, B., Worku, A., & Abrha, H. (2022). Fuelwood use and carbon emission reduction of improved biomass cookstoves: Evidence from kitchen performance tests in Tigray, Ethiopia. *Energy, Sustainability and Society*, *12*. https://doi.org/10.1186/s13705-022-00355-3

Mengistu, K. (2002, December). *FAO - Forestry—Workshop on Tropical Secondary Forest Management in Africa: Reality and Perspectives*. Fao.Org. https://www.fao.org/3/j0628e/J0628E50.htm

Mohammed, N. (2008). *Impact of 'Katikala' Production on the Degradation of Woodland Vegetation and Emission of CO and PM during Distillation in Arsi-Negele Woreda, Central Rift Valley of Ethiopia*.

Muluken Biadgelegn Wollele & Debre Markos University. (2020). Quantifying Energy Losses on Electric Cooking Stove. *International Journal of Engineering Research And*, *V9*(05), IJERTV9IS050577. https://doi.org/10.17577/IJERTV9IS050577

New England Temperature Solutions. (2023, June 28). *PID Temperature Controllers: Everything You Need to Know*. https://nets-inc.com/resources/pid-temperature-controllers/

OEM Heaters. (n.d.). *Comparison of Temperature Controller Styles*. Retrieved December 29, 2024, from https://oemheaters.com/topic/temperature-controller-styles

OMEGA Engineering. (n.d.-a). *Data Loggers*. Https://Www.Omega.Com/En-Us/. Retrieved December 29, 2024, from https://www.omega.com/en-us/resources/data-loggers

OMEGA Engineering. (n.d.-b). *Introduction to Temperature Controllers*. Retrieved June 29, 2024, from https://br.omega.com/omegaFiles/temperature/Z/pdf/z110-114.pdf

OMEGA Engineering. (n.d.-c). *What is a Temperature Controller?* Https://Www.Omega.Com/En-Us/. Retrieved December 28, 2024, from https://www.omega.com/en-us/resources/temperature-controllers

Selinus, R. (1971). The Traditional Foods of the Central Ethiopian Highlands. *The Scandinavian Institute of African Studies*. https://ethnomed.org/resource/the-traditional-foods-of-the-central-ethiopian-highlands/

Shah, D. U., Konnerth, J., Ramage, M. H., & Gusenbauer, C. (2019). Mapping thermal conductivity across bamboo cell walls with scanning thermal microscopy. *Scientific Reports*, *9*(1), 16667. https://doi.org/10.1038/s41598-019-53079-4

Sibongiseni, G., Sampson, M., David, K., & Edson, M. (2024). (PDF) The Properties and Suitability of Various Biomass/Coal Blends for Co-Gasification Purposes. *ResearchGate*. https://doi.org/10.4236/jsbs.2014.43016

Sinny. (2024a, June 20). *Exploring Pid Temperature Controllers: Key Components-Sinny*. Sinny Temperature Controller. https://www.sinny.com/exploring-pid-temperature-controllers-key-components.html

Sinny. (2024b, November 2). *How Temperature Controllers Work: Components, Types, And Application-Sinny*. Sinny Temperature Controller. https://www.sinny.com/how-temperature-controllers-work-components-types-and-application.html

Someswararao, C., Kumar, G. P., & Satyanarayana, C. V. V. (2012). Performance Evaluation of Improved Cook Stoves. *Nature Environment and Pollution Technology*, *11*(4).

Tafere, G. (2015). *A review on Traditional Fermented Beverages of Ethiopian*.

Tesfay, A. H., Tsegay, K., Kahsay, M. B., Hailu, M. H., & Adaramola, M. S. (2024). Performance comparison of three prototype biomass stoves with traditional and Mirt stoves for baking Injera. *Energy, Sustainability and Society*, *14*(1), 11. https://doi.org/10.1186/s13705-024-00443-6

Testbook Edu Solutions Pvt. Ltd. (2023, June 8). *Asbestos Products: Know Properties, Uses, Types and Applications*. Testbook. https://testbook.com/civil-engineering/asbestos-products

The Engineering Toolbox. (n.d.). *Ethanol Water Mixtures—Densities vs. Temperature*. Retrieved January 3, 2025, from https://www.engineeringtoolbox.com/ethanol-water-mixture-density-d_2162.html

The SHORTFOR research project. (n.d.). *Preliminary results on the physical & chemical properties of Eucalyptus in Ireland*. The SHORTFOR research project. Retrieved December 8, 2024, from https://www.teagasc.ie/media/website/crops/forestry/research/shortfor_euc_handout_DPlant_210515.pdf

Thermcraft, Inc. (2016). *Electrical Resistance Heating Elements: An Overview*. Thermcraft. https://thermcraftinc.com/wp-content/uploads/2018/01/Heating_Element_Seminar_Nov_2_2016.pdf

Types and Properties of Heating Elements. (2025). https://www.iqsdirectory.com/articles/heating-element.html

Vizzuality. (2022). *Ethiopia Deforestation Rates & Statistics | GFW*. https://www.globalforestwatch.org/dashboards/country/ETH?category=undefined

Vu, V.-A., Cloutier, A., Bissonnette, B., Blanchet, P., & Duchesne, J. (2019). The Effect of Wood Ash as a Partial Cement Replacement Material for Making Wood-Cement Panels. *Materials*, *12*(17), Article 17. https://doi.org/10.3390/ma12172766

VZPS. (n.d.). *NiCr 8020 alloy*. Retrieved January 8, 2025, from https://en.vlzps.ru/alloys/electrical-resistance-alloys/nicr-80-20/

Wedajo Lemi, B. (2020). Microbiology of Ethiopian Traditionally Fermented Beverages and Condiments. *International Journal of Microbiology*, *2020*, 1478536. https://doi.org/10.1155/2020/1478536

Yohannes, T., Melak, F., & Siraj, K. (2013). Preparation and physicochemical analysis of some Ethiopian traditional alcoholic beverages. *African Journal of Food Sciences*, *7*, 399–403. https://doi.org/10.5897/AJFS2013.1066

Appendix-A: Calculation Tables

Table A-1: S/R_o ratio as a function of wire diameter for nichrome 80 alloy, valid for resistivity $\rho = 1.08\ ohm.mm^2/m$ and density = 8.3 g/cm^3 (Hegbom, 1997).

B&S no.	d (mm)	R/l (ohm/m)	S/R (cm^2/ohm)	W/l (g/m)	B&S no.	d (mm)	R/l (ohm/m)	S/R (cm^2/ohm)	W/l (g/m)
0	8.253	0.0202	12,828	444	20.5	0.766	2.34	10.3	3.82
0.5	7.788	0.0227	10,780	395	21	0.723	2.63	8.62	3.40
1	7.349	0.0255	9,059	352	21.5	0.682	2.96	7.24	3.03
1.5	6.935	0.0286	7,613	313	22	0.644	3.32	6.09	2.70
2	6.545	0.0321	6,398	279	22.5	0.607	3.73	5.12	2.40
2.5	6.176	0.0361	5,377	249	23	0.573	4.19	4.30	2.14
3	5.828	0.0405	4,518	221	23.5	0.541	4.70	3.61	1.91
3.5	5.500	0.0455	3,797	197	24	0.510	5.28	3.04	1.70
4	5.190	0.0511	3,191	176	24.5	0.482	5.93	2.55	1.51
4.5	4.898	0.0574	2,682	156	25	0.455	6.66	2.14	1.35
5	4.622	0.0644	2,253	139	25.5	0.429	7.48	1.80	1.20
5.5	4.362	0.0723	1,894	124	26	0.405	8.39	1.51	1.07
6	4.116	0.0812	1,591	110	26.5	0.382	9.43	1.27	0.951
6.5	3.884	0.0912	1,337	98.3	27	0.361	10.6	1.07	0.847
7	3.665	0.102	1,124	87.5	27.5	0.340	11.9	0.899	0.754
7.5	3.459	0.115	944	78.0	28	0.321	13.3	0.755	0.672
8	3.264	0.129	794	69.4	28.5	0.303	15.0	0.635	0.598
8.5	3.080	0.145	667	61.8	29	0.286	16.8	0.533	0.533
9	2.907	0.163	561	55.1	29.5	0.270	18.9	0.448	0.474
9.5	2.743	0.183	471	49.0	30	0.255	21.2	0.377	0.422
10	2.589	0.205	396	43.7	30.5	0.240	23.8	0.317	0.376
10.5	2.443	0.231	333	38.9	31	0.227	26.8	0.266	0.335
11	2.305	0.259	280	34.6	31.5	0.214	30.1	0.224	0.298
11.5	2.175	0.291	235	30.8	32	0.202	33.7	0.188	0.266
12	2.053	0.326	197	27.5	32.5	0.191	37.9	0.158	0.237
12.5	1.937	0.367	166	24.5	33	0.180	42.6	0.133	0.211
13	1.828	0.412	139	21.8	33.5	0.170	47.8	0.111	0.188
13.5	1.725	0.462	117	19.4	34	0.160	53.7	0.0937	0.167
14	1.628	0.519	98.5	17.3	34.5	0.151	60.3	0.0787	0.149
14.5	1.536	0.583	82.7	15.4	35	0.143	67:7	0.0662	0.132
15	1.450	0.655	69.5	13.7	35.5	0.135	76.0	0.0556	0.118
15.5	1.368	0.735	58.4	12.2	36	0.127	85.3	0.0467	0.105
16	1.291	0.825	49.1	10.9	36.5	0.120	95.8	0.0393	0.0936
16.5	1.218	0.927	41.3	9.67	37	0.113	108	0.0330	0.0833
17	1.150	1.04	34.7	8.61	37.5	0.107	121	0.0277	0.0742
17.5	1.085	1.17	29.1	7.67	38	0.101	136	0.0233	0.0661
18	1.024	1.31	24.5	6.83	38.5	0.0950	152	0.0196	0.0588
18.5	0.966	1.47	20.6	6.08	39	0.0897	171	0.0165	0.0524
19	0.912	1.66	17.3	5.42	39.5	0.0846	192	0.0138	0.0467
19.5	0.860	1.86	14.5	4.82	40	0.0799	216	0.0116	0.0416
20	0.812	2.09	12.2	4.30	40.5	0.0754	242	0.0098	0.0370

Table A-2: Representative values of the overall heat transfer coefficients in heat exchangers (Cengel & Ghajar, 2019).

Type of Heat Exchanger	U, W/m^2·K*
Water-to-water	850–1700
Water-to-oil	100–350
Water-to-gasoline or kerosene	300–1000
Water-to-brine	600–1200
Feedwater heaters	1000–8500
Steam-to-light fuel oil	200–400
Steam-to-heavy fuel oil	50–200
Steam condenser	1000–6000
Freon condenser (water cooled)	300–1000
Ammonia condenser (water cooled)	800–1400
Alcohol condensers (water cooled)	250–700
Gas-to-gas	10–40
Gas-to-brine	10–250
Oil-to-oil	50–400
Organic vapors-to-water	700–1000
Organic solvents-to-organic solvents	100–300
Water-to-air in finned tubes (water in tubes)	30–60† 400–850‡
Steam-to-air in finned tubes (steam in tubes)	30–300† 400–4000‡

*Multiply the listed values by 0.176 to convert them to Btu/h·ft^2·°F.
†Based on air-side surface area.
‡Based on water- or steam-side surface area.

Appendix-B: LabVIEW VI Diagrams

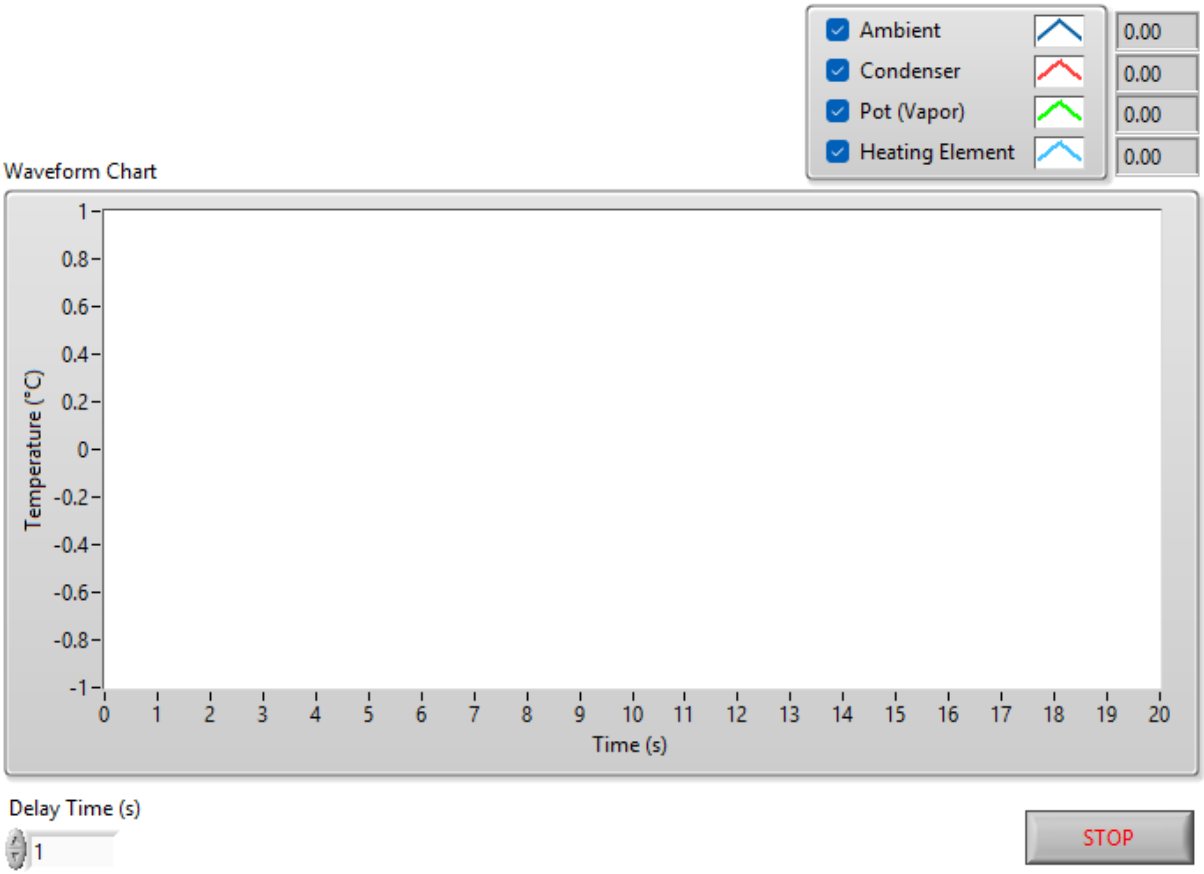

Figure B-1: Front Panel of LabVIEW VI used to log data for CCT.

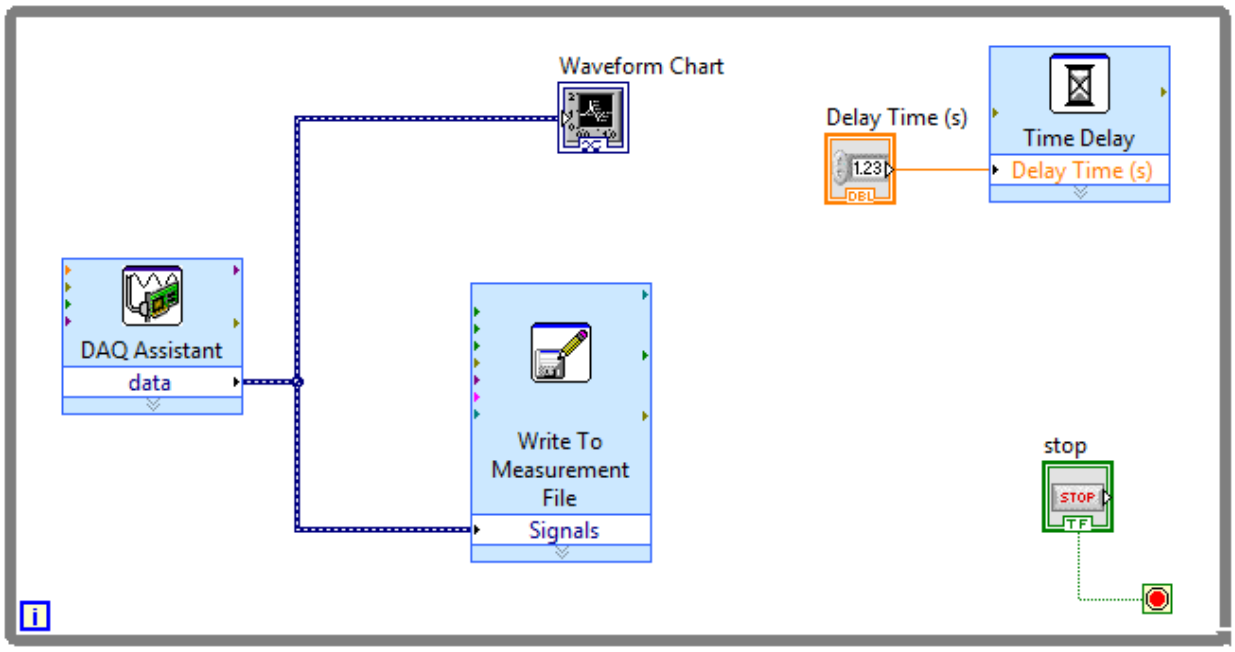

Figure B-2: Block diagram of LabVIEW VI used to log data for CCT.

Appendix-C: Drawings

Item	Name	Quantity	Item	Name	Quantity
10	Insulation	1	1	Aluminum Flask	1
11	Plastic Hose 1	1	2	Aluminum Pot	1
12	Plastic Hose 2	1	3	Barrel	1
13	Pot Lid	1	4	Bowl	1
14	Stove Cover	1	5	Clay Pot	1
15	Submersible Pump	1	6	Condenser Shell	1
16	Water Container	1	7	Condenser Tube	1
17	Wooden Chair	1	8	Heating Element	1
			9	Heating Element 2	1

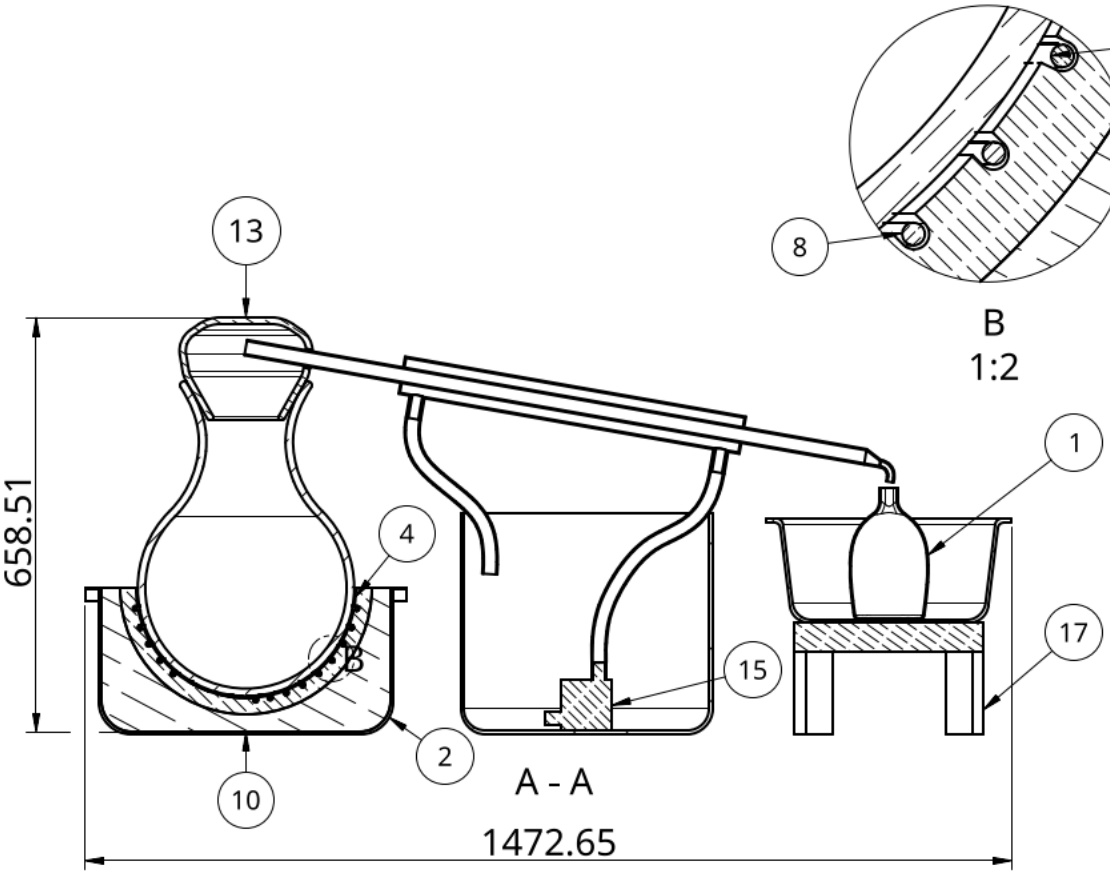

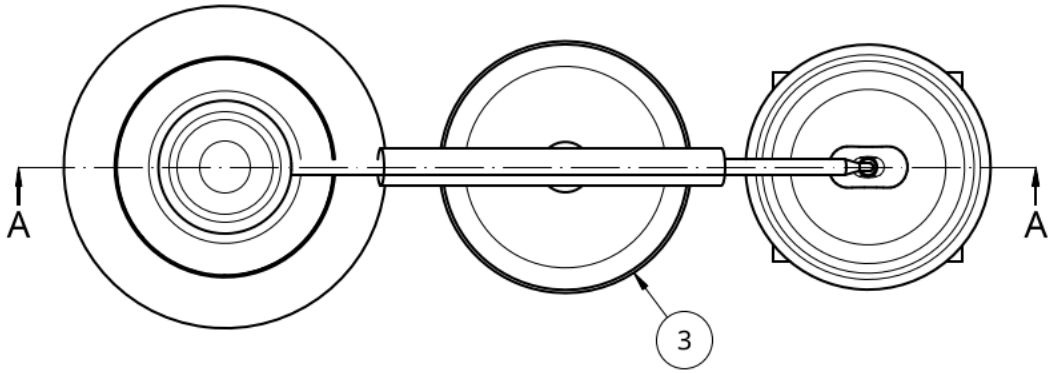

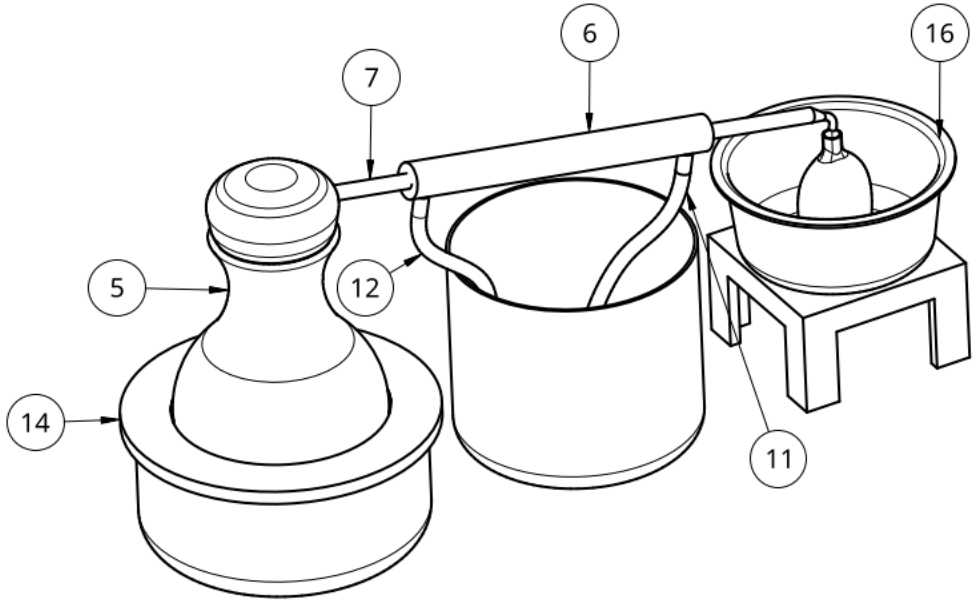

All dimensions are in millimeters	Title: **Electrical Areke Distillation Stove**		
Created By: Dawit Debash	Date: 2025-01-17	Scale: 1:12	Size: A4
Aprroved By: Kamil D. Adem (PhD)	Material: N/A		Sheet: 1/8

Item	Name	Quantity
2	Aluminum Pot	1
4	Bowl	1
5	Clay Pot	1
8	Heating Element	1
9	Heating Element 2	1
10	Insulation	1
13	Pot Lid	1
14	Stove Cover	1

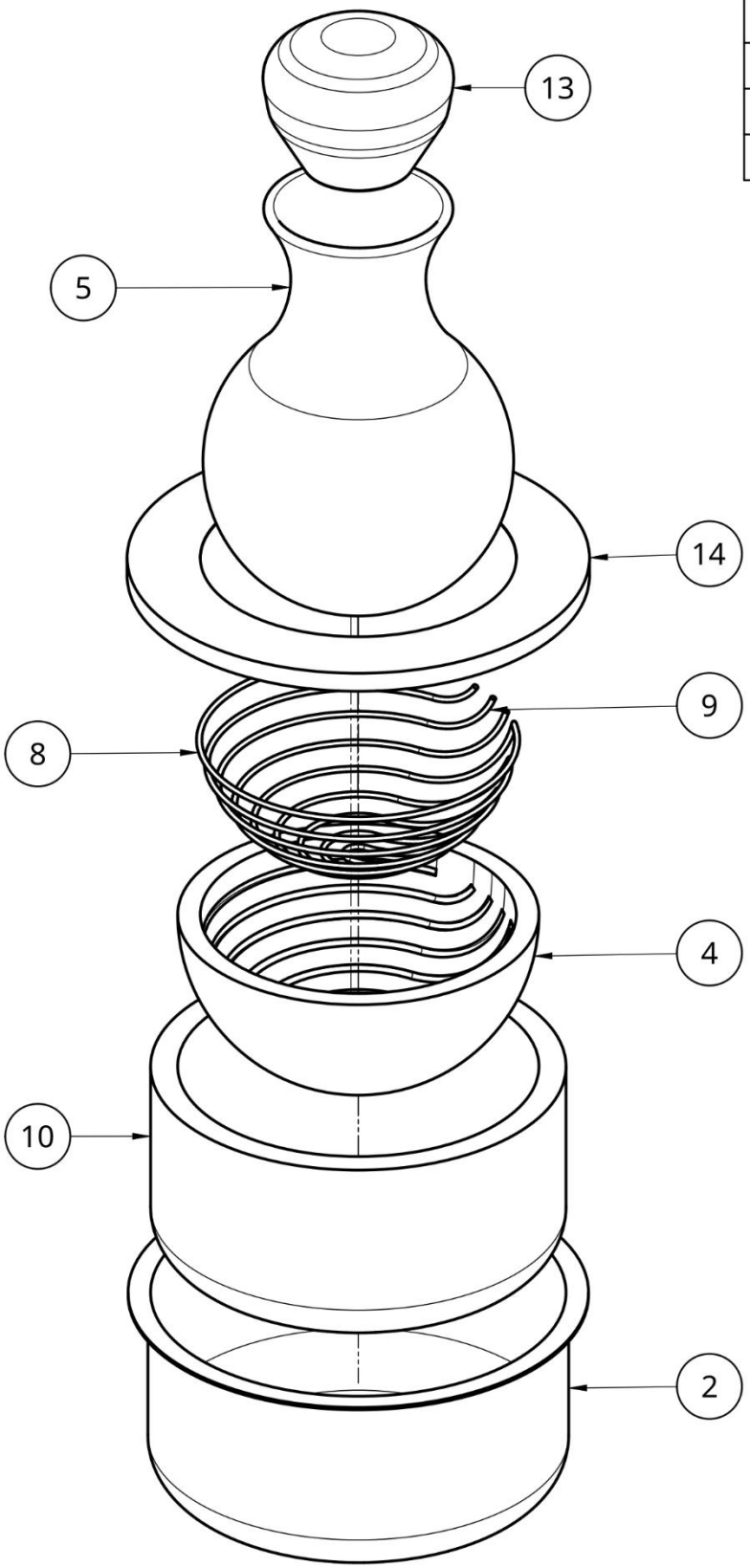

All dimensions are in millimeters	Title: **Stove Assembly**		
Created By: Dawit Debash	Date: 2025-01-17	Scale: 1:8	Size: A4
Aprroved By: Kamil D. Adem (PhD)	Material: N/A		Sheet: 2/8

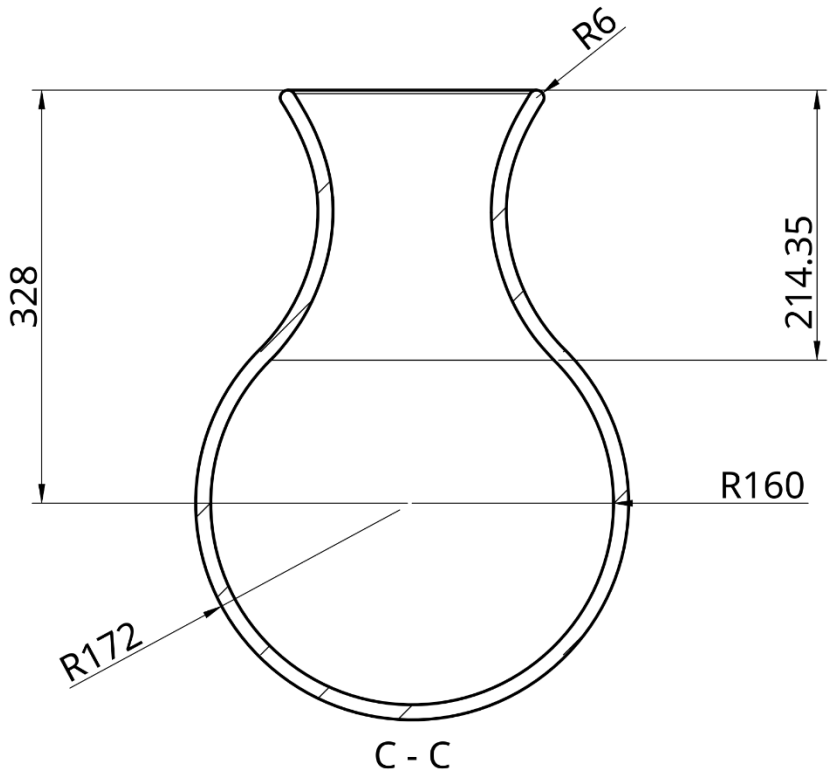

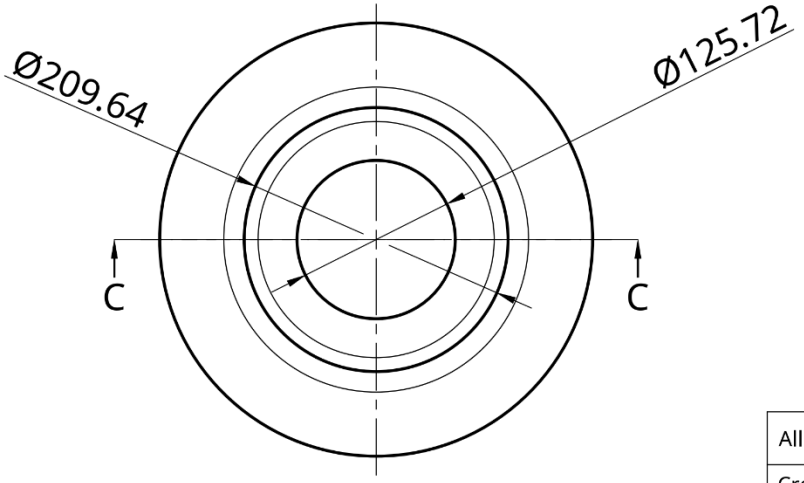

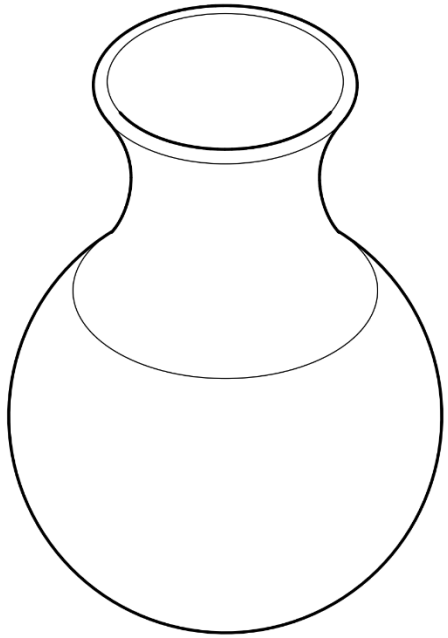

All dimensions are in millimeters	Title: **Clay Pot**		
Created By: Dawit Debash	Date: 2025-01-17	Scale: 1:6	Size: A4
Aprroved By: Kamil D. Adem (PhD)	Material: Clay		Sheet: 3/8

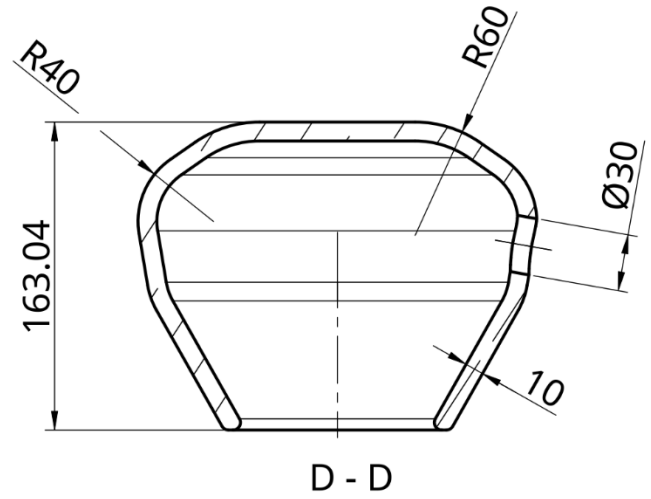

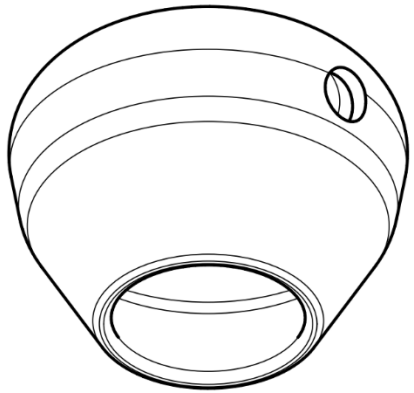

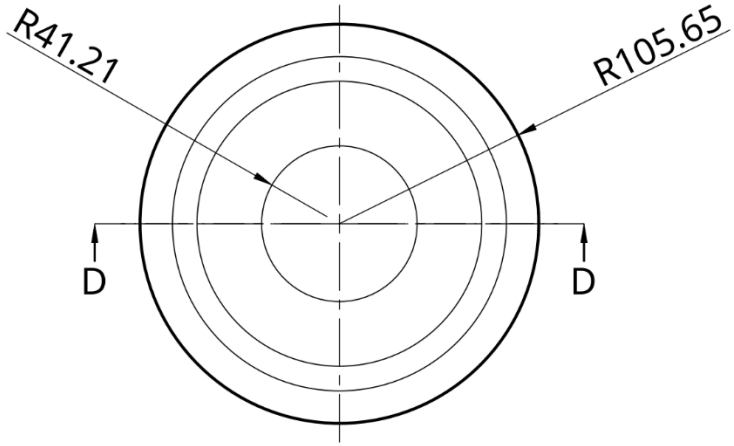

All dimensions are in millimeters	Title: **Pot Lid**		
Created By: Dawit Debash	Date: 2025-01-17	Scale: 1:4	Size: A4
Aprroved By: Kamil D. Adem (PhD)	Material: Clay		Sheet: 4/8

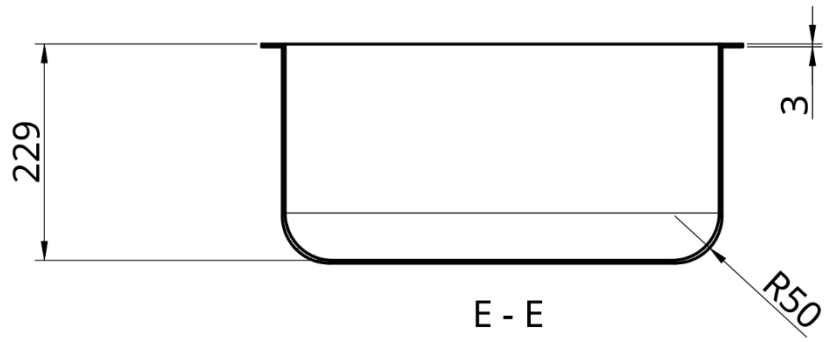

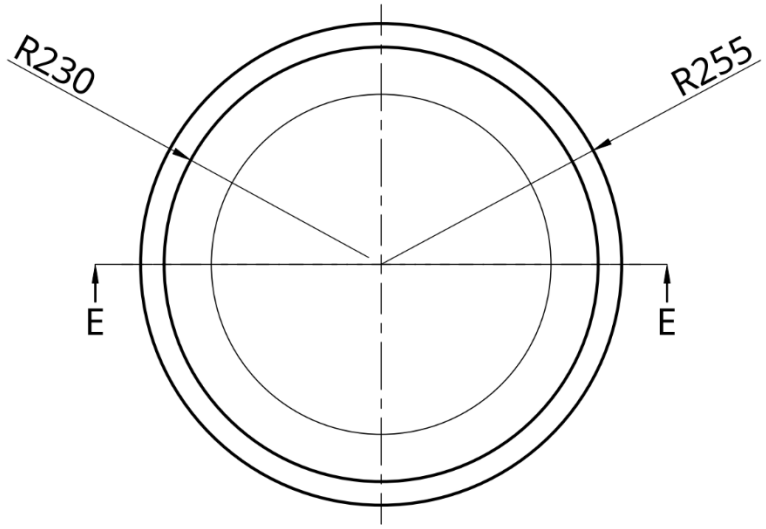

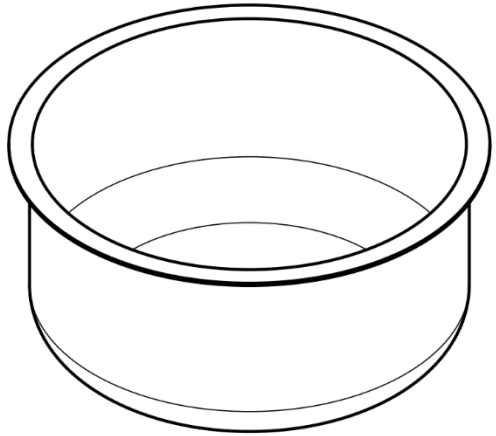

All dimensions are in millimeters	Title: **Aluminum Pot**		
Created By: Dawit Debash	Date: 2025-01-17	Scale: 1:8	Size: A4
Aprroved By: Kamil D. Adem (PhD)	Material: Aluminum		Sheet: 5/8

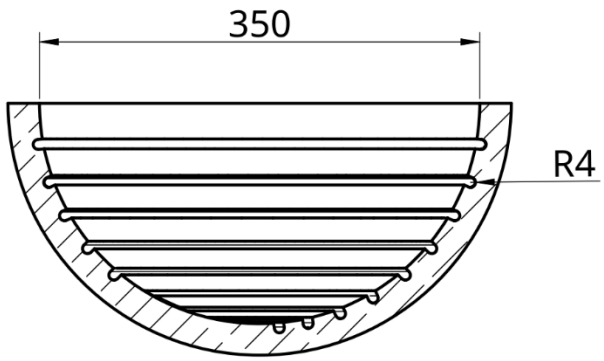

F - F

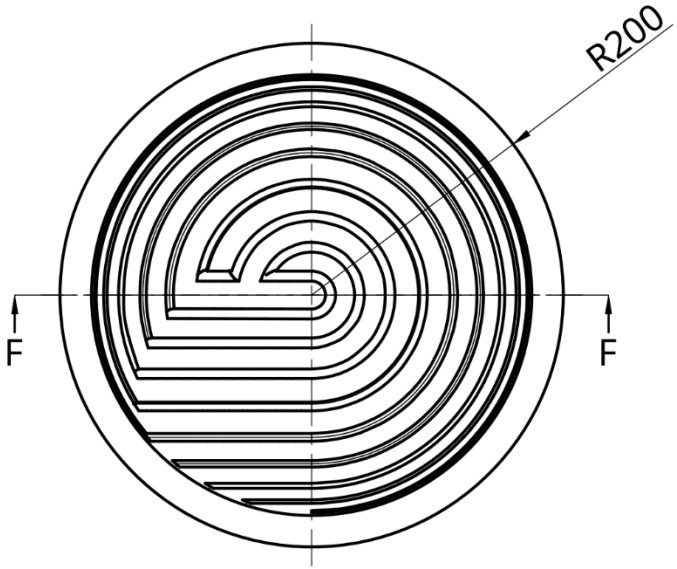

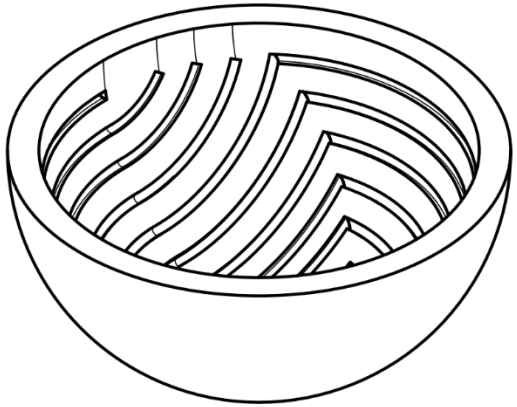

All dimensions are in millimeters	Title: **Bowl**		
Created By: Dawit Debash	Date: 2025-01-17	Scale: 1:6	Size: A4
Aprroved By: Kamil D. Adem (PhD)	Material: CLAY		Sheet: 6/8

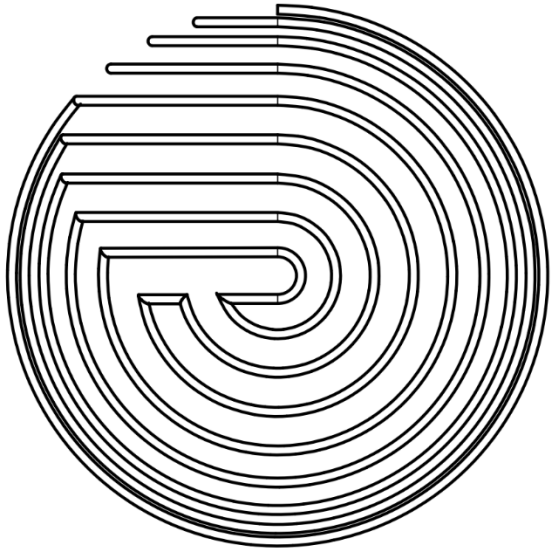

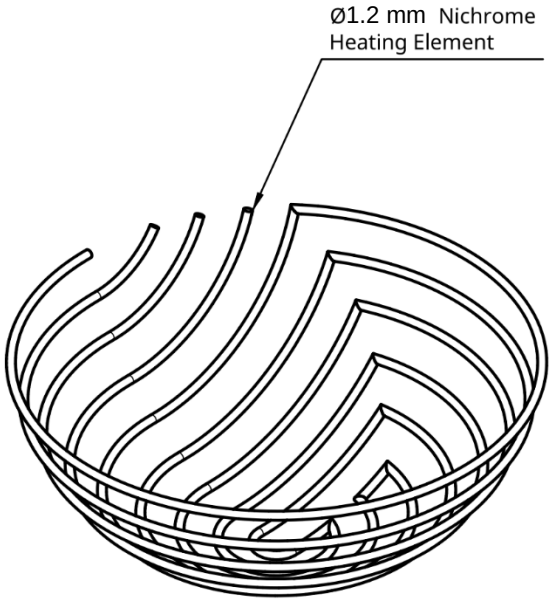

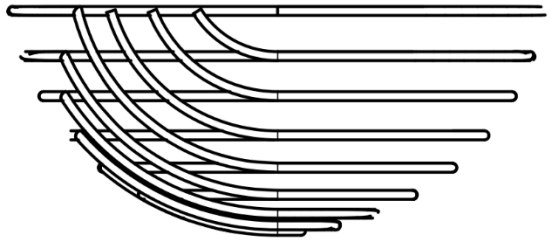

Note: Two 30 ohm resistance Heating elements coils connected in pareallel.
- Coil diameter = 0.6 mm
- Wire diameter = 0.12 mm

All dimensions are in millimeters	Title: **Heating Element Assembly**		
Created By: Dawit Debash	Date: 2025-01-17	Scale: 1:5	Size: A4
Aprroved By: Kamil D. Adem (PhD)	Material: Nichrome 80		Sheet: 7/8

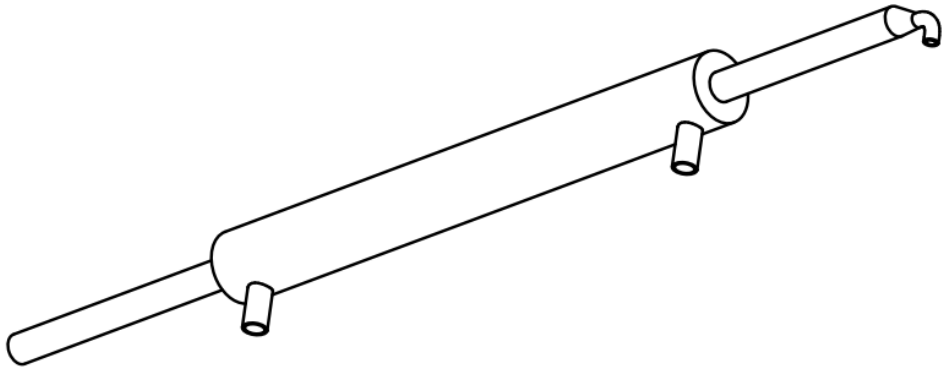

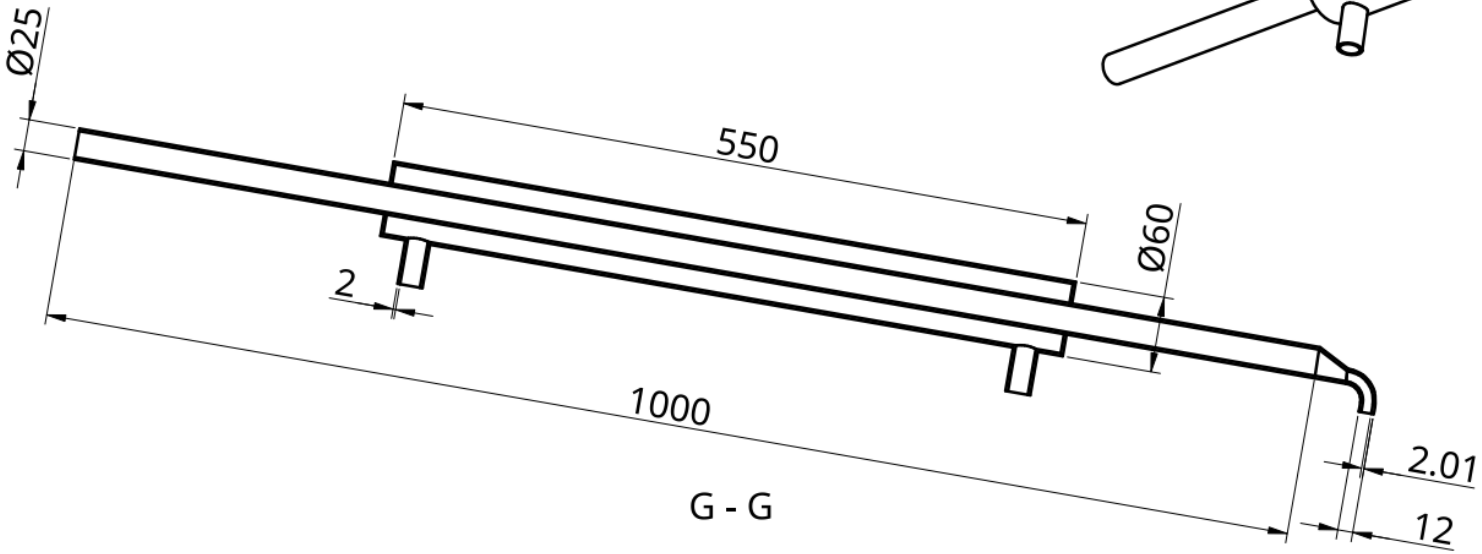

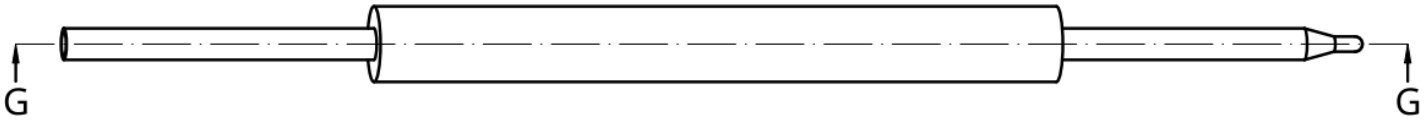

All dimensions are in millimeters	Title: **Shell And Tube Condenser Assembly**		
Created By: Dawit Debash	Date: 2025-01-17	Scale: 1:6	Size: A4
Aprroved By: Kamil D. Adem (PhD)	Material: N/A		Sheet: 8/8